論文 / 著書情報
Article / Book Information

題目(和文)	
Title(English)	Applications of Exact WKB analysis to Spectral problems and N = 2 gauge theories
著者(和文)	今泉恵太
Author(English)	Keita Imaizumi
出典(和文)	学位:博士(理学), 学位授与機関:東京工業大学, 報告番号:甲第12309号, 授与年月日:2023年3月26日, 学位の種別:課程博士, 審査員:伊藤 克司,今村 洋介,慈道 大介,須山 輝明,関澤 一之
Citation(English)	Degree:Doctor (Science), Conferring organization: Tokyo Institute of Technology, Report number:甲第12309号, Conferred date:2023/3/26, Degree Type:Course doctor, Examiner:,,,,
学位種別(和文)	博士論文
Type(English)	Doctoral Thesis

Ph.D Thesis

Applications of Exact WKB analysis to Spectral problems and $\mathcal{N} = 2$ gauge theories

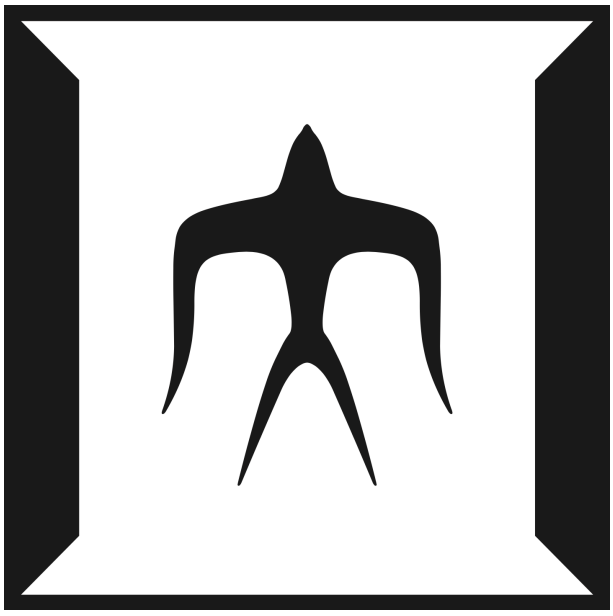

Keita Imaizumi

Department of Physics, Tokyo Institute of Technology
Tokyo, 152-8551, Japan

February, 2023

Abstract

The Exact Wentzel-Kramers-Brillouin (WKB) analysis is an exact approach to study the complex one-dimensional stationary Schrödinger equation. In this thesis, we apply the Exact WKB analysis to study quantum mechanics, the quasi-normal modes (QNMs) for the extremal D3/M5-branes and 4-dimensional $\mathcal{N} = 2$ SU(2) supersymmetric gauge theories. This thesis is composed of three parts. In the first part, we introduce the Exact WKB analysis. We explain the connection formula for the Borel resummation of the WKB solutions. In the second part, we solve the spectral problems for the bound states of quantum mechanical systems and the QNMs of the extremal D3/M5-branes based on the Exact WKB analysis. The connection formula for the Borel resummed WKB solutions determines exact conditions for the spectra. The exact conditions show that the discontinuity of the perturbative part of the spectra leads the non-perturbative part of themselves. In the third part, we derive the Thermodynamic Bethe Ansatz (TBA) equations that determine the spectra by combining with the exact conditions. We also derive the TBA equations for the quantum Seiberg-Witten curves of 4-dimensional $\mathcal{N} = 2$ SU(2) supersymmetric gauge theories with $N_f = 0, 2$ fundamental hypermultiplets. The TBA equations for the quantum Seiberg-Witten curves determine the renormalized masses of the Bogomol'nyi-Prasad-Sommerfield (BPS) particles in the low-energy effective theory of the models exactly.

Acknowledgements

First and foremost, I would like to express my sincere gratitude to my supervisor Katsushi Ito for his guidance and helps during my Ph.D course. He has been a great help to me in all the time of my studies. I couldn't have done it without him.

I would like to thank all the former and current members of the particle physics group at Tokyo Institute of Technology. In particular, I would like to thank Yosuke Imamura for his guidance. I would also like to thank Hongfei Shu, Naoto Kan, Takafumi Okubo, Reona Arai, Saki Koizumi, Kohei Kuroda, Takayasu Kondo, Shota Fujiwara, Tatsuya Mori, Shuichi Murayama, Mingshuo Zhu and Jingjing Yang for discussions.

I must also thank Yasuyuki Hatsuda, Naohisa Sueishi for their very helpful discussions.

My Ph.D course is supported in part by the Sasakawa Scientific Research Grant from The Japan Science Society and JSPS Research Fellowship 22J15182 for Young Scientists, from Japan Society for the Promotion of Science (JSPS).

Last but not least, I am very grateful to my parents.

Contents

Chapter 1

Introduction

The perturbation theory is the approximation method that expands physical observables in powers of a parameter. In particle physics, computations in the standard model and string theory are done by the perturbation theory, where the physical observables take the form of power series in the coupling constant. In the weak coupling region, the perturbation theory gives a good approximation to the physical observables.

In the strong coupling region, the perturbation theory is not applicable. Nevertheless, strong coupling theories appear in particle physics. For example, Quantum Chromodynamics is an asymptotically free theory and becomes a strong coupling theory in the low energy region. The strong coupling theory also appears in string theory, where the strong coupling limit of the theory becomes M-theory. To study the strong coupling theories, we need other methods (numerically, exactly, ...) to compute physical observables.

The perturbation theory can be promoted to exact analysis by combining with resummation methods. The goal of this thesis is to establish an exact method that enables us to study even the strong coupling theories based on the Borel resummation. In this thesis, as a first step to this goal, we will demonstrate that the Borel resummation provides exact results in the study of the quasi-normal modes (QNMs) and the low-energy effective dynamics of the $\mathcal{N} = 2$ gauge theories. In the study of the QNMs, we will derive exact QNMs conditions written by the Borel resummation. The exact conditions not only determine the QNMs exactly, but also clarify that the discontinuity of the perturbative part of the QNMs leads the non-perturbative part of themselves. This result shows we can study non-perturbative aspects of theories by using the Borel resummation. In the $\mathcal{N} = 2$ gauge theories, we will study the Borel resummation of the renormalized masses of the Bogomol'nyi-Prasad-Sommerfield (BPS) particles appearing in the low-energy effective theory of the models.

We determine the discontinuity structure of the Borel resummation of the masses and show that the discontinuity and the asymptotic behavior of the masses derive the Thermodynamic Bethe Ansatz (TBA) equations satisfied by the Borel resummation of the masses. We would like to emphasize that the discontinuity and the asymptotic behavior we will use in the derivation of the TBA equations are universal properties of the observables. This opens the possibility to formulate the exact approach based on the discontinuity and the asymptotic behavior.

In the rest of this chapter, we review each topic, the perturbation theory, the Borel resummation, the QNMs and N=2 gauge theories.

1.1 Perturbation theory

In the computation of observables (partition functions, energy eigenvalues, ...), there are cases in which we cannot get exact answers. We then try to compute the observables by using approximation methods. The perturbation theory expands the observables in powers of a parameter g that we can tune to be small:

$$\mathcal{O}(g) = \sum_{m=0}^{\infty} c_m g^m = c_0 + c_1 g + c_2 g^2 + \cdots , \tag{1.1.1}$$

where $\mathcal{O}(g)$ is an observable. The perturbation theory has good agreements with experimental results, for example the anomalous magnetic moment of the electron spin g-factor and its calculation in Quantum Electrodynamics.

If it is impossible to obtain the general term for the coefficient c_n, we compute the terms of the perturbative series (1.1.1) order by order. The perturbative series are then approximated by the partial sum,

$$\mathcal{O}(g) \sim \sum_{m=0}^{n} c_m g^m. \tag{1.1.2}$$

The numerical value of the the partial sum (1.1.2) is expected to approach to the true value of the observable as n increases, but it may deviates from the true value when n exceeds a certain number. As an example, let us consider the partition function for 0-dimensional

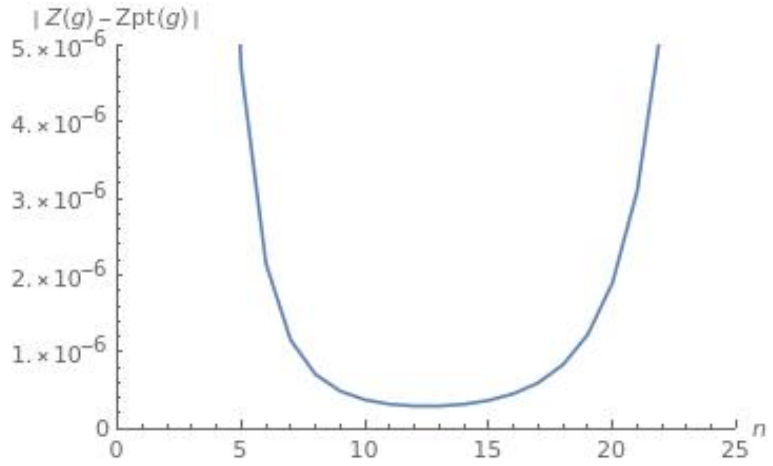

Figure 1.1: The numerical value of $|Z(g) - Z_{\rm pt}(g)|$ at $g = 1/100$. The horizon axis is the upper limit of the partial sum of $Z_{\rm pt}(g)$.

quantum field theory with a double well potential:

$$Z(g) = \int_{-\infty}^{+\infty} \frac{e^{-S}}{\sqrt{2\pi}} d\phi, \quad S = \frac{1}{2}\phi^2 + \frac{g}{2}\phi^4, \tag{1.1.3}$$

where $g > 0$. (1.1.3) can be evaluated for a given value of g numerically. On the other hand, expanding $e^{-\frac{g}{2}\phi^4}$ in powers of g and exchanging the integral and the sum without considering convergence, we obtain the perturbative series for (1.1.3),

$$Z_{\rm pt}(g) = \sum_{m=0}^{\infty} c_m g^m, \quad c_m = \frac{(-2)^m}{\sqrt{\pi}} \frac{\Gamma\left(2m + \frac{1}{2}\right)}{\Gamma\left(m+1\right)}. \tag{1.1.4}$$

Fig.1.1 shows the numerical value of $|Z(g) - Z_{\rm pt}(g)|$ at $g = 1/100$ where we have approximated $Z_{\rm pt}(g)$ as the partial sum up to order n. In small n region, $|Z(g) - Z_{\rm pt}(g)|$ goes to zero as n increases, while in large n region, it is getting bigger as n increases. As a result, the perturbative series (1.1.4) has a lack of the accuracy for large n.

The limit of the accuracy of the perturbative series occurs if the radius of convergence of the series (1.1.1) is zero. The radius of convergence of (1.1.4) is zero because the coefficient is factorially growth as $c_m \sim \frac{(-8)^m}{\sqrt{2}\pi} (n-1)!$. The origin of the factorial growth of c_m is the rapid growth of the number of the Feynman diagrams [1, 2]. We encounter the similar factorial growth of the coefficients of the perturbative series in quantum field theory [3], quantum mechanics [4–6] and string theory [7, 8].

1.2 Borel resummation

If the coefficients of (1.1.1) show factorial growth, we can define the Borel resummation by the following Laplace integral, which provides an analytic function on g,

$$\mathcal{B}\left[\mathcal{O}\right](g) = \int_0^\infty e^{-\xi/g}\tilde{\mathcal{O}}\left(\xi\right)d\xi, \quad \tilde{\mathcal{O}}\left(\xi\right) = \sum_{n=0}^{\infty}\frac{c_n}{\Gamma\left(n\right)}\xi^{n-1}. \tag{1.2.1}$$

For the series $\tilde{\mathcal{O}}\left(\xi\right)$, the factorial growth of c_n is suppressed by the factor $1/\Gamma\left(n\right)$. The Borel resummation $\mathcal{B}\left[\mathcal{O}\right](g)$ has $\mathcal{O}(g)$ as the asymptotic series at $g = 0$. For (1.1.4), the Borel resummation is given by

$$\mathcal{B}\left[Z_{\rm pt}\right](g) = \int_0^\infty e^{-\xi/g}\tilde{Z}_{\rm pt}\left(\xi\right)d\xi = \frac{1}{g}\int_0^\infty e^{-\xi/g}\frac{2}{\pi}\sqrt{1-2k^2(\xi)}K\left(k^2(\xi)\right)d\xi, \tag{1.2.2}$$

where $k^2(\xi) := \frac{1}{2}\left(1-\frac{1}{\sqrt{1+8\xi}}\right)$ and $K\left(k^2(\xi)\right)$ is the elliptic integral of the first kind. We have calculated $|Z(g) - \mathcal{B}\left[Z_{\rm pt}\right](g)|$ at $g = 1/100$ and the result is 6.38378×10^{-14}. The Borel resummation determines the observables exactly (e.g. [9–11]).

The Borel resummation also clarifies that the non-perturbative contribution to the observables can be captured from the discontinuity of the Borel resummation of the perturbative series (1.1.1). The analytic continuation of $\tilde{\mathcal{O}}\left(\xi\right)$ may have singularities on the complex ξ-plane. If there is a singularity on the positive real axis, we need to redefine the integral of (1.2.1) so that the integration contour avoids the singularity. We then have the ambiguity that the integration contour avoids the singularity to the left or right. We denote each integral as

$$\mathcal{B}_\pm\left[\mathcal{O}\right](g) = \int_0^{\infty e^{\pm i\delta}} e^{-\xi/g}\tilde{\mathcal{O}}\left(\xi\right)d\xi, \quad \delta \ll 1. \tag{1.2.3}$$

An example that the discontinuity of the Borel resummation appears is given by (1.1.3) with inverting the sign of $g \to -g$:

$$Z(g) = \int_{-\infty}^{+\infty}\frac{e^{-S}}{\sqrt{2\pi}}d\phi, \quad S = \frac{1}{2}\phi^2 - \frac{g}{2}\phi^4. \tag{1.2.4}$$

By expanding $e^{\frac{g}{2}\phi^4}$ in powers of g and exchanging the integral and the sum without considering convergence, we obtain the perturbative series for (1.2.4),

$$Z_{\rm pt}(g) = \sum_{m=0}^{\infty}c_m g^m, \quad c_m = 2^m\sqrt{\frac{2}{\pi}}\frac{\Gamma\left(2m+\frac{1}{2}\right)}{\Gamma\left(m+1\right)}, \tag{1.2.5}$$

and then,

$$\tilde{Z}_{\rm pt}\left(\xi\right) = \frac{2}{\pi g}\sqrt{2-k^2(\xi)}K(k^2(\xi)), \tag{1.2.6}$$

where $k^2(\xi) := \frac{\sqrt{32g\xi}}{1+\sqrt{8g\xi}}$. The Borel resummation of (1.2.6) has the discontinuity because the elliptic integral has the branch cut on the half line $\xi > 1/8g$. The difference of $\mathcal{B}_{\pm}\left[Z_{\rm pt}\right](g)$ is given by

$$\mathcal{B}_{+}\left[Z_{\rm pt}\right](g) - \mathcal{B}_{-}\left[Z_{\rm pt}\right](g) = \frac{i}{\sqrt{2\pi g}}e^{-\frac{1}{16g}}\frac{\pi}{2\sqrt{2}}\left(I_{-\frac{1}{4}}\left(\frac{1}{16g}\right) - I_{\frac{1}{4}}\left(\frac{1}{16g}\right)\right), \tag{1.2.7}$$

where $I_{\alpha}(x)$ is the modified Bessel function of the first kind. At $g \to 0$, the discontinuity (1.2.7) is suppressed by the non-perturbative factor $e^{-\frac{1}{16g}}$, which cannot be expressed by the power series in g.

The property that the discontinuity of the perturbative series provides the non-perturbative contribution is called resurgence. In quantum field theory, the discontinuity of the perturbative expansion of the partition function around a classical vacuum leads the non-perturbative parts that are the contributions from other saddle points [12–15]. The resurgence is also found for the vacuum energy, where the discontinuity of the perturbative part determines the IR renormalon of itself [16–19].

1.3 Exact WKB analysis

The Borel resummation of the perturbative series provides the exact observables. In this thesis, we will study the application of the Borel resummation to the Wentzel-Kramers-Brillouin (WKB) method in quantum mechanics.

WKB method

In quantum mechanics, the state of a particle is described by the wavefunction. For a time-independent potential $V(x)$ in one-dimensional space, the wavefunction is governed by the one-dimensional stationary Schrödinger equation:

$$\left[-\frac{\hbar^2}{2m}\frac{d^2}{dx^2} + V(x)\right]\psi(x) = E\psi(x), \tag{1.3.1}$$

where $\hbar$ is the reduced Planck constant, m is the mass of the particle, E is the energy of the particle and $\psi(x)$ is the wavefunction.

The WKB method provides the solution of (1.3.1) with a phase $S_{\rm WKB}(x)$ (see Chapter 2 for details):

$$\psi(x) = \exp\left[\frac{i}{\hbar} S_{\rm WKB}(x)\right]. \tag{1.3.2}$$

If we expand $S_{\rm WKB}(x)$ in powers of $\hbar$, the solution (1.3.2) becomes a power series solution called the WKB solution. On the x-axis, each classical allowed or forbidden region of the potential has different WKB solution. By solving the connection problem of the WKB solution in each region, we can obtain for example the energy quantization condition perturbatively.

Exact WKB analysis

The WKB solution is an asymptotic solution of (1.3.1), the radius of convergence of which is $\hbar = 0$. To obtain an exact solution, we can take the Borel resummation of the WKB solution [21, 22]. The Borel resummed WKB solution provides an exact wavefunction of the particle. In this method, the Schrödinger equation (1.3.1) is formulated in a complex plane. The Borel resummed WKB solution is a local solution at a point. The global structure of the Borel resummed WKB solution is determined by the Stokes graph, which is a set of integral curves drawn on the complex plane. If we connect the Borel resummed WKB solution across any line on the Stokes graph, the solutions are discontinuously changed (Stokes phenomenon of the WKB solution) [23–26]. Combining the boundary conditions, the connection formula for the Borel resummed WKB solution provides exact energy quantization conditions, which include the non-perturbative contributions arising from the quantum tunneling effect [27–32].

1.4 Quasi-normal modes

In this thesis, we will study the spectral problem of perturbations to curved spacetimes. The perturbations ingoing to the horizon (or the origin) and outgoing to the infinity damp over time. The damped modes of the perturbations are explained by the complex resonant eigenfrequencies called the quasi-normal modes (QNMs). The imaginary part of the QNMs measures the timescale that the perturbations damp. One of the examples of appearing QNMs is the gravitational waves in the ring-down phase of binary black holes merger, firstly observed by [33]. The gravitational waves in the ring-down phase can be described as a linear perturbation to the metrics. The symmetries of the background spacetimes then reduce the gravitational linear perturbation to a scalar or a vector perturbation. The grav-

itational waves are ingoing to the horizon and outgoing to the infinity, and the frequencies are explained by the QNMs.

The QNMs also studied in string theory. String theory has solitonic objects called Dp-branes, where p indicates the spacial dimension that Dp-branes extend. The open string is attached to the Dp-branes. The Dp-branes have the mass and can curve the background spacetime [34]. In [35], the QNMs of the dilaton field, which is a massless scalar state of the closed string, propagating in the parallel D3-branes geometry were computed. It was demonstrated that the QNMs can also be computed by the picture that the dilaton field interacts with massless fields explaining massless states of the open string on the D3-branes.

Another example of appearing QNMs is the Anti-de Sitter space/Conformal field theory (AdS/CFT) correspondence [36, 37]. Under the AdS/CFT correspondence, an AdS black hole geometry corresponds to a thermal equilibrium state of the CFT [38]. Then a perturbation to the AdS black hole corresponds to a perturbation to the thermal equilibrium state of the CFT. As the QNMs in the AdS black hole describe the damped modes of the perturbation, the QNMs in the CFT describe the damped perturbation to the thermal equilibrium state over time. Then the imaginary part of the QNMs measure the timescale that the CFT returns to the thermal equilibrium [39].

The QNMs are complex resonant eigenvalues of the Schrödinger type differential equations. In [40], we derived an exact condition for the QNMs of the dilaton field in the extremal D3-branes geometry based on the Exact WKB analysis. The QNMs computed by the exact condition agree with the Leaver's numerical method [42], and the results of the classical WKB approximation at large frequency [43]. We also derive exact QNMs conditions for a massless scalar field in the extremal M5-branes [41], which are objects in M-theory appearing the strong coupling limit of string theory. The exact conditions not only determined the QNMs non-perturbatively, but also showed that the discontinuity of the perturbative part of the QNMs leads the non-perturbative part of themselves. These results show that the Exact WKB analysis is a powerful tool to study the QNMs spectral problems.

1.5 WKB periods and TBA equations

WKB periods

In the Exact WKB analysis, the exact conditions for the energy spectra and the QNMs are given as functional relations of the Borel resummation of the WKB periods, which are the

following period integrals of the classical allowed and forbidden regions by the potential in (1.3.1):

$$\Pi_{[x_i,x_j]} := 2\int_{x_i}^{x_j} S_{\mathrm{WKB}}(x)dx, \tag{1.5.1}$$

where $[x_i, x_j]$ is a classical allowed or forbidden region. The WKB periods (1.5.1) are asymptotic series in $\hbar$, which coefficients has a factorial growth (e.g. [28]). The WKB periods can be computed order by order, for example the higher order coefficients of the WKB periods are computed by applying differential operators with respect to the energy E and the moduli parameters of the potential $V(x)$ to the leading term of the WKB periods (e.g. [44–46]). By computing the Borel resummation of the WKB periods and substituting into the exact conditions, we can obtain the spectra exactly.

TBA equation

In [21], the author pointed out that the discontinuity structure and the asymptotic behavior of the Borel resummed WKB periods determine themselves completely (called analytic bootstrap program or Riemann-Hilbert problem [21]). Recently, the solution to this problem has been explicitly given for arbitrary polynomial potentials [28], and for potentials with a regular singularity [47]. The solutions in [28, 47] take the form of the Thermodynamic Bethe Ansatz (TBA) equations, which are the integral equations appearing in the study of the integrable field theories represented by 2-dimensional CFT. By solving the TBA equations, we can compute the Borel resummed WKB periods without knowing the higher order coefficients of the WKB periods.

1.6 Quantum Seiberg-Witten curve

It is also important to derive the TBA equations for 4-dimensional $\mathcal{N} = 2$ supersymmetric gauge theories. The low-energy effective dynamics of 4-dimensional $\mathcal{N} = 2$ gauge theories is determined by a single holomorphic function called the prepotential [48]. According to the Seiberg-Witten theory [49, 50], the prepotential can be exactly computed from the Seiberg-Witten periods, which are the period integrals of the Seiberg-Witten differential on the Seiberg-Witten curve describing the Coulomb moduli space of the vacua. The prepotential obtained from the Seiberg-Witten periods enables us to understand non-perturbative aspects of the gauge theories such as the global structure of the BPS spectra [51–54]. The prepotential can also be obtained from the Nekrasov partition function [55, 56], which is

defined on the Ω-deformed background parametrized by two deformation parameters ϵ_1 and ϵ_2.

Under the Ω-background, the prepotential and the Seiberg-Witten periods also receive the correction by the deformation. In [44], it was argued that the deformed Seiberg-Witten periods for the $SU(2)$ super Yang-Mills theory in the Nekrasov-Shatashvili limit $\epsilon_2 \to 0$ [57] are identical to the WKB periods for the Mathieu differential equation. This identification was generalized to pure $SU(N)$ case [58] and with matters [59] later. The corresponding differential equations are called the quantum Seiberg-Witten curves, which are obtained from the canonical quantization of the symplectic structure of the Seiberg-Witten curves. The WKB periods for the quantum Seiberg-Witten curves determine the mass of the BPS particles perturbatively with respect to ϵ_1. The quantization of the Seiberg-Witten curves has been investigated with various examples [46,60–62]. The quantum Seiberg-Witten curves also appear in the Alday-Gaiotto-Tachikawa (AGT) correspondence, where the differential equations are satisfied by the one-point function of a degenerate primary field with respect to the Gaiotto states [63, 64].

In [65, 66], we studied the Exact WKB analysis for the quantum Seiberg-Witten curves for 4-dimensional $\mathcal{N} = 2$ SU(2) supersymmetric gauge theories with $N_f = 0, 2$ fundamental hypermultiplets and derived the TBA equations for the WKB periods. The TBA equations for the quantum Seiberg-Witten curves compute the Borel resummed WKB periods, which determine the mass of the BPS particles exactly. The TBA equations also show that the effective central charge of the underlying CFT is proportional to the one-loop beta function of the gauge theory.

The quantum Seiberg-Witten curve is also studied in the context of the QNMs. In [67], the authors showed that the E.O.M. for perturbations to the 4-dimensional Schwarzschild black hole and the Kerr black hole can be transformed to the quantum Seiberg-Witten curve for 4-dimensional $\mathcal{N} = 2$ SU(2) supersymmetric QCD with $N_f = 2, 3$ fundamental hypermultiplets [46]. This transformation enables us to utilize gauge theory techniques for solving the QNMs spectral problems. The Seiberg-Witten/gravity correspondence has extended to other geometries including D3 and M5-branes, fuzzballs and exotic compact objects later [41, 68, 69].

1.7 Outline of the thesis

In this thesis, we study the QNMs spectral problems and the quantum Seiberg-Witten curves exactly based on the Exact WKB analysis. For the QNMs spectral problems, we will obtain exact conditions determining the QNMs exactly. The exact conditions show that the discontinuity of the perturbative part of the QNMs leads the non-perturbative part of themselves. For the quantum Seiberg-Witten curves, we will derive the TBA equations computing the Borel resummed WKB periods exactly. The TBA equations provide an efficient way to compute the renormalized masses of the BPS particles and the QNMs by combining with the exact conditions.

This thesis is composed of three parts. The first part presents the basics of the Exact WKB analysis. The second part studies the exact conditions for the spectrum based on the Exact WKB analysis. We first review the exact energy quantization conditions for the bound states of quantum mechanical systems. Next, we derive the exact conditions for the QNMs, which are the complex resonant eigenfrequencies. The third part explores the derivation of the TBA equations governing the Borel resummed WKB periods. We review the TBA equations for arbitrary polynomial potentials and Central-Centrifugal potentials. We generalize the derivation of the TBA equations to the quantum Seiberg-Witten curves for 4-dimensional $\mathcal{N} = 2$ SU(2) $N_f = 0, 2$ supersymmetric gauge theories. This thesis is organized as follows:

Chapter 2 We introduce the Exact WKB analysis. We first review the classical WKB approximation. We present the connection formula for the Borel resummed WKB solution and the discontinuity formula for the Borel resummed WKB periods, which play a key role in this thesis. We do not enter the mathematical details of the proof of the formulae.

Chapter 3 We derive exact quantization conditions for energy spectrum of quantum mechanical systems based on the Exact WKB analysis. We study the bound states for the harmonic oscillator and in the double-well potential.

Chapter 4 We derive the exact conditions for the quasi-normal modes of massless scalar perturbations to the extremal D3-branes metric and the extremal M5-branes metric. We numerically check our exact conditions by using the Borel-Padé approximation. We also present analytic forms and asymptotic behaviors of the QNMs. The exact conditions show that the discontinuity of the perturbative part of the QNMs leads the non-perturbative part

of themselves. We also find examples of the Seiberg-Witten/gravity correspondence, which helps us to compute the QNMs from our conditions.

Chapter 5 We derive the TBA equations governing the Borel resummed WKB periods for arbitrary polynomial potentials and Central-Centrifugal potentials. Combining with the exact energy quantization condition, the TBA equations calculate the spectrum exactly.

Chapter 6 We generalize the derivation of the TBA equations to the quantum Seiberg-Witten curves for 4-dimensional $\mathcal{N} = 2$ SU(2) $N_f = 0, 2$ supersymmetric gauge theories (or Super Quantum Chromodynamics (SQCD)). We also compute the effective central charge of the underlying CFT, which is shown to be proportional to the one-loop beta function of the SQCD.

Chapter 4 and 6 are based on the author's paper [40, 41, 65, 66]. The review part in Chapter 2, 3 and 5 is inspired by various literature.

Chapter 2

Exact WKB analysis

This chapter aims to introduce the Exact WKB analysis. We first review the classical WKB approximation. The classical WKB approximation gives the wavefunction that is valid in the semiclassical limit. We derive the Bohr-Sommerfeld energy quantization condition, which is also valid in the semiclassical limit, from the connection formula for the wavefunction given by the WKB approximation. Next, we introduce the Exact WKB analysis. The Exact WKB analysis provides an exact wavefunction. The connection problem of the exact wavefunction is formulated on a Riemann surface called the WKB curve. We also introduce the WKB periods, which are the period integrals on the WKB curve. We basically follow the notations of [25, 26].

2.1 Classical WKB approximation

In quantum mechanics, a particle moving in a time-independent potential obeys the one-dimensional stationary Schrödinger equation,

$$\left[-\frac{\hbar^2}{2m}\frac{d^2}{dx^2} + V(x,\hbar)\right]\psi(x) = E\psi(x), \tag{2.1.1}$$

where x is the spacial coordinate, $\hbar$ is the reduced Planck constant, m is the mass of the particle, E is the energy of the particle, $V(x,\hbar)$ is the potential and $\psi(x)$ is the wavefunction.

Let us consider the bound state of the particle moving in a potential schematically described by Fig.2.1. There are two turning points x_1, x_2 satisfying $V(x_1,\hbar) = V(x_2,\hbar) = E$. We denote the region $[x_1, x_2]$ as II, in which the motion of the particle is classically allowed, and the regions $(-\infty, x_1]$ and $[x_2, +\infty)$ as I and III respectively, in which the motion of the

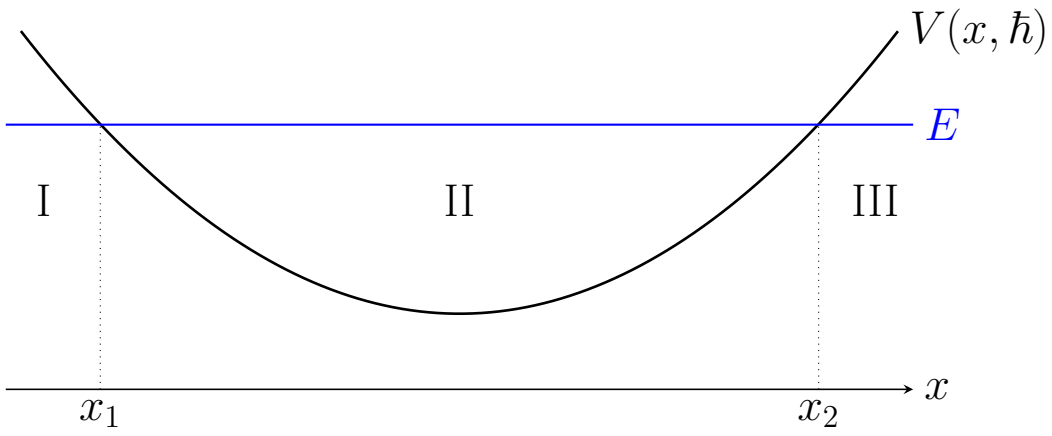

Figure 2.1: The potential graph describing a bound state of the particle.

particle is classically forbidden. For the bound state, we impose the boundary conditions that the wavefunction $\psi(z)$ decays at $x \to \pm\infty$. Then we obtain a spectrum of the energy taking discrete values.

In the semiclassical limit, where the de Broglie wavelength $\lambda(x) := \frac{\hbar}{ip(x,\hbar)}$ with $p(x,\hbar) := 2m\left(V(x,\hbar) - E\right)$ satisfies $|\lambda'(x)| \ll 1$, the wavefunction of (2.1.1) is given by the following solutions,

$$\psi_a(x) = \frac{1}{\sqrt{p(x,\hbar)}} \exp\left[\pm\frac{1}{\hbar}\int_a^x \sqrt{p(x',\hbar)}dx'\right] \tag{2.1.2}$$

where a is a parameter controlling the normalization of the wavefunction. (2.1.2) is called the WKB approximation of the wavefunction. The decaying solution in the region I at $E \gg 1$ is given by the plus signed solution of (2.1.2),

$$\psi_{x_1,\mathrm{I}}(x) = \frac{A}{\sqrt{p(x,\hbar)}} \exp\left[\frac{1}{\hbar}\int_{x_1}^x \sqrt{p(x',\hbar)}dx'\right], \quad x \in (-\infty, x_1] \tag{2.1.3}$$

where A is a constant and we have denoted the solution in I normalized at $a = x_1$ as $\psi_{x_1,\mathrm{I}}(x)$. Similarly, the decaying solution in the region III at $E \gg 1$ is given by the minus signed solution of (2.1.2),

$$\psi_{x_2,\mathrm{III}}(x) = \frac{C}{\sqrt{p(x,\hbar)}} \exp\left[-\frac{1}{\hbar}\int_{x_2}^x \sqrt{p(x',\hbar)}dx'\right], \quad x \in [x_2, +\infty) \tag{2.1.4}$$

where C is a constant and we have denoted the solution in III normalized at $a = x_2$ as $\psi_{x_2,\mathrm{III}}(x)$.

$\psi_{x_1,\mathrm{I}}(x)$ is connected into the region II as

$$\psi_{x_1,\mathrm{I}}(x) \to \psi_{\mathrm{II}}(x) = \frac{2A}{\sqrt{p(x,\hbar)}} \cos\left[\frac{1}{\hbar}\int_{x_1}^{x} \sqrt{p(x',\hbar)}dx' - \frac{\pi}{4}\right], \quad x \in [x_1, x_2] \tag{2.1.5}$$

where we have denoted the solution in II as $\psi_{\mathrm{II}}(x)$. On the other hand, $\psi_{x_2,\mathrm{III}}(x)$ is connected into the region II as

$$\psi_{x_2,\mathrm{III}}(x) \to \psi_{\mathrm{II}}(x) = \frac{2C}{\sqrt{p(x,\hbar)}} \cos\left[-\frac{1}{\hbar}\int_{x_2}^{x} \sqrt{p(x',\hbar)}dx' - \frac{\pi}{4}\right]. \quad x \in [x_1, x_2] \tag{2.1.6}$$

The wavefunction must be unique in the region II. Demanding that (2.1.5) and (2.1.6) match, one obtains the following condition,

$$A\cos\left[\frac{1}{\hbar}\int_{x_1}^{x} \sqrt{p(x',\hbar)}dx' - \frac{\pi}{4}\right] = C\cos\left[-\frac{1}{\hbar}\int_{x_2}^{x} \sqrt{p(x',\hbar)}dx' - \frac{\pi}{4}\right]. \tag{2.1.7}$$

This condition is satisfied by the discrete set of the value of E satisfying the following conditions,

$$\frac{1}{\hbar}\int_{x_1}^{x_2} p(x,\hbar)dx - i\frac{\pi}{2} = in\pi, \quad A = (-1)^n C, \tag{2.1.8}$$

where $n \in \mathbb{Z}_{\geq 0}$. The first condition for E in (2.1.8) is called the Bohr-Sommerfeld condition.

As an example, let us consider the harmonic oscillator. The potential is given by

$$V(x,\hbar) = \frac{1}{2}m\omega^2 x^2, \tag{2.1.9}$$

where ω is the angular frequency. The bound state for (2.1.9) has the positive energy $E > 0$, then the turning points $x_1 = -\frac{\sqrt{2E}}{\sqrt{m\omega^2}}$ and $x_2 = \frac{\sqrt{2E}}{\sqrt{m\omega^2}}$ are real. By substituting (2.1.9) and the turning points into the integral of the first condition in (2.1.8), we obtain

$$\frac{1}{\hbar}\int_{x_1}^{x_2} p(x,\hbar)dx = \frac{\sqrt{2m}}{\hbar}\int_{-\frac{\sqrt{2E}}{\sqrt{m\omega^2}}}^{\frac{\sqrt{2E}}{\sqrt{m\omega^2}}} \sqrt{\frac{1}{2}m\omega^2x^2 - E}dx = i\frac{m\omega}{\hbar}\int_{-\frac{\sqrt{2E}}{\sqrt{m\omega^2}}}^{\frac{\sqrt{2E}}{\sqrt{m\omega^2}}} \sqrt{\frac{2E}{m\omega^2} - x^2}dx. \tag{2.1.10}$$

Because the integral in the last equation is the area of the half circle, we obtain

$$i\frac{m\omega}{\hbar}\int_{-\frac{\sqrt{2E}}{\sqrt{m\omega^2}}}^{\frac{\sqrt{2E}}{\sqrt{m\omega^2}}} \sqrt{\frac{2E}{m\omega^2} - x^2}dx = i\pi\frac{E}{\hbar\omega}, \tag{2.1.11}$$

and then the first condition in (2.1.8) becomes

$$i\pi\frac{E}{\hbar\omega} = i\pi\left(n+\frac{1}{2}\right) \quad \Rightarrow \quad E = \hbar\omega\left(n+\frac{1}{2}\right). \tag{2.1.12}$$

The WKB approximation is only valid for the semiclassical limit, but the energy spectrum of the harmonic oscillator (2.1.12) coincides with the exact result.

Except for a few example represented by the harmonic oscillator, the WKB approximation and the Bohr-Sommerfeld condition are only valid for the semiclassical limit. One of the way to determine the exact wavefunction and the exact spectrum is using the Exact WKB analysis instead of the WKB approximation. In this thesis, we study the Schrödinger equations appearing in spectral problems and $\mathcal{N} = 2$ gauge theories based on the Exact WKB analysis.

2.2 Exact WKB analysis

2.2.1 WKB method

We consider the second-order ordinary differential equation of the Schrödinger type on a compact Riemann surface Σ (usually taken as the Riemann sphere $\Sigma = \mathbb{C}^*$),

$$\left[\frac{d^2}{dz^2} - \eta^2 Q_0(z) - Q_2(z)\right]\psi(z) = 0, \tag{2.2.1}$$

where z is a local complex coordinate on Σ, and η is a complex parameter, which plays a role of the reduced Planck constant $\eta = 1/\hbar$ [1]. Assume that $Q_0(z)$ and $Q_2(z)$ are meromorphic functions on Σ [2] .

Let us consider the following ansatz of the solution to (2.2.1),

$$\psi_a(z) = \exp\left[\eta\int_a^z S(z')dz'\right], \tag{2.2.2}$$

where a is a constant governing the normalization of the solution. Substituting the ansatz

[1] We follow the notation of [25, 26].

[2] In general, the potential function takes the form $\eta^2 Q_0(z) + \eta Q_1(z) + Q_2(z) + \eta^{-1}Q_3(z) + \cdots$. But, in this thesis, it is enough to consider only $Q_0(z)$ and $Q_2(z)$.

(2.2.2) into the Schrödinger equation (2.2.1), we obtain the equation satisfied by $S(z)$,

$$S^2(z) + \eta^{-1}\frac{d}{dz}S(z) - Q_0(z) - \eta^{-2}Q_2(z) = 0. \tag{2.2.3}$$

(2.2.3) is called the Riccati equation. To solve the Riccati equation, we expand $S(z)$ as a formal Laurent series in η^{-1},

$$S(z) = \sum_{n=0}^{\infty} S_n(z)\eta^{-n} = S_0(z) + S_1(z)\eta^{-1} + S_2(z)\eta^{-2} + \cdots . \tag{2.2.4}$$

Plugging the series (2.2.4) into the Riccati equation (2.2.3) and equating the coefficients of the powers of η^{-1}, one finds that $S_n(z)$ must satisfy the following recursion relation,

$$\begin{aligned}
&S_0^2(z) = Q_0(z),\\
&2S_0(z)S_1(z) + \frac{d}{dz}S_0(z) = 0,\\
&2S_0(z)S_2(z) + S_1^2(z) + \frac{d}{dz}S_1(z) = Q_2(z),\\
&2S_0(z)S_n(z) + \sum_{i,j\geq 1, i+j=n} S_i(z)S_j(z) + \frac{d}{dz}S_{n-1}(z) = 0, \quad (n \geq 3).
\end{aligned} \tag{2.2.5}$$

Depending on the choice of the sign for the root of the first equation in (2.2.5), we obtain two sets of functions $\{+S_n(z)\}_{n\geq 0}$ and $\{-S_n(z)\}_{n\geq 0}$ with $S_0(z) = \sqrt{Q_0(z)}$. They give two linearly independent solutions to the Schrödinger equation (2.2.1), which are denoted as follows,

$$\psi_a^{\pm}(z) = \exp\left[\pm\eta\int_a^z S(z')dz'\right]. \tag{2.2.6}$$

One can split (2.2.4) into even and odd powers of η^{-1} as,

$$S(z) = \sum_{n=0}^{\infty} S_{2n}(z)\eta^{-2n} + \sum_{n=0}^{\infty} S_{2n+1}(z)\eta^{-(2n+1)} = S_{\text{even}}(z) + S_{\text{odd}}(z). \tag{2.2.7}$$

Substituting this split into the Ricatti equation (2.2.3), we obtain

$$S_{\text{even}}^2(z) + 2S_{\text{even}}(z)S_{\text{odd}}(z) + S_{\text{odd}}^2(z) + \eta^{-1}\frac{d}{dz}\left(S_{\text{even}}(z) + S_{\text{odd}}(z)\right) - Q_0(z) - \eta^{-2}Q_2(z) = 0. \tag{2.2.8}$$

This equation can also be parted into even and odd collections of η^{-1},

$$\begin{aligned} &S^2_{\rm even}(z) + S^2_{\rm odd}(z) + \eta^{-1}\frac{d}{dz}S_{\rm odd}(z) - Q_0(z) - \eta^{-2}Q_2(z) = 0, \quad \text{(even power)}, \\ &2S_{\rm even}(z)S_{\rm odd}(z) + \eta^{-1}\frac{d}{dz}S_{\rm even}(z) = 0, \qquad\qquad\qquad\qquad \text{(odd power)}. \end{aligned} \tag{2.2.9}$$

The odd power collection shows that $S_{\rm odd}(z)$ is a total derivative,

$$S_{\rm odd}(z) = -\frac{\eta^{-1}}{2S_{\rm even}(z)}\frac{d}{dz}S_{\rm even}(z) = -\frac{\eta^{-1}}{2}\frac{d}{dz}\log S_{\rm even}(z) = \eta^{-1}\frac{d}{dz}\log\left(S_{\rm even}(z)\right)^{-\frac{1}{2}}. \tag{2.2.10}$$

Therefore the solutions (2.2.6) can be expressed by only using $S_{\rm even}(z)$,

$$\begin{aligned} \psi^{\pm}_a(z) &= \exp\left[\pm\int_a^z\left(\eta S_{\rm even}(z') + \frac{d}{dz'}\log\left(S_{\rm even}(z')\right)^{-\frac{1}{2}}\right)dz'\right] \\ &= \pm\left(S_{\rm even}(a)\right)^{-\frac{1}{2}}\left(S_{\rm even}(z)\right)^{-\frac{1}{2}}\exp\left[\pm\eta\int_a^z S_{\rm even}(z')dz'\right] \end{aligned} \tag{2.2.11}$$

Absorbing the constant $\pm\left(S_{\rm even}(a)\right)^{-\frac{1}{2}}$ into the normalization, we obtain

$$\psi^{\pm}_a(z) = \frac{1}{\sqrt{S_{\rm even}(z)}}\exp\left[\pm\eta\int_a^z S_{\rm even}(z')dz'\right]. \tag{2.2.12}$$

We refer to the solutions (2.2.12) as WKB solutions. The WKB solutions can be expanded as the series in η^{-1},

$$\psi^{\pm}_a(z) = \exp\left[\pm\eta\int_a^z S_0(z')dz'\right]\sum_{n=0}^{\infty}\psi^{\pm}_{a,n}(z)\,\eta^{-n}. \tag{2.2.13}$$

At a point z on Σ, the leading term $S_0(z) = \sqrt{Q_0(z)}$ has two values. For $Q_0(z) = e^{i\theta}|Q_0(z)| = e^{i(\theta+2\pi)}|Q_0(z)|$,

$$S_0(z) = \sqrt{Q_0(z)} = \sqrt{e^{i\theta}|Q_0(z)|} = e^{i\theta/2}\sqrt{|Q_0(z)|}, \tag{2.2.14}$$

and

$$S_0(z) = \sqrt{Q_0(z)} = \sqrt{e^{i(\theta+2\pi)}|Q_0(z)|} = e^{i(\theta/2+\pi)}\sqrt{|Q_0(z)|} = -e^{i\theta/2}\sqrt{|Q_0(z)|}. \tag{2.2.15}$$

Using this property, the WKB solutions can be regarded as not two independent solutions but one solution that is a two-valued function by the sign indefiniteness on Σ. As the zeros

of $Q_0(z)$ be branch points and taking the branch cuts on Σ, we can define a double covering $\hat{\Sigma}$. On $\hat{\Sigma}$, the leading term $S_0(z) = \sqrt{Q_0(z)}$ and the WKB solutions are single-valued functions. If the coordinate z cross a branch cut of $\hat{\Sigma}$, the sign of $\pm\sqrt{Q_0(z)}$ is reversed and the WKB solutions are also changed $\psi_a^{\pm}(z) \to \psi_a^{\mp}(z)$.

$\hat{\Sigma}$ can also be constructed by using the following algebraic curve,

$$y^2 = Q_0(x), \tag{2.2.16}$$

where (x, y) are real coordinates. It has been shown that the set of the complex numbers $w = x + iy$ where (x, y) satisfy the relation (2.2.16) has an isomorphism to $\hat{\Sigma}$. For this reason, we refer to $\hat{\Sigma}$ as WKB curve.

Along a closed curve γ on $\hat{\Sigma}$ that cannot shrink to a point, we define the integral of $S_{\text{even}}(z)$ as follows,

$$\Pi_\gamma := \oint_\gamma S_{\text{even}}(z)dz. \tag{2.2.17}$$

We refer to (2.2.17) as WKB period. γ is an element in 1-dimensional homology group $H_1(\hat{\Sigma})$ and the WKB periods are the periods of the one-form $S_{\text{even}}(z)dz$ on $\hat{\Sigma}$. The WKB periods are even power series in η^{-1} as $S_{\text{even}}(z)$,

$$\Pi_\gamma = \sum_{n=0}^{\infty} \Pi_\gamma^{(2n)} \eta^{-2n}, \quad \Pi_\gamma^{(2n)} = \oint_\gamma S_{2n}(z)dz. \tag{2.2.18}$$

If one finds the following relation,

$$S_{2n}(z) = \mathcal{O}_{2n} S_0(z) + \frac{d}{dz}(\cdots), \tag{2.2.19}$$

where $\mathcal{O}_{2n}$ is a differential operator with respect to the parameters in $Q_0(z)$ and $Q_2(z)$ and $\frac{d}{dz}(\cdots)$ is a total derivative, then the higher order coefficient of the WKB period $\Pi_\gamma^{(2n)}$ can be computed from the leading order coefficient $\Pi_\gamma^{(0)}$ as follows,

$$\Pi_\gamma^{(2n)} = \mathcal{O}_{2n} \Pi_\gamma^{(0)}, \tag{2.2.20}$$

because the WKB period is the integral on the closed curve with respect to z. This method is called the differential operator method (e.g. [44–46]).

2.2.2 Borel resummation

The WKB solutions and the WKB periods are asymptotic series which only converge at $\eta = \infty$. They can be promoted to analytic functions by the Borel resummation, which is defined as follows: Let us consider a general asymptotic series,

$$f = e^{-\eta A} \sum_{n=0}^{\infty} a_n \eta^{-(n+\alpha)}, \quad (\alpha \notin \{-1, -2, -3, \cdots\}), \tag{2.2.21}$$

where A is complex and $e^{-\eta A}$ is the factor that cannot be expressed as the power series in η^{-1}. The Borel transformation of f is defined by,

$$\hat{f}(\xi) = \sum_{n=0}^{\infty} \frac{a_n}{\Gamma(n+\alpha)} (\xi - A)^{n+\alpha-1}. \tag{2.2.22}$$

If $a_n \sim \mathcal{O}(n!)$, $\hat{f}(\xi)$ defines a power series around A with finite convergence of radius. If the Borel transformation $\hat{f}(\xi)$ converges near $\xi = A$ and can be analytically continued to the complex ξ-plane, and satisfies

$$|\hat{f}(\xi)| \leq C_1 e^{C_2|\xi|}, \tag{2.2.23}$$

with positive constants C_1 and C_2, f is said to be Borel summable (definition 2.10 of [25]). If f is Borel summable, the Borel resummation of f for the direction $\varphi = \arg(\eta)$ is defined as the following integral of the Borel transformation,

$$\mathcal{B}_\varphi[f] = \int_A^{\infty e^{-i\varphi}} e^{-\eta\xi} \hat{f}(\xi)\, d\xi, \tag{2.2.24}$$

where $\infty e^{-i\varphi}$ indicates that the path of the integral in (2.2.24) is taken along the half line $\{\xi = A + re^{-i\varphi} | r \geq 0\}$ (e.g. Fig.2.2). Due to (2.2.23), the Borel resummaton converges and gives an analytic function of η. If we take $\eta \to \infty$, the integrand $e^{-\eta\xi}\hat{f}(\xi)$ is suppressed at large ξ by the factor $e^{-\eta\xi}$. Then the Borel resummation can be approximated by

$$\mathcal{B}_0[f] = \int_A^{\infty} e^{-\eta\xi} \left[\sum_{n=0}^{\infty} \frac{a_n}{\Gamma(n+\alpha)} (\xi - A)^{n+\alpha-1} \right] d\xi. \tag{2.2.25}$$

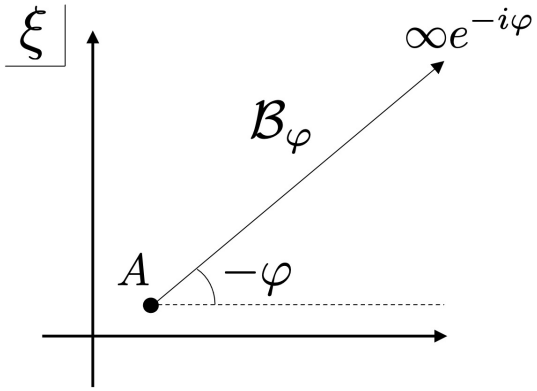

Figure 2.2: An integration contour of the Borel resummation.

Formally exchanging the integral and the sum, we obtain

$$\mathcal{B}_0[f] = \sum_{n=0}^{\infty} a_n \int_A^{\infty} \frac{e^{-\eta\xi}}{\Gamma(n+\alpha)} (\xi - A)^{n+\alpha-1} d\xi = e^{-\eta A} \sum_{n=0}^{\infty} a_n \eta^{-(n+\alpha)} = f. \tag{2.2.26}$$

Therefore the Borel resummation has f as the asymptotic expansion at $\eta \to \infty$.

For any Borel summable series f, g, the Borel resummation commutes with addition and multiplication (proposition 2.11 of [25]),

$$\begin{aligned} \mathcal{B}_\varphi[f+g] &= \mathcal{B}_\varphi[f] + \mathcal{B}_\varphi[g], \\ \mathcal{B}_\varphi[fg] &= \mathcal{B}_\varphi[f]\,\mathcal{B}_\varphi[g]. \end{aligned} \tag{2.2.27}$$

The Borel transformation $\hat{f}(\xi)$ of f may have singularities and branch cuts on the complex ξ-plane. If there are the singularities and the branch cuts on the integration contour of (2.2.24), we have to deform the integral contour so that it avoids the singularities and the branch cuts. In the Exact WKB analysis, we take the integration contours which avoid the singularities and the branch cuts left or right (Fig.2.3),

$$\mathcal{B}_{\varphi\pm}[f] = \lim_{\varepsilon \to 0} \mathcal{B}_{\varphi\pm\varepsilon}[f]. \tag{2.2.28}$$

(2.2.28) is called lateral Borel resummations. The lateral Borel resummations provide different analytic functions, but they have same asymptotic expansion f at $\eta \to \infty$.

$\mathcal{B}_{\varphi\pm}$ can be seen as operators acting on the asymptotic series. The lateral Borel resummations map an asymptotic series to different analytic functions. Then we can define the

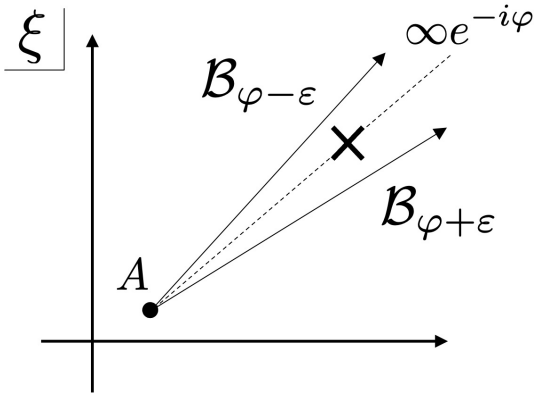

Figure 2.3: Integration contours of the lateral Borel resummations. The cross indicates a singularity.

automorphism $\mathfrak{S}_\varphi$ mapping an asymptotic series to another so that

$$\mathcal{B}_{\varphi-} = \mathcal{B}_{\varphi+} \circ \mathfrak{S}_\varphi. \tag{2.2.29}$$

$\mathfrak{S}_\varphi$ is called the Stokes automorphism. If two Borel summable series f and g satisfy $\mathfrak{S}_\varphi[f] = g$, then $\mathcal{B}_{\varphi-}[f] = \mathcal{B}_{\varphi+}[g]$, which indicates the different series f and g are mapped to a same analytic function by the lateral Borel resummations. By using the Stokes automorphism, we define a resummation $\mathcal{B}_{\varphi,\mathrm{med}}$ as follows,

$$\mathcal{B}_{\varphi,\mathrm{med}} := \mathcal{B}_{\varphi-} \circ \mathfrak{S}_\varphi^{-1/2} = \mathcal{B}_{\varphi+} \circ \mathfrak{S}_\varphi^{1/2}, \tag{2.2.30}$$

where $\mathfrak{S}_\varphi^{\pm 1/2}$ is defined as the formal Taylor series expanded at $\mathfrak{S}_\varphi = 1$,

$$\begin{aligned}
\mathfrak{S}_\varphi^{1/2} &= \sum_{n=0}^{\infty} \binom{\frac{1}{2}}{n} (\mathfrak{S}_\varphi - 1)^n = 1 + \frac{1}{2}(\mathfrak{S}_\varphi - 1) - \frac{1}{8}(\mathfrak{S}_\varphi - 1)^2 + \cdots, \\
\mathfrak{S}_\varphi^{-1/2} &= \sum_{n=0}^{\infty} \binom{-\frac{1}{2}}{n} (\mathfrak{S}_\varphi - 1)^n = 1 - \frac{1}{2}(\mathfrak{S}_\varphi - 1) + \frac{3}{8}(\mathfrak{S}_\varphi - 1)^2 + \cdots.
\end{aligned} \tag{2.2.31}$$

$\mathcal{B}_{\varphi,\mathrm{med}}$ is called median resummation. If we approximate (2.2.31) by first two term, then the median resummation becomes

$$\mathcal{B}_{\varphi,\mathrm{med}} \sim \mathcal{B}_{\varphi+} \circ \left[1 + \frac{1}{2}(\mathfrak{S}_\varphi - 1)\right] = \frac{1}{2}\left(\mathcal{B}_{\varphi+} + \mathcal{B}_{\varphi-}\right), \tag{2.2.32}$$

where we have used (2.2.29). (2.2.32) indicates that the median resummation can be seen

like the average of the lateral Borel resummations.

Borel summability of the WKB solutions

In this thesis, we impose the following assumptions (Assumption 2.3. of [26]):

Let ϕ be $Q_0(z)$ times the square of the infinitesimal interval dz,

$$\phi = Q_0(z)dzdz. \tag{2.2.33}$$

The square root of ϕ is $\sqrt{Q_0(z)}dz$, which appears in the exponential factor of the WKB solutions (2.2.13). $dzdz$ is the tensor product $dz \otimes dz$ and ϕ is a meromorphic quadratic differential on Σ locally given by (2.2.33). For ϕ, we assume,

- ϕ has at least one zero and one pole.
- All zeros of ϕ are simple (that is, the order of the zeros of ϕ is one).
- If a point $p \in \Sigma$ is a pole of $Q_2(z)$, then p is a pole of ϕ.
- If a point $s \in \Sigma$ is a simple pole of ϕ, then $Q_2(z)$ has a pole of order at most 2 at s.
- If a point $p \in \Sigma$ is a double pole of ϕ, and z be a local coordinate around p satisfying $z(p) = 0$, then $Q_2(z)$ has the following asymptotic behavior,

$$Q_2(z) = -\frac{1}{4z^2}(1 + \mathcal{O}(z)) \text{ as } z \to 0. \tag{2.2.34}$$

- If a point $p \in \Sigma$ is a pole of ϕ of order $m \geq 3$, then $Q_2(z)$ has may has a pole at p satisfying

$$(\text{pole order of } Q_2(z) \text{ at } p) < 1 + \frac{m}{2}. \tag{2.2.35}$$

Under the above assumption, the WKB solutions are Borel summable [25, 26].

2.2.3 Stokes graph

The Borel resummation of the WKB solutions $\mathcal{B}_\varphi\left[\psi^{\pm}_{z_a}\right](z)$ is local solutions at z on Σ. To obtain the solutions in the whole of Σ, we need to analytically continue the Borel resummation of the WKB solutions. The global structure of the Borel resummation of the WKB

solutions is determined by the Stokes lines, which are defined by the following equation,

$$\Im\left[e^{i\varphi}\int_{z_*}^{z} S_0\left(z'\right)dz'\right] = 0, \tag{2.2.36}$$

where z_* is a zero or a simple pole of the quadratic differential ϕ (2.2.33). The endpoints of the stokes lines are connected to the zeros or the poles of ϕ. In particular, the Stokes line both endpoints of which are connected to the zeros or the simple pole is called Stokes segment. The Stokes lines can be assigned the orientation defined by the following conditions,

$$\begin{cases} \Re\left[e^{i\varphi}\int_{z_*}^{z} S_0\left(z'\right)dz'\right] > 0 \rightarrow \text{positive orientation}, \\ \Re\left[e^{i\varphi}\int_{z_*}^{z} S_0\left(z'\right)dz'\right] < 0 \rightarrow \text{negative orientation}. \end{cases} \tag{2.2.37}$$

The graph on the WKB curve $\hat{\Sigma}$ depicted by the Stokes lines is called Stokes graph. The Stokes graph splits $\hat{\Sigma}$ into some regions, which can be mapped into a triangulation of $\hat{\Sigma}$ [25, 70]. Each region divided by the Stokes graph is called Stokes region.

The Stokes lines are steepest descent lines of the WKB solutions. Along a Stokes line emanating from z_*, the WKB solutions normalized at z_* don't oscillate because the exponential factor of the solutions (2.2.13) is always real by (2.2.36). If the Stokes line has the positive orientation, the minus signed WKB solution decays along the Stokes line asymptotically. On the other hand, if the Stokes line has the negative orientation, the plus signed WKB solution decays along the Stokes line.

Connection formula for the WKB solutions

The Borel resummation of the WKB solutions is analytic in each Stokes region. If the path of the analytic continuation crosses any stokes line, then the form of the solutions is changed. From the point of view of the ordinary WKB method, this is the Stokes phenomenon of the WKB solutions.

Let us consider the connection around a simple zero and a simple pole of ϕ. First, the Stokes graphs around a simple zero z_* is shown in Fig.2.4, where the black lines are the Stokes lines, the orange points are the simple zero z_*, the dashed red lines are the branch cuts, the arrow on each Stokes line indicates the orientation of them (for the negative orientation, the arrow points to the simple zero along the Stokes line, and for the positive orientation, the arrow points to the opposite of the simple zero) and I_1 and I_2 are the Stokes regions. There are two possible assignment of the orientation of the Stokes lines around a

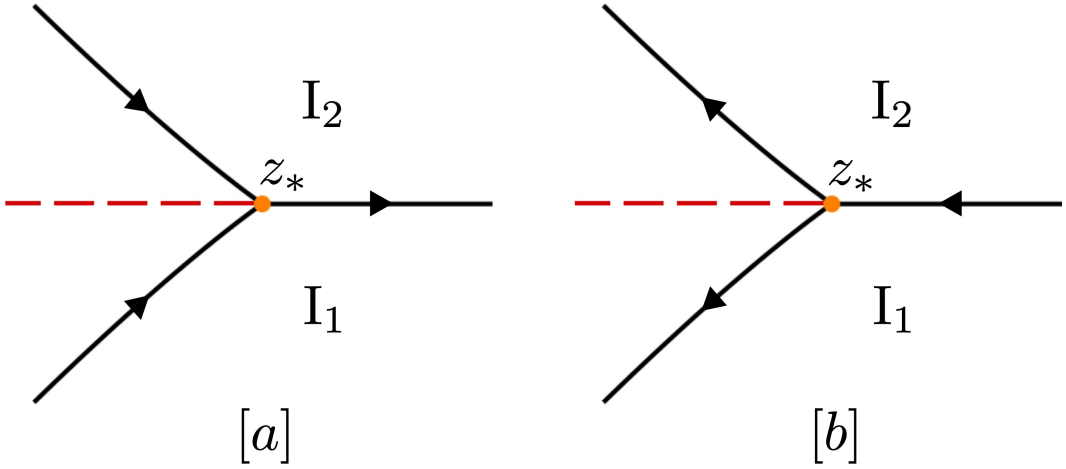

Figure 2.4: The Stokes graphs around a simple zero.

simple zero. As Fig.2.4, exactly three Stokes lines emanate from a simple zero.

Assume that the Stokes graph has no Stokes segments for a direction $\arg(\eta) = \varphi$, the Borel resummation of the WKB solutions in the region I_1 and I_2 are shown to be analytically connected as follows [21, 23, 25],

- For $[a]$ in Fig.2.4,

$$\begin{pmatrix} \mathcal{B}_\varphi\left[\psi^+_{z_*,\mathrm{I}_1}\right](z) \\ \mathcal{B}_\varphi\left[\psi^-_{z_*,\mathrm{I}_1}\right](z) \end{pmatrix} = \begin{pmatrix} 1 & i \\ 0 & 1 \end{pmatrix} \begin{pmatrix} \mathcal{B}_\varphi\left[\psi^+_{z_*,\mathrm{I}_2}\right](z) \\ \mathcal{B}_\varphi\left[\psi^-_{z_*,\mathrm{I}_2}\right](z) \end{pmatrix}, \tag{2.2.38}$$

- For $[b]$ in Fig.2.4,

$$\begin{pmatrix} \mathcal{B}_\varphi\left[\psi^+_{z_*,\mathrm{I}_1}\right](z) \\ \mathcal{B}_\varphi\left[\psi^-_{z_*,\mathrm{I}_1}\right](z) \end{pmatrix} = \begin{pmatrix} 1 & 0 \\ i & 1 \end{pmatrix} \begin{pmatrix} \mathcal{B}_\varphi\left[\psi^+_{z_*,\mathrm{I}_2}\right](z) \\ \mathcal{B}_\varphi\left[\psi^-_{z_*,\mathrm{I}_2}\right](z) \end{pmatrix}, \tag{2.2.39}$$

where we have denoted the WKB solutions in the region I_1 as $\psi^\pm_{z_*,\mathrm{I}_1}$, and in the region I_2 as $\psi^\pm_{z_*,\mathrm{I}_2}$. These formulae are the exact extension on the complex plane of the connection formula for the WKB approximation considered in Sec.2.1.

Next, the Stokes graphs around a simple zero z_* is shown in Fig.2.5, where the black lines are the Stokes lines, the green points are the simple pole z_*, the dashed red lines are the branch cuts, the arrow on each Stokes line indicates the orientation of them (for the negative orientation, the arrow points to the simple pole along the Stokes line, and for the positive orientation, the arrow points to the opposite of the simple pole) and I_1 and I_2 are the

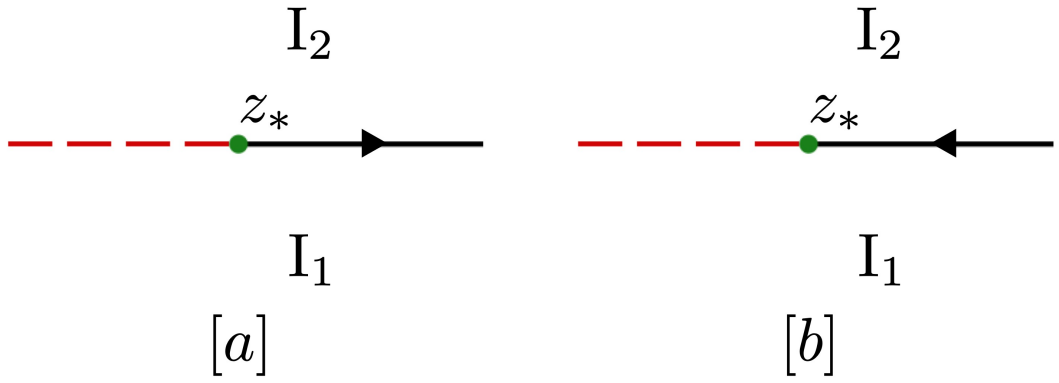

Figure 2.5: The Stokes graphs around a simple pole.

Stokes regions. As Fig.2.5, only one Stokes line emanates from a simple pole. Assume that the Stokes graph has no Stokes segments for a direction $\arg(\eta) = \varphi$, the Borel resummation of the WKB solutions in the region I_1 and I_2 are shown to be analytically connected as follows [26],

- For $[a]$ in Fig.2.5,

$$\begin{pmatrix} \mathcal{B}_\varphi\left[\psi^+_{z_*,\mathrm{I}_1}\right](z) \\ \mathcal{B}_\varphi\left[\psi^-_{z_*,\mathrm{I}_1}\right](z) \end{pmatrix} = \begin{pmatrix} 1 & i(t+t^{-1}) \\ 0 & 1 \end{pmatrix} \begin{pmatrix} \mathcal{B}_\varphi\left[\psi^+_{z_*,\mathrm{I}_2}\right](z) \\ \mathcal{B}_\varphi\left[\psi^-_{z_*,\mathrm{I}_2}\right](z) \end{pmatrix}, \tag{2.2.40}$$

- For $[b]$ in Fig.2.5,

$$\begin{pmatrix} \mathcal{B}_\varphi\left[\psi^+_{z_*,\mathrm{I}_1}\right](z) \\ \mathcal{B}_\varphi\left[\psi^-_{z_*,\mathrm{I}_1}\right](z) \end{pmatrix} = \begin{pmatrix} 1 & 0 \\ i(t+t^{-1}) & 1 \end{pmatrix} \begin{pmatrix} \mathcal{B}_\varphi\left[\psi^+_{z_*,\mathrm{I}_2}\right](z) \\ \mathcal{B}_\varphi\left[\psi^-_{z_*,\mathrm{I}_2}\right](z) \end{pmatrix}, \tag{2.2.41}$$

where

$$t = \exp\left(i\pi\sqrt{1+4b}\right), \quad b = \lim_{z\to z_*}\left((z-z_*)^2 Q_2(z)\right). \tag{2.2.42}$$

Discontinuity formula for the WKB periods

The Stokes graph also determine the discontinuity of the WKB periods. Rotating $\arg(\eta)$, Stokes segments often appear in the Stokes graphs at some direction. If Stokes segments appear at $\arg(\eta) = \varphi$, then the Borel transformation of a WKB period Π_γ whose one-cycle γ intersects with any Stokes segment has singularities on the complex ξ-plane in the direction $\arg(\xi) = -\varphi$. As rotating $\arg(\eta)$, the integration contour of the Borel resummation

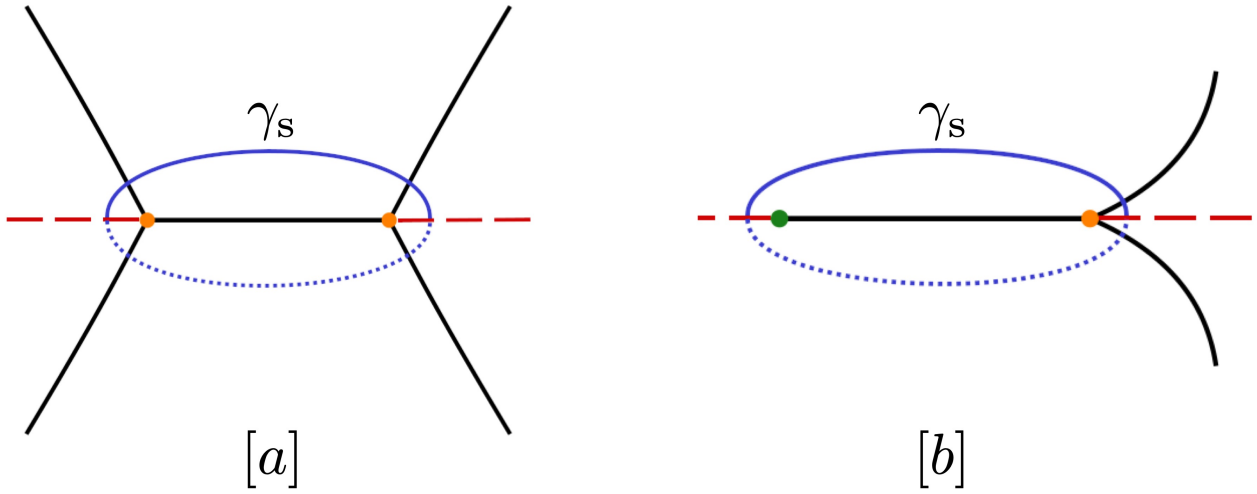

Figure 2.6: The Stokes segments in the presence of [a] the simple zero and [b] the simple pole. The orange points are the simple zeros and the green point is the simple pole. γ_s is the one-cycle on the WKB curve $\hat{\Sigma}$ encircling the Stokes segments. The dashed segment in each cycle lies on the other sheet of $\hat{\Sigma}$.

for Π_γ collides with the singularities on the complex ξ-plane at $\arg(\eta) = \varphi$. To ensure the analyticity in η of the Borel resummation, we must take the contributions from the integration contours encircling the singularities into account. These new integration contours cause the discontinuity of the WKB periods.

Fig.2.6 shows examples of the Stokes segment in the presence of the simple zeros and the simple pole. γ_s in Fig.2.6 is the one-cycle on the WKB curve $\hat{\Sigma}$ encircling the Stokes segments. We take the orientation of γ_s so that

$$\Pi^{(0)}_{\gamma_s} = \oint_{\gamma_s} S_0(z)dz < 0. \tag{2.2.43}$$

Assume that the Stokes graph for a direction $\arg(\eta) = \varphi$ has a unique Stokes segment of $[a]$ in Fig.2.6, it is showed that any WKB period Π_γ satisfies the following equation [23, 25],

$$e^{\eta\mathcal{B}_{\varphi-}[\Pi_\gamma]} = e^{\eta\mathcal{B}_{\varphi+}[\Pi_\gamma]} \left(1 + e^{\eta\mathcal{B}_{\varphi+}[\Pi_{\gamma_s}]}\right)^{-(\gamma_s,\gamma)}, \tag{2.2.44}$$

where (γ_s, γ) is the intersection number normalized as $(x\text{−axis}, y\text{−axis}) = +1$. This is called the Delabaere-Pham formula. The term $e^{\eta\mathcal{B}_{\varphi+}[\Pi_{\gamma_s}]}$ in r.h.s. of (2.2.44) is the contribution from the singularity of the Borel transformation of Π_γ. (2.2.44) can also be expressed by

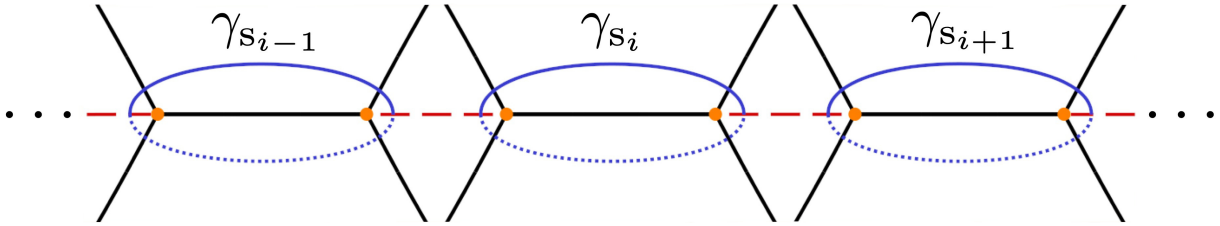

Figure 2.7: The Stokes graph with multiple Stokes segments connecting the simple zeros.

using the Stokes automorphism as follows,

$$\mathfrak{S}_{\varphi}\left[e^{\eta\Pi_{\gamma}}\right] = e^{\eta\Pi_{\gamma}}\left(1+e^{\eta\Pi_{\gamma_{\mathrm{s}}}}\right)^{-(\gamma_{\mathrm{s}},\gamma)}. \tag{2.2.45}$$

In particular, for γ_{s} itself, $(\gamma_{\mathrm{s}},\gamma_{\mathrm{s}})=0$ and (2.2.44) leads $e^{\eta\mathcal{B}_{\varphi-}[\Pi_{\gamma_{\mathrm{s}}}]} = e^{\eta\mathcal{B}_{\varphi+}[\Pi_{\gamma_{\mathrm{s}}}]} = e^{\eta\mathcal{B}_{\varphi}[\Pi_{\gamma_{\mathrm{s}}}]}$. Therefore (2.2.44) can also be express as,

$$e^{\eta\mathcal{B}_{\varphi-}[\Pi_{\gamma}]} = e^{\eta\mathcal{B}_{\varphi+}[\Pi_{\gamma}]}\left(1+e^{\eta\mathcal{B}_{\varphi}[\Pi_{\gamma_{\mathrm{s}}}]}\right)^{-(\gamma_{\mathrm{s}},\gamma)}. \tag{2.2.46}$$

Similarly, assume that the Stokes graph for a direction $\arg(\eta)=\varphi$ has a unique Stokes segment of $[b]$ in Fig.2.6, it is showed that any WKB period Π_{γ} satisfies the following equation [26],

$$e^{\eta\mathcal{B}_{\varphi-}[\Pi_{\gamma}]} = e^{\eta\mathcal{B}_{\varphi+}[\Pi_{\gamma}]}\left(1+\left(t+t^{-1}\right)e^{\eta\mathcal{B}_{\varphi+}[\Pi_{\gamma_{\mathrm{s}}}]}+e^{2\eta\mathcal{B}_{\varphi+}[\Pi_{\gamma_{\mathrm{s}}}]}\right)^{-(\gamma_{\mathrm{s}},\gamma)}, \tag{2.2.47}$$

where t is defined in (2.2.42). (2.2.47) can also be expressed by using the Stokes automorphism as follows,

$$\mathfrak{S}_{\varphi}\left[e^{\eta\Pi_{\gamma}}\right] = e^{\eta\Pi_{\gamma}}\left(1+\left(t+t^{-1}\right)e^{\eta\Pi_{\gamma_{\mathrm{s}}}}+e^{2\eta\Pi_{\gamma_{\mathrm{s}}}}\right)^{-(\gamma_{\mathrm{s}},\gamma)}. \tag{2.2.48}$$

In particular, for γ_{s} itself, $(\gamma_{\mathrm{s}},\gamma_{\mathrm{s}})=0$ and (2.2.47) leads $e^{\eta\mathcal{B}_{\varphi-}[\Pi_{\gamma_{\mathrm{s}}}]} = e^{\eta\mathcal{B}_{\varphi+}[\Pi_{\gamma_{\mathrm{s}}}]} = e^{\eta\mathcal{B}_{\varphi}[\Pi_{\gamma_{\mathrm{s}}}]}$. Therefore (2.2.47) can also be express as,

$$e^{\eta\mathcal{B}_{\varphi-}[\Pi_{\gamma}]} = e^{\eta\mathcal{B}_{\varphi+}[\Pi_{\gamma}]}\left(1+\left(t+t^{-1}\right)e^{\eta\mathcal{B}_{\varphi}[\Pi_{\gamma_{\mathrm{s}}}]}+e^{2\eta\mathcal{B}_{\varphi}[\Pi_{\gamma_{\mathrm{s}}}]}\right)^{-(\gamma_{\mathrm{s}},\gamma)}. \tag{2.2.49}$$

The discontinuity formulae (2.2.44)$\sim$(2.2.49) can be generalized for the presence of more than one Stokes segment. For example, for the Stokes graph having n Stokes segments for the simple zeros as Fig.2.7, then any WKB period Π_{γ} satisfies the following Delabaere-Phan

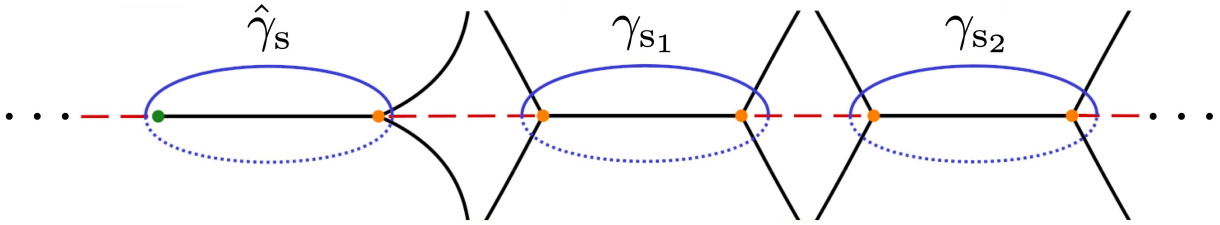

Figure 2.8: The Stokes graph with multiple Stokes segments connecting the simple zeros and a Stokes segment for the simple pole.

formula [23, 28],

$$e^{\eta\mathcal{B}_{\varphi-}[\Pi_\gamma]} = e^{\eta\mathcal{B}_{\varphi+}[\Pi_\gamma]} \prod_i^n \left(1 + e^{\eta\mathcal{B}_\varphi[\Pi_{\gamma_{\mathrm{s}_i}}]}\right)^{-\left(\gamma_{\mathrm{s}_i},\gamma\right)}. \tag{2.2.50}$$

If there is also a Stokes segment for the simple pole as Fig.2.8, the formula (2.2.50) is generalized as follows,

$$e^{\eta\mathcal{B}_{\varphi-}[\Pi_\gamma]} = e^{\eta\mathcal{B}_{\varphi+}[\Pi_\gamma]} \left(1 + \left(t + t^{-1}\right) e^{\eta\mathcal{B}_\varphi[\Pi_{\hat{\gamma}_{\mathrm{s}}}]} + e^{2\eta\mathcal{B}_\varphi[\Pi_{\hat{\gamma}_{\mathrm{s}}}]}\right)^{-(\hat{\gamma}_{\mathrm{s}},\gamma)} \prod_i^n \left(1 + e^{\eta\mathcal{B}_\varphi[\Pi_{\gamma_{\mathrm{s}_i}}]}\right)^{-\left(\gamma_{\mathrm{s}_i},\gamma\right)}. \tag{2.2.51}$$

Summary

In this chapter, we have considered the complex one-dimensional second order differential equation of the Schrödinger type having a complex parameter η. The WKB method provides the WKB solutions, which are asymptotic series in η^{-1}. The WKB solutions are promoted to exact solutions by applying the Borel resummation. The global structure of the Borel resummed WKB solutions are determined by the Stokes graph. Based on the Stokes graphs, we have explained the connection formula for the Borel resummed WKB solutions. We have also introduced the WKB periods, which are even power series in η^{-1}. The Borel resummed WKB periods have the discontinuity and it is captured by the Delabaere-Pham formula.

Chapter 3

Energy quantization conditions in quantum mechanics

The Exact WKB analysis provides an exact approach to study the spectral problem. In this chapter, we review the application of the Exact WKB analysis to study the exact energy quantization conditions in quantum mechanics. We solve the spectral problem for the bound state of the harmonic oscillator and the double-well potential as concrete examples. The Exact WKB analysis gives exact energy quantization conditions, which are expressed by the Borel resummed WKB periods. This review chapter is mainly based on [27, 29].

3.1 Harmonic oscillator

Let us consider the following differential equation on the Riemann sphere $\mathbb{C}^* = \mathbb{C} \cup \{\infty\}$,

$$\left[\frac{d^2}{dz^2} - \eta^2 Q_0(z)\right] \psi(z) = 0, \tag{3.1.1}$$

with

$$Q_0(z) = V(z) - E = z^2 - E. \tag{3.1.2}$$

For $\arg(\eta) = 0$ and under the identification $\eta = 1/\hbar$ (the reduced Planck constant), the differential equation (3.1.1) on the real-z axis agrees with the stationary Schrödinger equation for the one-dimensional harmonic oscillator.

We solve the eigenvalue problem of (3.1.1) for $\arg(\eta) = 0$ and $E > 0$ case, i.e. the bound state in quantum mechanics. The Stokes graph for $\arg(\eta) = 0$ and $E > 0$ is drawn in Fig.3.1. For $E > 0$, the simple zeros $z_1 = -\sqrt{E}$, $z_2 = \sqrt{E}$ are real. First, we solve the

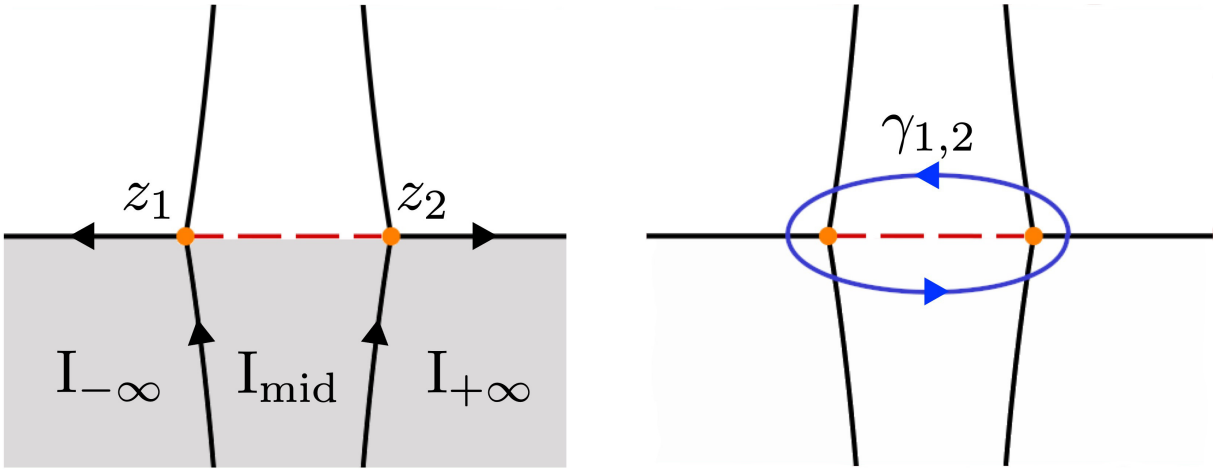

Figure 3.1: The Stokes graph for the harmonic oscillator with $\arg(\eta) = 0$ and $E > 0$. The sheet of the WKB curve is taken so that $S_{\mathrm{even}}(z)dz$ has the positive sign. The orange points $z_1 = -\sqrt{E}$, $z_2 = \sqrt{E}$ are the simple zeros and $\gamma_{1,2}$ is the one-cycle encircling them. The gray regions named $\mathrm{I}_{+\infty}$, $\mathrm{I}_{\mathrm{mid}}$, $\mathrm{I}_{-\infty}$ are the Stokes regions. The stokes lines going out of the frame flow at $z = \infty$.

connection problem of the Borel resummation of the WKB solutions from $\mathrm{I}_{+\infty}$ to $\mathrm{I}_{\mathrm{mid}}$ and $\mathrm{I}_{\mathrm{mid}}$ to $\mathrm{I}_{-\infty}$.

The regions $\mathrm{I}_{+\infty}$ and $\mathrm{I}_{\mathrm{mid}}$ are separated by the Stokes line emanating from the simple zero z_2 and having the negative orientation. Therefore the Borel resummation of the WKB solutions normalized at z_2 in each region are connected by the formula (2.2.39) as follows,

$$\begin{pmatrix} \mathcal{B}_0\left[\psi^{+}_{z_2,\mathrm{I}_{+\infty}}\right](z) \\ \mathcal{B}_0\left[\psi^{-}_{z_2,\mathrm{I}_{+\infty}}\right](z) \end{pmatrix} = \begin{pmatrix} 1 & 0 \\ -i & 1 \end{pmatrix} \begin{pmatrix} \mathcal{B}_0\left[\psi^{+}_{z_2,\mathrm{I}_{\mathrm{mid}}}\right](z) \\ \mathcal{B}_0\left[\psi^{-}_{z_2,\mathrm{I}_{\mathrm{mid}}}\right](z) \end{pmatrix}, \tag{3.1.3}$$

where we have used the inverse of (2.2.39). Next, the regions $\mathrm{I}_{\mathrm{mid}}$ and $\mathrm{I}_{-\infty}$ are separated by the Stokes line emanating from z_1 and having the negative orientation. In order to apply the connection formula (2.2.39), we have to change the normalization of the solutions in the

r.h.s. of (3.1.3) from z_2 to z_1. From the definition of the WKB solutions (2.2.12),

$$\begin{aligned}\mathcal{B}_0\left[\psi^{\pm}_{z_2,\mathrm{I_{mid}}}\right](z) &= \mathcal{B}_0\left[\frac{1}{\sqrt{S_{\mathrm{even}}(z)}}\exp\left[\pm\eta\int_{z_2}^{z}S_{\mathrm{even}}(z')dz'\right]\right]\\ &= \mathcal{B}_0\left[\frac{1}{\sqrt{S_{\mathrm{even}}(z)}}\exp\left[\pm\eta\left(\int_{z_2}^{z_1}S_{\mathrm{even}}(z')dz'+\int_{z_1}^{z}S_{\mathrm{even}}(z')dz'\right)\right]\right]\\ &= \exp\left[\pm\eta\mathcal{B}_0\left[\int_{z_2}^{z_1}S_{\mathrm{even}}(z')dz'\right]\right]\mathcal{B}_0\left[\frac{1}{\sqrt{S_{\mathrm{even}}(z)}}\exp\left[\pm\eta\int_{z_1}^{z}S_{\mathrm{even}}(z')dz'\right]\right].\end{aligned} \tag{3.1.4}$$

(3.1.4) can be written in the matrix form as,

$$\begin{pmatrix}\mathcal{B}_0\left[\psi^{+}_{z_2,\mathrm{I_{mid}}}\right](z)\\ \mathcal{B}_0\left[\psi^{-}_{z_2,\mathrm{I_{mid}}}\right](z)\end{pmatrix} = \begin{pmatrix}e^{-\eta\mathcal{B}_0\left[\int_{z_1}^{z_2}S_{\mathrm{even}}(z)dz\right]} & 0\\ 0 & e^{\eta\mathcal{B}_0\left[\int_{z_1}^{z_2}S_{\mathrm{even}}(z)dz\right]}\end{pmatrix}\begin{pmatrix}\mathcal{B}_0\left[\psi^{+}_{z_1,\mathrm{I_{mid}}}\right](z)\\ \mathcal{B}_0\left[\psi^{-}_{z_1,\mathrm{I_{mid}}}\right](z)\end{pmatrix}, \tag{3.1.5}$$

where we have reversed the contour of the integrals $\pm\int_{z_2}^{z_1}S_{\mathrm{even}}(z)dz = \mp\int_{z_1}^{z_2}S_{\mathrm{even}}(z)dz$. After changing the normalization, the solutions in $\mathrm{I_{mid}}$ and $\mathrm{I}_{-\infty}$ are connected by (2.2.39),

$$\begin{pmatrix}\mathcal{B}_0\left[\psi^{+}_{z_1,\mathrm{I_{mid}}}\right](z)\\ \mathcal{B}_0\left[\psi^{-}_{z_1,\mathrm{I_{mid}}}\right](z)\end{pmatrix} = \begin{pmatrix}1 & 0\\ -i & 1\end{pmatrix}\begin{pmatrix}\mathcal{B}_0\left[\psi^{+}_{z_1,\mathrm{I}_{-\infty}}\right](z)\\ \mathcal{B}_0\left[\psi^{-}_{z_1,\mathrm{I}_{-\infty}}\right](z)\end{pmatrix}. \tag{3.1.6}$$

By multiplying (3.1.3), (3.1.5) and (3.1.6) and finally restoring the normalization of the solutions in the r.h.s. of (3.1.6) from z_1 to z_2, we obtain the connection formula of the WKB solutions,

$$\begin{pmatrix}\mathcal{B}_0\left[\psi^{+}_{z_2,\mathrm{I}_{+\infty}}\right](z)\\ \mathcal{B}_0\left[\psi^{-}_{z_2,\mathrm{I}_{+\infty}}\right](z)\end{pmatrix} = \begin{pmatrix}1 & 0\\ -i\left(1+e^{\eta\mathcal{B}\left[2\int_{z_1}^{z_2}S_{\mathrm{even}}(z)dz\right]}\right) & 1\end{pmatrix}\begin{pmatrix}\mathcal{B}_0\left[\psi^{+}_{z_2,\mathrm{I}_{-\infty}}\right](z)\\ \mathcal{B}_0\left[\psi^{-}_{z_2,\mathrm{I}_{-\infty}}\right](z)\end{pmatrix}. \tag{3.1.7}$$

The integral $2\int_{z_1}^{z_2}S_{\mathrm{even}}(z)dz$ is equivalent to the WKB period for the one-cycle $\gamma_{1,2}$ in Fig.3.1. Therefore the connection formula (3.1.7) can be expressed by using the WKB period as follows,

$$\begin{pmatrix}\mathcal{B}_0\left[\psi^{+}_{z_2,\mathrm{I}_{+\infty}}\right](z)\\ \mathcal{B}_0\left[\psi^{-}_{z_2,\mathrm{I}_{+\infty}}\right](z)\end{pmatrix} = \begin{pmatrix}1 & 0\\ -i\left(1+e^{\eta\mathcal{B}_0\left[\Pi_{\gamma_{1,2}}\right]}\right) & 1\end{pmatrix}\begin{pmatrix}\mathcal{B}_0\left[\psi^{+}_{z_2,\mathrm{I}_{-\infty}}\right](z)\\ \mathcal{B}_0\left[\psi^{-}_{z_2,\mathrm{I}_{-\infty}}\right](z)\end{pmatrix}. \tag{3.1.8}$$

The energy eigenvalue for the bound state can be obtained by imposing the boundary

conditions that the solutions decay at $z \to \pm\infty$. As z goes to $+\infty$, the integral $\int_{z_2}^{z} S_0(z')dz'$ becomes large because the Stokes line lying on the $[z_2, +\infty)$ in Fig.3.1 has the positive orientation. Therefore the minus signed WKB solution $\psi^{-}_{z_2,\mathrm{I}_{+\infty}}(z)$ decays at $z \to +\infty$. According to the connection formula (3.1.8), the solution $\psi^{-}_{z_2,\mathrm{I}_{+\infty}}(z)$ is connected to $z \to -\infty$ as follows,

$$\mathcal{B}_0\left[\psi^{-}_{z_2,\mathrm{I}_{+\infty}}\right](z) = -i\left(1 + e^{\eta\mathcal{B}\left[\Pi_{\gamma_{1,2}}\right]}\right)\mathcal{B}_0\left[\psi^{+}_{z_2,\mathrm{I}_{-\infty}}\right](z) + \mathcal{B}_0\left[\psi^{-}_{z_2,\mathrm{I}_{-\infty}}\right](z). \tag{3.1.9}$$

The Stokes line lying on the $(-\infty, z_1]$ in Fig.3.1 has the positive orientation and the minus signed WKB solution $\psi^{-}_{z_2,\mathrm{I}_{-\infty}}(z)$ decays at $z \to -\infty$. Therefore to satisfy the boundary conditions, the coefficient of $\mathcal{B}_0\left[\psi^{+}_{z_2,\mathrm{I}_{-\infty}}\right](z)$ in (3.1.9) has to be zero,

$$1 + e^{\eta\mathcal{B}\left[\Pi_{\gamma_{1,2}}\right]} = 0. \tag{3.1.10}$$

Taking the logarithm of (3.1.10), we obtain

$$\mathcal{B}\left[\Pi_{\gamma_{1,2}}\right] = 2\pi i\eta^{-1}\left(n + \frac{1}{2}\right) \quad (n \in \mathbb{Z})\,. \tag{3.1.11}$$

This is the exact energy quantization condition for the harmonic oscillator. In the present case, the WKB period $\Pi_{\gamma_{1,2}}$ is equivalent to the residue at $z = \infty$ on the Riemann sphere,

$$\Pi_{\gamma_{1,2}} = \oint_{\gamma_{1,2}} S_{\mathrm{even}}(z)dz = 2\pi i\mathrm{Res}_{z=\infty}S_{\mathrm{even}}(z). \tag{3.1.12}$$

For the harmonic oscillator case, it has been shown that the higher order coefficient $S_n(z)$ $(n \geq 1)$ is holomorphic at $z = \infty$ (Proposition 2.8. in [25]). Therefore

$$\Pi_{\gamma_{1,2}} = -2\pi i\mathrm{Res}_{z=\infty}S_0(z) = \pi iE. \tag{3.1.13}$$

Substituting (3.1.13) into (3.1.11), we obtain the well-known result of the energy eigenvalue for the harmonic oscillator,

$$E = 2\eta^{-1}\left(n + \frac{1}{2}\right). \tag{3.1.14}$$

Because $E > 0$, n is restricted to $\mathbb{Z}_{\geq 0}$.

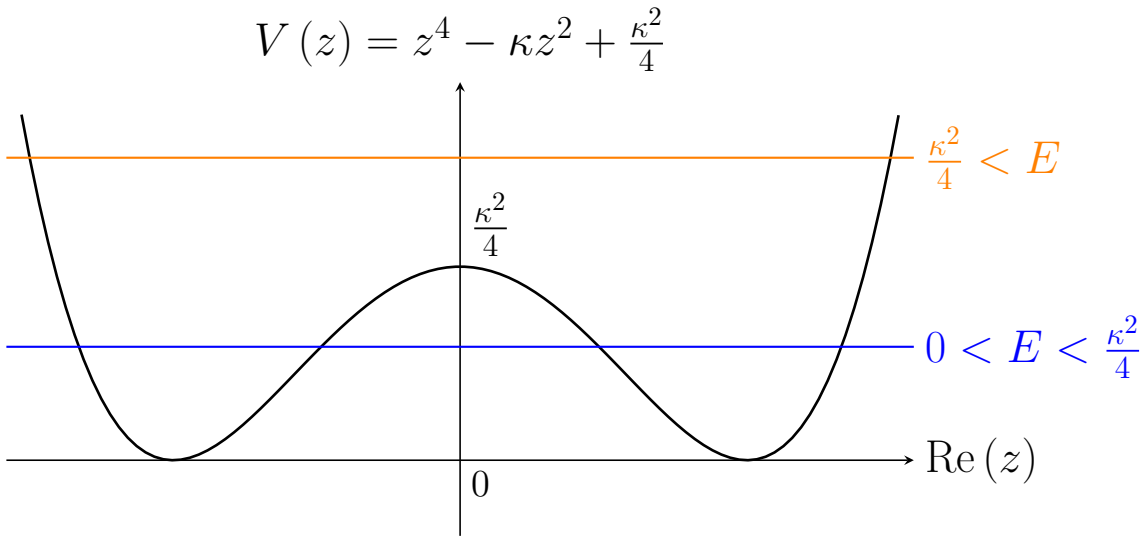

Figure 3.2: The potential $V(z)$ on the real z-axis.

3.2 Double-well potential

The second example is the following differential equation on the Riemann sphere $\mathbb{C}^* = \mathbb{C} \cup \{\infty\}$,

$$\left[\frac{d^2}{dz^2} - \eta^2 Q_0(z)\right] \psi(z) = 0, \tag{3.2.1}$$

with

$$Q_0(z) = V(z) - E = z^4 - \kappa z^2 + \frac{\kappa^2}{4} - E \quad (\kappa > 0). \tag{3.2.2}$$

For $\arg(\eta) = 0$ and under the identification $\eta = 1/\hbar$, the differential equation (3.2.1) on the real-z axis agrees with the one-dimensional stationary Schrödinger equation with the double-well potential $V(z) = z^4 - \kappa z^2 + \frac{\kappa^2}{4}$ and the energy E.

We solve the eigenvalue problem of (3.2.1) for $\arg(\eta) = 0$ and $E > 0$ case. The potential $V(z)$ on the real-z axis is shown in Fig.3.2. There are two bound state $0 < E < \frac{\kappa^2}{4}$ (below the potential barrier) and $\frac{\kappa^2}{4} < E$ (above the potential barrier).

3.2.1 Below the potential barrier

Fig.3.3 shows the Stokes graph for $0 < E < \frac{\kappa^2}{4}$. The simple zeros $z_1 = -\sqrt{\sqrt{E} + \frac{\kappa}{2}}$, $z_2 = -\sqrt{-\sqrt{E} + \frac{\kappa}{2}}$, $z_3 = \sqrt{-\sqrt{E} + \frac{\kappa}{2}}$, $z_4 = \sqrt{\sqrt{E} + \frac{\kappa}{2}}$ are real. The intervals $[z_1, z_2]$ and $[z_3, z_4]$ are the classically allowed intervals in the potential graph Fig.3.2, and $[z_2, z_3]$ is the classically forbidden interval by the potential barrier. There is the Stokes segment on

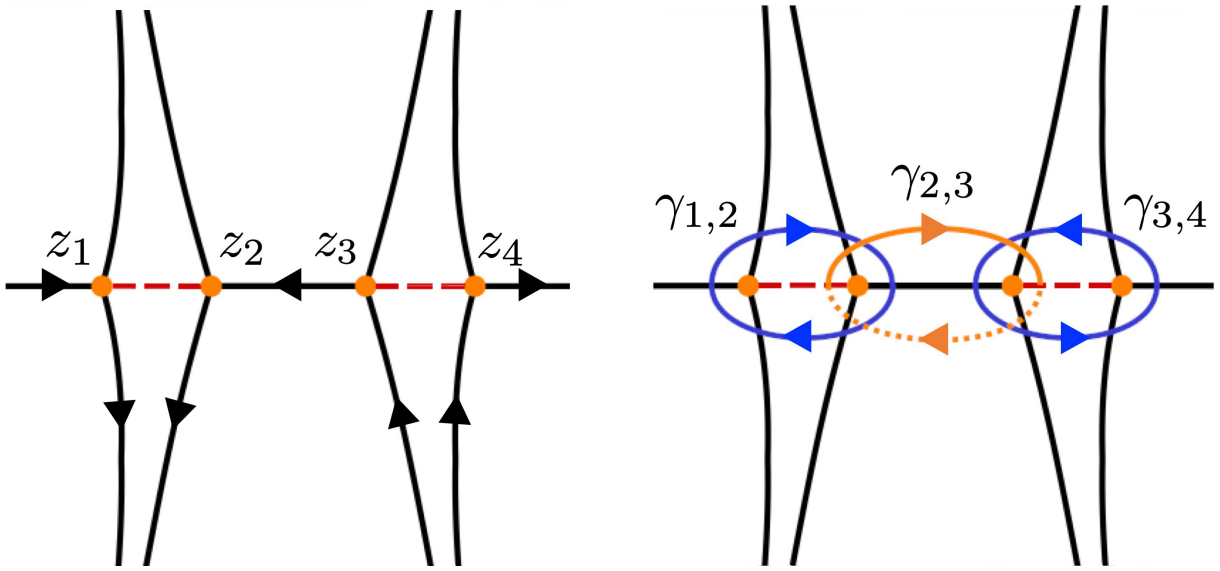

Figure 3.3: The Stokes graph for the double-well potential with $\arg(\eta) = 0$ and $0 < E < \frac{\kappa^2}{4}$. The sheet of the WKB curve is taken so that $S_{\rm even}(z)dz$ has the positive sign. The orange points $z_1 = -\sqrt{\sqrt{E} + \frac{\kappa}{2}}$, $z_2 = -\sqrt{-\sqrt{E} + \frac{\kappa}{2}}$, $z_3 = \sqrt{-\sqrt{E} + \frac{\kappa}{2}}$, $z_4 = \sqrt{\sqrt{E} + \frac{\kappa}{2}}$ are the simple zeros and $\gamma_{1,2}, \gamma_{2,3}, \gamma_{3,4}$ are the one-cycles. The stokes lines going out of the frame flow at $z = \infty$. The arrow on the Stokes segment on $[z_2, z_3]$ indicates $\int_{z_2}^{z_3} S_0(z)dz < 0$.

$[z_2, z_3]$ and therefore we cannot use the formulae (2.2.38), (2.2.39) for $\arg(\eta) = 0$ because the formulae (2.2.38), (2.2.39) are assumed that there are no Stokes segments in the Stokes graph. We instead compute the lateral Borel resummation (2.2.28) as the exact energy quantization for $\arg(\eta) = 0$.

The lateral Borel resummation can be obtained by solving the connection problems for $\arg(\eta) = \pm\varepsilon$ ($\varepsilon \ll 1$). The Stokes graph for $\arg(\eta) = \pm\varepsilon$ is given in Fig.3.4. In Fig.3.4, the Stokes segment on $[z_2, z_3]$ in Fig.3.3 is separated and the new Stokes regions appear (the region I_3 for $[a]$ in Fig.3.4 and the region I_2 for $[b]$). The Stokes graph is then discontinuously changed between $\arg(\eta) > -\varepsilon$, $\arg(\eta) = 0$ and $\arg(\eta) < +\varepsilon$ cases. This phenomenon is called the saddle reduction of the Stokes graph [25]. First, we compute the connection formula for $\arg(\eta) = -\varepsilon$ along the Stokes regions $\mathrm{I}_{+\infty} \to \mathrm{I}_1 \to \mathrm{I}_2 \to \mathrm{I}_3 \to \mathrm{I}_4 \to \mathrm{I}_{-\infty}$. We can compute the connection formula for the solutions by using the formulae (2.2.38), (2.2.39) repeatedly according to the orientations of the Stokes lines.

- $\mathrm{I}_{+\infty} \to \mathrm{I}_1$

$$\begin{pmatrix} \mathcal{B}_{0-}\left[\psi^{+}_{z_4,\mathrm{I}_{+\infty}}\right](z) \\ \mathcal{B}_{0-}\left[\psi^{-}_{z_4,\mathrm{I}_{+\infty}}\right](z) \end{pmatrix} = \begin{pmatrix} 1 & 0 \\ -i & 1 \end{pmatrix} \begin{pmatrix} \mathcal{B}_{0-}\left[\psi^{+}_{z_4,\mathrm{I}_1}\right](z) \\ \mathcal{B}_{0-}\left[\psi^{-}_{z_4,\mathrm{I}_1}\right](z) \end{pmatrix}. \tag{3.2.3}$$

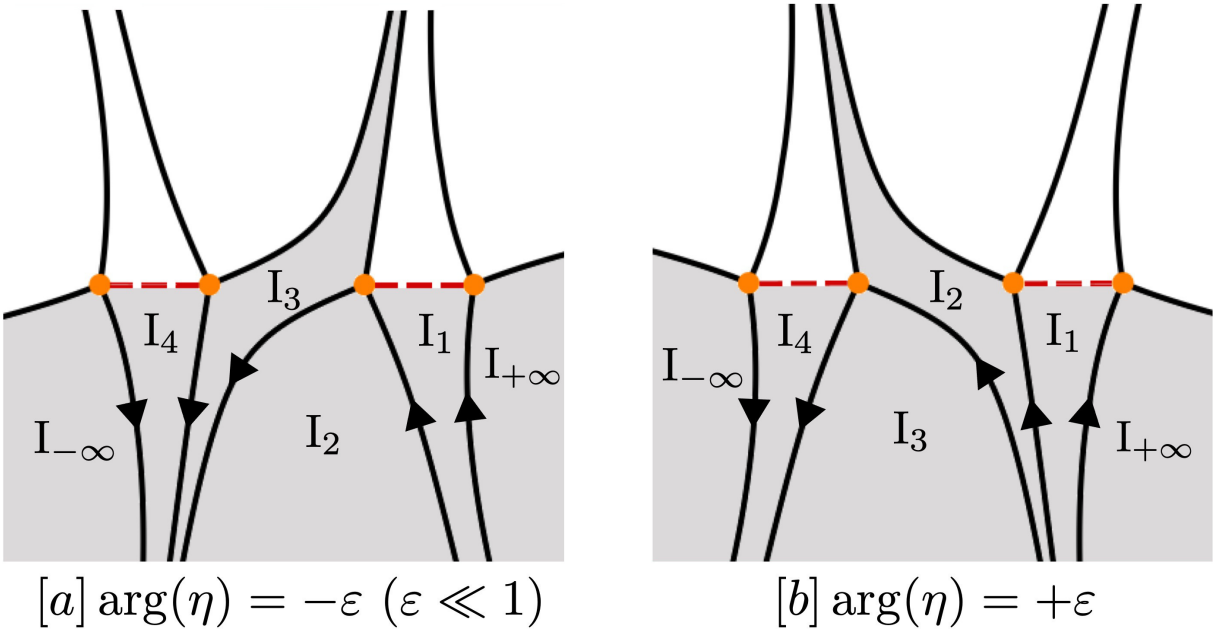

Figure 3.4: The Stokes graph for the double-well potential with $\arg(\eta) = \pm\varepsilon$ ($\varepsilon \ll 1$) and $0 < E < \frac{\kappa^2}{4}$. The gray regions named $\mathrm{I}_{+\infty}$, I_1, I_2, I_3, I_4, $\mathrm{I}_{-\infty}$ are the Stokes regions.

- Change of the normalization $z_4 \to z_3$

$$\begin{pmatrix} \mathcal{B}_{0-}\left[\psi^{+}_{z_4,\mathrm{I}_1}\right](z) \\ \mathcal{B}_{0-}\left[\psi^{-}_{z_4,\mathrm{I}_1}\right](z) \end{pmatrix} = \begin{pmatrix} e^{-\eta\mathcal{B}_{0-}\left[\int_{z_3}^{z_4} S_{\mathrm{even}}(z)dz\right]} & 0 \\ 0 & e^{\eta\mathcal{B}_{0-}\left[\int_{z_3}^{z_4} S_{\mathrm{even}}(z)dz\right]} \end{pmatrix} \begin{pmatrix} \mathcal{B}_{0-}\left[\psi^{+}_{z_3,\mathrm{I}_1}\right](z) \\ \mathcal{B}_{0-}\left[\psi^{-}_{z_3,\mathrm{I}_1}\right](z) \end{pmatrix}. \tag{3.2.4}$$

- $\mathrm{I}_1 \to \mathrm{I}_2$

$$\begin{pmatrix} \mathcal{B}_{0-}\left[\psi^{+}_{z_3,\mathrm{I}_1}\right](z) \\ \mathcal{B}_{0-}\left[\psi^{-}_{z_3,\mathrm{I}_1}\right](z) \end{pmatrix} = \begin{pmatrix} 1 & 0 \\ -i & 1 \end{pmatrix} \begin{pmatrix} \mathcal{B}_{0-}\left[\psi^{+}_{z_3,\mathrm{I}_2}\right](z) \\ \mathcal{B}_{0-}\left[\psi^{-}_{z_3,\mathrm{I}_2}\right](z) \end{pmatrix}. \tag{3.2.5}$$

- $\mathrm{I}_2 \to \mathrm{I}_3$

$$\begin{pmatrix} \mathcal{B}_{0-}\left[\psi^{+}_{z_3,\mathrm{I}_2}\right](z) \\ \mathcal{B}_{0-}\left[\psi^{-}_{z_3,\mathrm{I}_2}\right](z) \end{pmatrix} = \begin{pmatrix} 1 & -i \\ 0 & 1 \end{pmatrix} \begin{pmatrix} \mathcal{B}_{0-}\left[\psi^{+}_{z_3,\mathrm{I}_3}\right](z) \\ \mathcal{B}_{0-}\left[\psi^{-}_{z_3,\mathrm{I}_3}\right](z) \end{pmatrix}. \tag{3.2.6}$$

- Change of the normalization $z_3 \to z_2$

$$\begin{pmatrix} \mathcal{B}_{0-}\left[\psi^{+}_{z_3,\mathrm{I}_3}\right](z) \\ \mathcal{B}_{0-}\left[\psi^{-}_{z_3,\mathrm{I}_3}\right](z) \end{pmatrix} = \begin{pmatrix} e^{-\eta\mathcal{B}_{0-}\left[\int_{z_2}^{z_3} S_{\mathrm{even}}(z)dz\right]} & 0 \\ 0 & e^{\eta\mathcal{B}_{0-}\left[\int_{z_2}^{z_3} S_{\mathrm{even}}(z)dz\right]} \end{pmatrix} \begin{pmatrix} \mathcal{B}_{0-}\left[\psi^{+}_{z_2,\mathrm{I}_3}\right](z) \\ \mathcal{B}_{0-}\left[\psi^{-}_{z_2,\mathrm{I}_3}\right](z) \end{pmatrix}. \tag{3.2.7}$$

- $\mathrm{I}_3 \to \mathrm{I}_4$

$$\begin{pmatrix} \mathcal{B}_{0-}\left[\psi^{+}_{z_2,\mathrm{I}_3}\right](z) \\ \mathcal{B}_{0-}\left[\psi^{-}_{z_2,\mathrm{I}_3}\right](z) \end{pmatrix} = \begin{pmatrix} 1 & -i \\ 0 & 1 \end{pmatrix} \begin{pmatrix} \mathcal{B}_{0-}\left[\psi^{+}_{z_2,\mathrm{I}_4}\right](z) \\ \mathcal{B}_{0-}\left[\psi^{-}_{z_2,\mathrm{I}_4}\right](z) \end{pmatrix}. \tag{3.2.8}$$

- Change of the normalization $z_2 \to z_1$

$$\begin{pmatrix} \mathcal{B}_{0-}\left[\psi^{+}_{z_2,\mathrm{I}_4}\right](z) \\ \mathcal{B}_{0-}\left[\psi^{-}_{z_2,\mathrm{I}_4}\right](z) \end{pmatrix} = \begin{pmatrix} e^{-\eta\mathcal{B}_{0-}\left[\int_{z_1}^{z_2} S_{\mathrm{even}}(z)dz\right]} & 0 \\ 0 & e^{\eta\mathcal{B}_{0-}\left[\int_{z_1}^{z_2} S_{\mathrm{even}}(z)dz\right]} \end{pmatrix} \begin{pmatrix} \mathcal{B}_{0-}\left[\psi^{+}_{z_1,\mathrm{I}_4}\right](z) \\ \mathcal{B}_{0-}\left[\psi^{-}_{z_1,\mathrm{I}_4}\right](z) \end{pmatrix}. \tag{3.2.9}$$

- $\mathrm{I}_4 \to \mathrm{I}_{-\infty}$

$$\begin{pmatrix} \mathcal{B}_{0-}\left[\psi^{+}_{z_1,\mathrm{I}_4}\right](z) \\ \mathcal{B}_{0-}\left[\psi^{-}_{z_1,\mathrm{I}_4}\right](z) \end{pmatrix} = \begin{pmatrix} 1 & -i \\ 0 & 1 \end{pmatrix} \begin{pmatrix} \mathcal{B}_{0-}\left[\psi^{+}_{z_1,\mathrm{I}_{-\infty}}\right](z) \\ \mathcal{B}_{0-}\left[\psi^{-}_{z_1,\mathrm{I}_{-\infty}}\right](z) \end{pmatrix}. \tag{3.2.10}$$

By multiplying (3.2.3)$\sim$(3.2.10) and finally restoring the normalization of the solutions in the r.h.s. of (3.2.10) from z_1 to z_2, z_2 to z_3, and z_3 to z_4, we obtain the connection formula,

$$\begin{pmatrix} \mathcal{B}_{0-}\left[\psi^{+}_{z_4,\mathrm{I}_{+\infty}}\right](z) \\ \mathcal{B}_{0-}\left[\psi^{-}_{z_4,\mathrm{I}_{+\infty}}\right](z) \end{pmatrix} = M_- \begin{pmatrix} \mathcal{B}_{0-}\left[\psi^{+}_{z_4,\mathrm{I}_{-\infty}}\right](z) \\ \mathcal{B}_{0-}\left[\psi^{-}_{z_4,\mathrm{I}_{-\infty}}\right](z) \end{pmatrix}, \tag{3.2.11}$$

with

$$M_- = \begin{pmatrix} 1 & -i\dfrac{1+\left(1+e^{\eta\mathcal{B}_{0-}\left[\Pi_{\gamma_{2,3}}\right]}\right)e^{-\eta\mathcal{B}_{0-}\left[\Pi_{\gamma_{1,2}}\right]}}{e^{-\eta\mathcal{B}_{0-}\left[\Pi_{\gamma_{1,2}}\right]}e^{\eta\mathcal{B}_{0-}\left[\Pi_{\gamma_{3,4}}\right]}e^{\eta\mathcal{B}_{0-}\left[\Pi_{\gamma_{2,3}}\right]}} \\ -i\left(1+e^{\eta\mathcal{B}_{0-}\left[\Pi_{\gamma_{3,4}}\right]}\right) & -\dfrac{1+e^{\eta\mathcal{B}_{0-}\left[\Pi_{\gamma_{3,4}}\right]}+\left(1+e^{\eta\mathcal{B}_{0-}\left[\Pi_{\gamma_{3,4}}\right]}+e^{\eta\mathcal{B}_{0-}\left[\Pi_{\gamma_{2,3}}\right]}\right)e^{-\eta\mathcal{B}_{0-}\left[\Pi_{\gamma_{1,2}}\right]}}{e^{-\eta\mathcal{B}_{0-}\left[\Pi_{\gamma_{1,2}}\right]}e^{\eta\mathcal{B}_{0-}\left[\Pi_{\gamma_{3,4}}\right]}e^{\eta\mathcal{B}_{0-}\left[\Pi_{\gamma_{2,3}}\right]}} \end{pmatrix}, \tag{3.2.12}$$

where we have identified the integrals $2\int_{z_1}^{z_2} S_{\mathrm{even}}(z)dz$, $2\int_{z_2}^{z_3} S_{\mathrm{even}}(z)dz$ and $2\int_{z_3}^{z_4} S_{\mathrm{even}}(z)dz$ with the WKB periods for the one-cycles $-\gamma_{1,2}$, $\gamma_{2,3}$ and $\gamma_{3,4}$ in Fig.3.3, respectively. The WKB periods for $\gamma_{3,4}$ and $\gamma_{1,2}$ satisfy the following relation,

$$\Pi_{\gamma_{3,4}} = 2\pi i \mathrm{Res}_{z=\infty} S_{\mathrm{even}}(z) + \Pi_{\gamma_{1,2}}. \tag{3.2.13}$$

As the harmonic oscillator case, it has been shown that the higher order coefficient $S_n(z)$ ($n \geq 1$) is holomorphic at $z = \infty$ (Proposition 2.8. in [25]). In the present case we can show that

$\mathrm{Res}_{z=\infty}S_0(z)=0$. Therefore we obtain

$$\Pi_{\gamma_{3,4}}=\Pi_{\gamma_{1,2}}. \tag{3.2.14}$$

By using the identity (3.2.14), the matrix (3.2.12) can be written as follows,

$$M_-=\begin{pmatrix} 1 & -i\frac{1+\left(1+e^{\eta\mathcal{B}_{0-}\left[\Pi_{\gamma_{2,3}}\right]}\right)e^{-\eta\mathcal{B}_{0-}\left[\Pi_{\gamma_{3,4}}\right]}}{e^{\eta\mathcal{B}_{0-}\left[\Pi_{\gamma_{2,3}}\right]}} \\ -i\left(1+e^{\eta\mathcal{B}_{0-}\left[\Pi_{\gamma_{3,4}}\right]}\right) & -\frac{2+e^{\eta\mathcal{B}_{0-}\left[\Pi_{\gamma_{3,4}}\right]}+e^{-\eta\mathcal{B}_{0-}\left[\Pi_{\gamma_{3,4}}\right]}+e^{\eta\mathcal{B}_{0-}\left[\Pi_{\gamma_{2,3}}\right]}e^{-\eta\mathcal{B}_{0-}\left[\Pi_{\gamma_{3,4}}\right]}}{e^{\eta\mathcal{B}_{0-}\left[\Pi_{\gamma_{2,3}}\right]}} \end{pmatrix}, \tag{3.2.15}$$

We can similarly compute the connection formula for $\arg(\eta)=+\varepsilon$ according to the Stokes graph [b] in Fig.3.4. Then we obtain

$$\begin{pmatrix} \mathcal{B}_{0+}\left[\psi^{+}_{z_4,\mathrm{I}_{+\infty}}\right](z) \\ \mathcal{B}_{0+}\left[\psi^{-}_{z_4,\mathrm{I}_{+\infty}}\right](z) \end{pmatrix}=M_+\begin{pmatrix} \mathcal{B}_{0+}\left[\psi^{+}_{z_4,\mathrm{I}_{-\infty}}\right](z) \\ \mathcal{B}_{0+}\left[\psi^{-}_{z_4,\mathrm{I}_{-\infty}}\right](z) \end{pmatrix}, \tag{3.2.16}$$

with

$$M_+=\begin{pmatrix} 1 & -i\frac{1+e^{-\eta\mathcal{B}_{0+}\left[\Pi_{\gamma_{3,4}}\right]}}{e^{\eta\mathcal{B}_{0+}\left[\Pi_{\gamma_{2,3}}\right]}} \\ -i\left(1+e^{\eta\mathcal{B}_{0+}\left[\Pi_{\gamma_{3,4}}\right]}\left(1+e^{\eta\mathcal{B}_{0+}\left[\Pi_{\gamma_{2,3}}\right]}\right)\right) & -\frac{2+e^{\eta\mathcal{B}_{0+}\left[\Pi_{\gamma_{3,4}}\right]}+e^{-\eta\mathcal{B}_{0+}\left[\Pi_{\gamma_{3,4}}\right]}+e^{\eta\mathcal{B}_{0+}\left[\Pi_{\gamma_{2,3}}\right]}e^{\eta\mathcal{B}_{0+}\left[\Pi_{\gamma_{3,4}}\right]}}{e^{\eta\mathcal{B}_{0+}\left[\Pi_{\gamma_{2,3}}\right]}} \end{pmatrix}. \tag{3.2.17}$$

The exact quantization conditions for the bound state can be obtained by imposing the boundary conditions that the solutions decay at $z\to\pm\infty$. The decaying solutions at $z\to+\infty$ are the solutions $\mathcal{B}_{0\pm}\left[\psi^{-}_{z_4,\mathrm{I}_{+\infty}}\right](z)$. According to the connection formulae (3.2.11) and (3.2.16), the solutions $\mathcal{B}_{0\pm}\left[\psi^{-}_{z_4,\mathrm{I}_{+\infty}}\right](z)$ are connected to $z\to-\infty$ as follows,

$$\begin{cases} \mathcal{B}_{0-}\left[\psi^{-}_{z_4,\mathrm{I}_{+\infty}}\right](z)=-i\left(1+e^{\eta\mathcal{B}_{0-}\left[\Pi_{\gamma_{3,4}}\right]}\right)\mathcal{B}_{0-}\left[\psi^{+}_{z_4,\mathrm{I}_{-\infty}}\right](z) \\ \qquad\qquad -\frac{2+e^{\eta\mathcal{B}_{0-}\left[\Pi_{\gamma_{3,4}}\right]}+e^{-\eta\mathcal{B}_{0-}\left[\Pi_{\gamma_{3,4}}\right]}+e^{\eta\mathcal{B}_{0-}\left[\Pi_{\gamma_{2,3}}\right]}e^{-\eta\mathcal{B}_{0-}\left[\Pi_{\gamma_{3,4}}\right]}}{e^{\eta\mathcal{B}_{0-}\left[\Pi_{\gamma_{2,3}}\right]}}\mathcal{B}_{0-}\left[\psi^{-}_{z_4,\mathrm{I}_{-\infty}}\right](z), \\ \mathcal{B}_{0+}\left[\psi^{-}_{z_4,\mathrm{I}_{+\infty}}\right](z)=-i\left(1+e^{\eta\mathcal{B}_{0+}\left[\Pi_{\gamma_{3,4}}\right]}\left(1+e^{-\eta\mathcal{B}_{0+}\left[\Pi_{\gamma_{2,3}}\right]}\right)\right)\mathcal{B}_{0+}\left[\psi^{+}_{z_4,\mathrm{I}_{-\infty}}\right](z) \\ \qquad\qquad -\frac{2+e^{\eta\mathcal{B}_{0+}\left[\Pi_{\gamma_{3,4}}\right]}+e^{-\eta\mathcal{B}_{0+}\left[\Pi_{\gamma_{3,4}}\right]}+e^{\eta\mathcal{B}_{0+}\left[\Pi_{\gamma_{2,3}}\right]}e^{\eta\mathcal{B}_{0+}\left[\Pi_{\gamma_{3,4}}\right]}}{e^{\eta\mathcal{B}_{0+}\left[\Pi_{\gamma_{2,3}}\right]}}\mathcal{B}_{0+}\left[\psi^{-}_{z_4,\mathrm{I}_{-\infty}}\right](z). \end{cases} \tag{3.2.18}$$

Contrary to the harmonic oscillator case, the decaying solutions at $z\to-\infty$ are the Borel resummations of the positive signed WKB solutions $\mathcal{B}_{0\pm}\left[\psi^{+}_{z_4,\mathrm{I}_{-\infty}}\right](z)$ because the Stokes

line lying on $(-\infty, z_1]$ in Fig.3.3 has the negative orientation. Therefore in order to satisfy the boundary conditions, the coefficients of $\mathcal{B}_{0\pm}\left[\psi^{-}_{z_4,\mathrm{I}_{-\infty}}\right](z)$ in (3.2.18) have to be zero,

$$\begin{cases} \mathcal{B}_{0-}[J_-] = 2 + e^{\eta\mathcal{B}_{0-}\left[\Pi_{\gamma_{3,4}}\right]} + e^{-\eta\mathcal{B}_{0-}\left[\Pi_{\gamma_{3,4}}\right]} + e^{\eta\mathcal{B}_{0-}\left[\Pi_{\gamma_{2,3}}\right]} e^{-\eta\mathcal{B}_{0-}\left[\Pi_{\gamma_{3,4}}\right]} = 0, \\ \mathcal{B}_{0+}[J_+] = 2 + e^{\eta\mathcal{B}_{0+}\left[\Pi_{\gamma_{3,4}}\right]} + e^{-\eta\mathcal{B}_{0+}\left[\Pi_{\gamma_{3,4}}\right]} + e^{\eta\mathcal{B}_{0+}\left[\Pi_{\gamma_{2,3}}\right]} e^{\eta\mathcal{B}_{0+}\left[\Pi_{\gamma_{3,4}}\right]} = 0, \end{cases} \tag{3.2.19}$$

here we have introduced the functions $J_\pm$, which are called Jost functions. Two exact quantization conditions (3.2.19) are equivalent [1],

$$\begin{aligned} \mathcal{B}_{0-}[J_-] &= 2 + e^{\eta\mathcal{B}_{0-}\left[\Pi_{\gamma_{3,4}}\right]} + \left(1 + e^{\eta\mathcal{B}_{0-}\left[\Pi_{\gamma_{2,3}}\right]}\right) e^{-\eta\mathcal{B}_{0-}\left[\Pi_{\gamma_{3,4}}\right]} \\ &= 2 + \left(1 + e^{\eta\mathcal{B}_{0+}\left[\Pi_{\gamma_{2,3}}\right]}\right) e^{\eta\mathcal{B}_{0+}\left[\Pi_{\gamma_{3,4}}\right]} + e^{-\eta\mathcal{B}_{0+}\left[\Pi_{\gamma_{3,4}}\right]} \\ &= \mathcal{B}_{0+}[J_+], \end{aligned} \tag{3.2.20}$$

where we have used the Delabaere-Pham formula (2.2.44) in the second line.

We can also define the Jost function for the median resummation J_{med} satisfying

$$\mathcal{B}_{0,\mathrm{med}}[J_{\mathrm{med}}] = \mathcal{B}_{0-}[J_-] = \mathcal{B}_{0+}[J_+]. \tag{3.2.21}$$

By acting the inverse of the definition of the median resummation (2.2.30) to (3.2.21), we obtain

$$J_{\mathrm{med}} = \mathfrak{S}_0^{1/2}[J_-] = \mathfrak{S}_0^{-1/2}[J_+]. \tag{3.2.22}$$

Let us compute $\mathfrak{S}_0^{1/2}[J_-]$. From (2.2.31), $\mathfrak{S}_0^{1/2}[J_-]$ can be express as,

$$\mathfrak{S}_0^{1/2}[J_-] = \sum_{n=0}^{\infty} \binom{\frac{1}{2}}{n} (\mathfrak{S}_0 - 1)^n [J_-]. \tag{3.2.23}$$

$(\mathfrak{S}_0 - 1)^n [J_-]$ can be computed by using the Delabaere-Pham formula (2.2.45) repeatedly. Then we obtain

$$(\mathfrak{S}_0 - 1)^n [J_-] = 2 + \left(e^{\eta\Pi_{\gamma_{2,3}}}\right)^n e^{\eta\Pi_{\gamma_{3,4}}} + \left(-\frac{e^{\eta\Pi_{\gamma_{2,3}}}}{1 + e^{\eta\Pi_{\gamma_{2,3}}}}\right)^n \left(1 + e^{\eta\Pi_{\gamma_{2,3}}}\right) e^{-\eta\Pi_{\gamma_{3,4}}}, \tag{3.2.24}$$

[1] We can also check that each matrix element of (3.2.12) and (3.2.17) are equivalent under the Delabaere-Pham formula.

and therefore

$$J_{\rm med} = \mathfrak{S}_0^{1/2}\left[J_-\right] = 2\left(1 + \left(1 + e^{\eta\Pi_{\gamma_{2,3}}}\right)^{\frac{1}{2}} \cosh\left(\eta\Pi_{\gamma_{3,4}}\right)\right). \tag{3.2.25}$$

The exact quantization condition is given by the median resummation of (3.2.25) [27],

$$\mathcal{B}_{0,\rm med}\left[J_{\rm med}\right] = 2\left(1 + \left(1 + e^{\eta\mathcal{B}_0\left[\Pi_{\gamma_{2,3}}\right]}\right)^{\frac{1}{2}} \cosh\left(\eta\mathcal{B}_{0,\rm med}\left[\Pi_{\gamma_{3,4}}\right]\right)\right) = 0, \tag{3.2.26}$$

where we have used that $\Pi_{\gamma_{2,3}}$ has no discontinuity for $\arg(\eta) = 0$ and therefore $e^{\eta\mathcal{B}_{0,\rm med}\left[\Pi_{\gamma_{2,3}}\right]} = e^{\eta\mathcal{B}_0\left[\Pi_{\gamma_{2,3}}\right]}$. The exact quantization condition (3.2.26) can also be written as [28],

$$i\eta\mathcal{B}_{0,\rm med}\left[\Pi_{\gamma_{3,4}}\right] \pm \tan^{-1}\left(e^{\frac{\eta}{2}\mathcal{B}_0\left[\Pi_{\gamma_{2,3}}\right]}\right) = 2\pi\left(k + \frac{1}{2}\right), \tag{3.2.27}$$

where $k \in \mathbb{Z}_{\geq 0}$. The sign $\pm$ corresponds to the parity of the quantum state. Depending on the parity, the n-th state of the spectrum is related as

$$n = 2k - \frac{-1 \pm 1}{2}. \tag{3.2.28}$$

The term $e^{\frac{\eta}{2}\mathcal{B}_0\left[\Pi_{\gamma_{2,3}}\right]}$ is exponentially small. $\mathcal{B}_0\left[\Pi_{\gamma_{2,3}}\right]$ is the contribution from the cycle encircling the classically forbidden interval $[z_2, z_3]$ in the potential graph Fig.3.2 and produces the instanton contributions from the tunnel effect to the asymptotic expansion of the energy eigenvalues (e.g. [27, 31, 71–73]).

3.2.2 Above the potential barrier

The Stokes graph for $\frac{\kappa^2}{4} < E$ is drawn in Fig.3.5. The simple zeros z_1, z_4 are real and z_2, z_3 are pure imaginary. As with $0 < E < \frac{\kappa^2}{4}$ case, z_2, z_3 are connected by the Stokes segment.

We compute the lateral Borel resummation to derive the exact energy quantization condition. The saddle reduction of the Stokes graph is given by Fig.3.6. The connection formula for $\arg(\eta) = -\varepsilon$ and $\frac{\kappa^2}{4} < E$ is same as the connection formula for $\arg(\eta) = +\varepsilon$ and $0 < E < \frac{\kappa^2}{4}$ given in (3.2.16) because, along the continuation from $\mathrm{I}_{+\infty}$ to $\mathrm{I}_{-\infty}$ on the graph [a] in Fig.3.6, we cross the Stokes lines that have the same orientation and emanating points as we cross along the continuation on the graph [b] in Fig.3.4. Therefore the Jost function

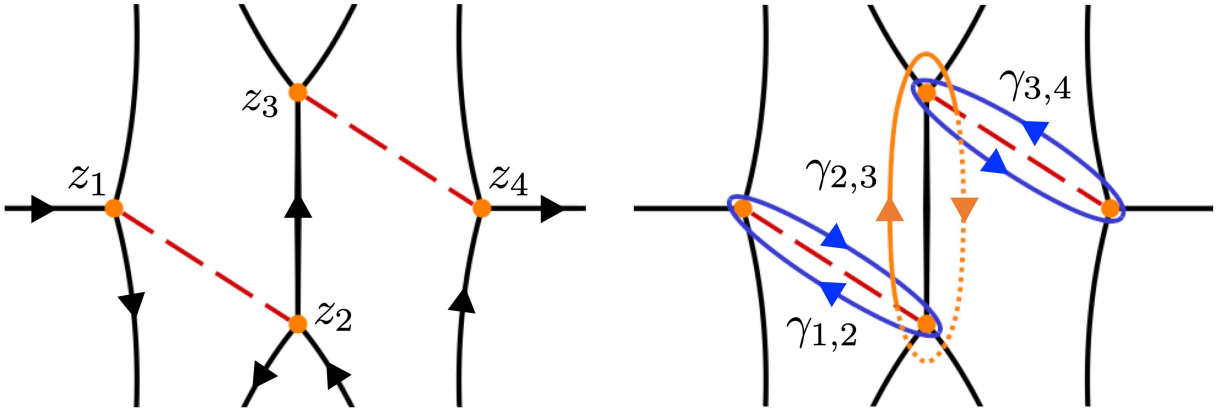

Figure 3.5: The Stokes graph and the one-cycles for the double-well potential with $\arg(\eta) = 0$ and $\frac{\kappa^2}{4} < E$.

J_- for $\frac{\kappa^2}{4} < E$ is also same as the Jost function J_+ for $0 < E < \frac{\kappa^2}{4}$,

$$J_- = 2 + e^{-\eta\Pi_{\gamma_{3,4}}} + \left(1 + e^{\eta\Pi_{\gamma_{2,3}}}\right) e^{\eta\Pi_{\gamma_{3,4}}}. \tag{3.2.29}$$

In Fig.3.5, γ_{23} encircles the Stokes segment and $\Pi^{(0)}_{\gamma_{23}} > 0$. The Delabaere-Pham formula (2.2.45) then leads

$$(\mathfrak{S}_0 - 1)^n [J_-] = 2 + \left(e^{-\eta\Pi_{\gamma_{2,3}}}\right)^n e^{-\eta\Pi_{\gamma_{3,4}}} + \left(e^{-\eta\Pi_{\gamma_{2,3}}}\right)^n e^{\eta\Pi_{\gamma_{2,3}}} e^{\eta\Pi_{\gamma_{3,4}}}. \tag{3.2.30}$$

Substituting this equation into (3.2.23), we obtain

$$\begin{aligned} J_{\text{med}} &= \mathfrak{S}_0^{1/2} [J_-] \\ &= 2 + \sqrt{1 + e^{-\eta\Pi_{\gamma_{2,3}}}} e^{-\eta\Pi_{\gamma_{3,4}}} + \sqrt{1 + e^{-\eta\Pi_{\gamma_{2,3}}}} e^{\eta\Pi_{\gamma_{2,3}}} e^{\eta\Pi_{\gamma_{3,4}}} \\ &= 2 + \sqrt{1 + e^{\eta\Pi_{\gamma_{2,3}}}} e^{-\frac{\eta}{2}\Pi_{\gamma_{2,3}}} e^{-\eta\Pi_{\gamma_{3,4}}} + \sqrt{1 + e^{\eta\Pi_{\gamma_{2,3}}}} e^{\frac{\eta}{2}\Pi_{\gamma_{2,3}}} e^{\eta\Pi_{\gamma_{3,4}}} \\ &= 2\left(1 + \sqrt{1 + e^{\eta\Pi_{\gamma_{2,3}}}} \cosh\left(\frac{\eta}{2}\Pi_{\gamma_{1,4}}\right)\right), \end{aligned} \tag{3.2.31}$$

where $\gamma_{1,4} = \gamma_{1,2} + \gamma_{2,3} + \gamma_{3,4}$ is the one-cycle encircling z_1, z_4 and we have used $\frac{1}{2}\Pi_{\gamma_{2,3}} + \Pi_{\gamma_{3,4}} = \frac{1}{2}\Pi_{\gamma_{2,3}} + \frac{1}{2}\Pi_{\gamma_{1,2}} + \frac{1}{2}\Pi_{\gamma_{3,4}} = \frac{1}{2}\Pi_{\gamma_{1,4}}$. The exact quantization condition is given by the median resummation of (3.2.31) [28, 30],

$$\mathcal{B}_{0,\text{med}} [J_{\text{med}}] = 2\left(1 + \left(1 + e^{\eta\mathcal{B}_0[\Pi_{\gamma_{2,3}}]}\right)^{\frac{1}{2}} \cosh\left(\frac{\eta}{2}\mathcal{B}_{0,\text{med}}\left[\Pi_{\gamma_{1,4}}\right]\right)\right) = 0. \tag{3.2.32}$$

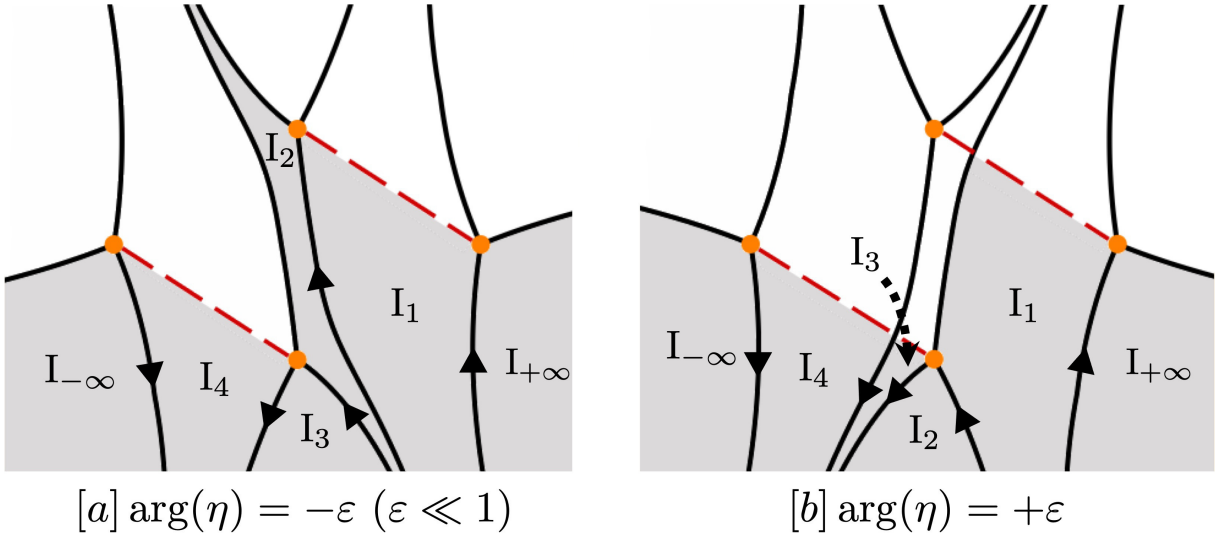

Figure 3.6: The Stokes graph for the double-well potential with $\arg(\eta) = \pm\varepsilon$ $(\varepsilon \ll 1)$ and $\frac{\kappa^2}{4} < E$.

(3.2.32) can be written as

$$i\frac{\eta}{2}\mathcal{B}_{0,\mathrm{med}}\left[\Pi_{\gamma_{1,4}}\right] \pm \tan^{-1}\left(e^{\frac{\eta}{2}\mathcal{B}_0\left[\Pi_{\gamma_{2,3}}\right]}\right) = 2\pi\left(k+\frac{1}{2}\right), \tag{3.2.33}$$

where $k \in \mathbb{Z}_{\geq 0}$ and the sign $\pm$ corresponds to the parity of the quantum state. The n-th state of the spectrum is related as (3.2.28). The first term in the l.h.s. of (3.2.33) is the perturbative contribution from the classically allowed interval $[z_1, z_4]$ and the second term is the non-perturbative contribution from the complex instanton.

Summary

In this chapter, we have solved the connection problem of the Borel resummed WKB solutions for the harmonic oscillator and the double-well potential based on the Stokes graphs and the connection formula of the solutions given in the previous chapter. Imposing the boundary conditions for the bound state, we have derived the exact energy quantization conditions written in terms of the Borel resummed WKB periods. The exact conditions for the double-well potential have the exponentially small terms, which provide the non-perturbative contributions arising from the quantum tunnel effect to the energy spectrum.

Chapter 4

Quasi-normal modes for D3/M5-branes

The Exact WKB analysis works not only in the study of the real-valued spectrum but also the complex-valued spectrum. In this chapter, we study the quasi-normal modes for massless scalar perturbations to the extremal D3/M5 branes by using the Exact WKB analysis. The exact conditions for the QNMs show that the discontinuity of the perturbative part of the QNMs leads the non-perturbative part of themselves. We also find examples of the Seiberg-Witten/gravity correspondence, which helps us to compute the QNMs from our conditions. This chapter is based on the author's papers [40, 41].

4.1 Massless dilaton perturbation to extremal D3-branes

4.1.1 E.O.M. and QNMs for dilaton field in extremal D3-branes metric

The geometry of a stack of the extremal D3-branes is given by the following line element [34],

$$ds^2 = H(r)^{-1/2}\left(-dt^2 + dx_1^2 + \cdots + dx_3^2\right) + H(r)^{1/2}\left(dr^2 + r^2 d\Omega_5^2\right), \tag{4.1.1}$$

where $H(r) = 1 + \frac{L^4}{r^4}$, L is a positive real parameter depending on the number of the extremal D3-branes, $(t, x_1, \cdots, x_3)$ are the coordinates on the D3-branes world-volume, r is the radial coordinate and $d\Omega_5^2$ is the metric on S^5 in the bulk of the D3-branes. We consider the massless dilaton field Φ, which describes a massless scalar state of the closed string.

The massless dilaton field in the extremal D3-branes geometry (4.1.1) obeys the following E.O.M.:

$$\Box\Phi = \frac{1}{\sqrt{-g}}\partial_M\left(\sqrt{-g}g^{MN}\partial_N\right)\Phi = 0, \tag{4.1.2}$$

where g_{MN} $(M, N = 0, 1, \cdots, 9)$ is the metric given by (4.1.1) and $g = \det g_{MN}$. Under the separation of the variables, the solution to (4.1.2) takes the form

$$\Phi = e^{-iEt+i\boldsymbol{k}\cdot\boldsymbol{x}}r^5\phi(r)\mathcal{Y}^l_{\boldsymbol{m}}(\boldsymbol{\theta}), \tag{4.1.3}$$

where $\mathcal{Y}^l_{\boldsymbol{m}}(\boldsymbol{\theta})$ is the spherical harmonics on S^5 obeying $\Delta_{S^5}\mathcal{Y}^l_{\boldsymbol{m}}(\boldsymbol{\theta}) = -l\,(l+4)\,\mathcal{Y}^l_{\boldsymbol{m}}(\boldsymbol{\theta})$, l and $\boldsymbol{m} = (m_1, m_2, m_3, m_4)$ are integers satisfying $|m_1| \le m_2 \le m_3 \le m_4 \le l$ and $\boldsymbol{\theta}$ denotes the angular coordinates on S^5. The radial part $\phi(r)$ of Ψ satisfies the second-order differential equation [74],

$$\left[\rho^{-5}\frac{d}{d\rho}\rho^5\frac{d}{d\rho} + 1 + \frac{(\omega R)^4}{\rho^4} - \frac{l\,(l+4)}{\rho^2}\right]\phi(\rho/\omega) = 0, \quad (\rho = \omega r) \tag{4.1.4}$$

where $\omega = \sqrt{E^2 - \boldsymbol{k}^2}$. Introducing z by $\rho = \omega L z$ and $\psi(z)$ by $\phi(\rho/\omega) = (\omega L z)^{-5/2}\psi(z)$, (4.1.4) becomes the second-order differential equation with absence of the first-order difference,

$$\left[\frac{d^2}{dz^2} - \eta^2 Q_0(z) - Q_2(z)\right]\psi(z) = 0, \tag{4.1.5}$$

with

$$Q_0(z) = -\frac{(\omega L)^2\,(z^4+1) - (l+2)^2\,z^2}{z^4}, \quad Q_2(z) = -\frac{1}{4z^2}, \tag{4.1.6}$$

and $\eta = 1$.

We will consider the solution to (4.1.5) satisfying the following boundary conditions: (i) only outgoing wave exists at $z \to +\infty$ along the real axis and (ii) only ingoing wave exists at $z \to 0$. Then we obtain the set of the spectrum of ω called the QNMs, which take discrete values with positive real and negative imaginary part.

The boundary conditions for the QNMs can be interpreted as follows. The potential $Q_0(z) + Q_2(z)$ has the maximum point z_c (Fig.4.1). z_c is called the photon sphere. The photon sphere is the unstable fixed point for the closed strings moving in the D3-branes geometry. By the potential, the closed strings on the photon sphere fall into the origin or go away to infinity. At the origin, the closed strings are absorbed by the D3-branes and there is no closed string emitted from the D3-branes. At the infinity, there is no incoming

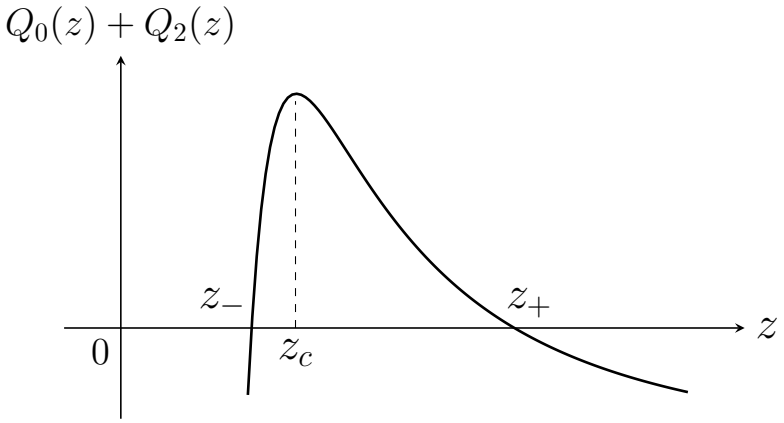

Figure 4.1: The potential graph of $Q_0(z)+Q_2(z)$.

closed string because there is no potential barrier reflecting the closed strings going away to infinity. In the end, all the closed strings leave from the photon sphere (This is expressed by that the scalar perturbation dumps over time.).

WKB approximation for extremal D3-branes

We first study the semiclassical value of the QNMs for large l, at which the QNMs can be determined from the Bohr-Sommerfeld quantization condition [43],

$$\int_{z_-}^{z_+} \sqrt{Q_0(z)+Q_2(z)}dz = \pi i\left(n+\frac{1}{2}\right), \tag{4.1.7}$$

where $n \in \mathbb{Z}_{\geq 0}$ and $z_\pm$ are the turning points satisfying $Q_0(z_\pm)+Q_2(z_\pm)=0$ (Fig.4.1). n is called overtone number. At large l, the turning points close each other and the l.h.s. of (4.1.7) can be integrated by approximating $Q_0(z)+Q_2(z)$ by its expansion at the maximum point z_c (Fig.4.1). Then (4.1.7) reduces to

$$\frac{Q_0(z_c)+Q_2(z_c)}{\sqrt{2\left(Q_0''(z_c)+Q_2''(z_c)\right)}} = i\left(n+\frac{1}{2}\right). \tag{4.1.8}$$

The condition (4.2.8) can be solved perturbatively with respect to the imaginary part of ωR. Up to the linear order, one finds

$$\omega L = \frac{1}{L}\sqrt{(l+2)^2-\frac{1}{4}} - i\left(n+\frac{1}{2}\right). \tag{4.1.9}$$

The formula (4.2.9) indicates that the real part of the QNMs only depends on l and the imaginary part only depends on n in the large l region.

The Bohr-Sommerfeld quantization condition is only valid for large l. One of the way to compute the QNMs even at small l is to determine exact conditions for the QNMs by using the Exact WKB analysis [40]. In this chapter, we study the QNMs spectral problem based on the Exact WKB analysis and derive exact conditions for the QNMs.

Leaver's method for extremal D3-branes

The QNMs can also be numerically calculated by the Leaver's method (e.g. [42, 75, 76]). Introducing the variable x as $z = (1-x)/x$ and the function $f(x)$ as

$$\psi(z) = x(1-x)e^{i\omega L\left(\frac{1}{x}+\frac{1}{1-x}\right)}f(x), \tag{4.1.10}$$

the equation (4.1.5) becomes

$$a(x)\frac{d^2}{dx^2}f(x) + b(x)\frac{d}{dx}f(x) + c(x)f(x) = 0, \tag{4.1.11}$$

with coefficients

$$\begin{aligned} a(x) &= 4(x-1)^2x^2, \\ b(x) &= 8(2x-1)\left(x^2 - x + i\omega L\right), \\ c(x) &= 8x^2 - 8x - 15 - 16l - 4l^2 + 8i\omega L + 8(\omega L)^2. \end{aligned} \tag{4.1.12}$$

Expanding $f(x)$ at $x = 1/2$ as

$$f(x) = \sum_{n=0}^{\infty} f_n \left(x - \frac{1}{2}\right)^n, \tag{4.1.13}$$

and substituting into (4.1.11), we find that the coefficient f_n satisfies two sets of three-term recurrence relations:

• For $n \in$ even

$$\begin{aligned} &\alpha_0 f_2 + \beta_0 f_0 = 0, \\ &\alpha_n f_{n+2} + \beta_n f_n + \gamma_n f_{n-2} = 0, \quad (n \geq 2), \end{aligned} \tag{4.1.14}$$

• For $n \in$ odd

$$\begin{aligned} &\alpha_1 f_3 + \beta_1 f_1 = 0, \\ &\alpha_n f_{n+2} + \beta_n f_n + \gamma_n f_{n-2} = 0, \quad (n \geq 3), \end{aligned} \tag{4.1.15}$$

with

$$\begin{aligned} \alpha_n &= \frac{1}{4}(1+n)(2+n), \\ \beta_n &= -2(-1+n)n - 4n + 16i\omega L n - 17 - 16l - 4l^2 + 8i\omega L + 8(\omega L)^2, \\ \gamma_n &= 4(-1+n)n + 16n + 8. \end{aligned} \tag{4.1.16}$$

From the first condition in (4.1.14), we obtain

$$\frac{f_2}{f_0} = -\frac{\beta_0}{\alpha_0}. \tag{4.1.17}$$

On the other hand, from the second condition in (4.1.14), the ration f_2/f_0 can be written by the infinite continuous fraction,

$$\frac{f_2}{f_0} = \frac{-\gamma_2}{\beta_2 - \alpha_2 \frac{\gamma_4}{\beta_4 - \alpha_4 \frac{\gamma_6}{\beta_6 - \cdots}}}, \tag{4.1.18}$$

or in the usual notation,

$$\frac{f_2}{f_0} = \frac{-\gamma_2}{\beta_2 -} \frac{\alpha_2\gamma_4}{\beta_4 -} \frac{\alpha_4\gamma_6}{\beta_6 -} \cdots . \tag{4.1.19}$$

Equating these expressions, we obtain

$$0 = \frac{\beta_0}{\alpha_0} + \frac{-\gamma_2}{\beta_2 -} \frac{\alpha_2\gamma_4}{\beta_4 -} \frac{\alpha_4\gamma_6}{\beta_6 -} \cdots . \tag{4.1.20}$$

Solving the equation (4.1.20) with fixed l by truncating the continuous fraction at a finite term, we obtain a value of ωL, which is the QNM at the overtone number $n = 0$ appearing in (4.1.7). Similarly, by considering the ratio f_3/f_1 and using (4.1.15), we obtain

$$0 = \frac{\beta_1}{\alpha_1} + \frac{-\gamma_3}{\beta_3 -} \frac{\alpha_3\gamma_5}{\beta_5 -} \frac{\alpha_5\gamma_7}{\beta_7 -} \cdots . \tag{4.1.21}$$

The equation (4.1.21) provides the QNM at the overtone number $n = 1$.

For higher overtone number, we can obtain the QNMs by considering the ration f_{n+2}/f_n.

By using the three-term recurrence relations, f_{n+2}/f_n can be expressed in two continuous fractions,

$$\frac{f_{n+2}}{f_n} = \begin{cases} -\frac{\beta_n}{\alpha_n} + \frac{1}{\alpha_n}\frac{\alpha_{n-2}\gamma_n}{\beta_{n-2}-}\frac{\alpha_{n-4}\gamma_{n-2}}{\beta_{n-4}-}\frac{\alpha_{n-6}\gamma_{n-4}}{\beta_{n-6}-}\cdots\frac{\alpha_0\gamma_2}{\beta_0}, & (n=2,4,6,\cdots) \\ -\frac{\beta_n}{\alpha_n} + \frac{1}{\alpha_n}\frac{\alpha_{n-2}\gamma_n}{\beta_{n-2}-}\frac{\alpha_{n-4}\gamma_{n-2}}{\beta_{n-4}-}\frac{\alpha_{n-6}\gamma_{n-4}}{\beta_{n-6}-}\cdots\frac{\alpha_1\gamma_3}{\beta_1}, & (n=3,5,7,\cdots) \end{cases} \tag{4.1.22}$$

and

$$\frac{f_{n+2}}{f_n} = \frac{-\gamma_{n+2}}{\beta_{n+2}-}\frac{\alpha_{n+2}\gamma_{n+4}}{\beta_{n+4}-}\frac{\alpha_{n+4}\gamma_{n+6}}{\beta_{n+6}-}\cdots. \tag{4.1.23}$$

By equating (4.1.22) and (4.1.23) and solving the resulting equation, we can obtain the QNMs with overtone number n numerically.

4.1.2 Exact QNMs condition for extremal D3-branes

We study the solution to (4.1.5) by using the Exact WKB analysis. The coordinate z is regarded as a complex variable and we keep η as a complex parameter, then (4.1.5) becomes the stationary Schrödinger equation (2.2.1) on the Riemann sphere $\mathbb{C}^* = \mathbb{C}\cup\{\infty\}$.

Connection problem

Let us solve a connection problem for the Borel resummation of the WKB solutions to (4.1.5) on the complex coordinate z from $z\to+\infty$ to the origin with $\arg(\eta)=0$. To illustrate the problem, we temporary fix the parameters $\omega L = \frac{13}{10} - i\frac{1}{16}$ and $l=0$. The Stokes graph is drawn in Fig.4.2.

The connection problem from $z\to+\infty$ to the origin is solved by continuing the solutions starting from the Stokes region I_∞ to $\mathrm{I}_{\mathrm{mid}}$ and $\mathrm{I}_{\mathrm{mid}}$ to I_0. First, the regions I_∞ and $\mathrm{I}_{\mathrm{mid}}$ are separated by a Stokes line emanating from z_4 and having the positive orientation. Then, by the formula (2.2.38), the Borel resummation of the WKB solutions in the region I_∞ and $\mathrm{I}_{\mathrm{mid}}$ are connected as follows,

$$\begin{pmatrix} \mathcal{B}_0\left[\psi^+_{z_4,\mathrm{I}_\infty}\right](z) \\ \mathcal{B}_0\left[\psi^-_{z_4,\mathrm{I}_\infty}\right](z) \end{pmatrix} = \begin{pmatrix} 1 & -i \\ 0 & 1 \end{pmatrix} \begin{pmatrix} \mathcal{B}_0\left[\psi^+_{z_4,\mathrm{I}_{\mathrm{mid}}}\right](z) \\ \mathcal{B}_0\left[\psi^-_{z_4,\mathrm{I}_{\mathrm{mid}}}\right](z) \end{pmatrix}. \tag{4.1.24}$$

Next, the regions $\mathrm{I}_{\mathrm{mid}}$ and I_0 are separated by a Stokes line emanating from z_3 and having the negative oreintation. In order to apply the formula (2.2.39), we have to change the normalization of the solutions in the r.h.s. of (4.1.24) as we have done in the derivation of

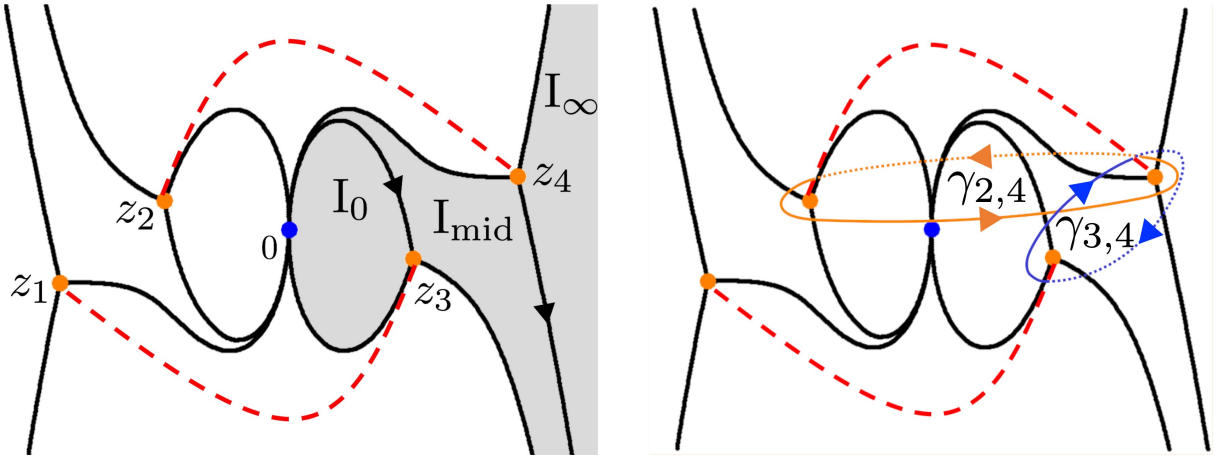

Figure 4.2: The Stokes graph at $\omega L = \frac{13}{10} - \frac{i}{16}$, $l = 0$ for $\arg(\eta) = 0$. The sheet of the WKB curve is taken so that $S_{\mathrm{even}}(z)dz$ has the positive sign. The orange points $z_1 = -z_4, z_2 = -z_3, z_3, z_4$ are the simple zeros and $\gamma_{2,4}, \gamma_{3,4}$ are the one-cycles on the WKB curve. The blue point indicates the origin, which is an irregular singularity of the differential equation (4.1.5). The black arrows on the stokes lines indicate the orientations of them (for the negative orientation, the arrow points to the branch point along the Stokes line, and for the positive orientation, the arrow points to the singular point.). The stokes lines going out of the frame flow at $z = \infty$, which is another irregular singularity of (4.1.5).

the exact energy quantization condition in the chapter 3 (e.g. (3.1.5)),

$$\begin{pmatrix} \mathcal{B}_0\left[\psi^+_{z_4,\mathrm{I}_{\mathrm{mid}}}\right](z) \\ \mathcal{B}_0\left[\psi^-_{z_4,\mathrm{I}_{\mathrm{mid}}}\right](z) \end{pmatrix} = \begin{pmatrix} e^{-\eta\mathcal{B}_0\left[\int_{z_3}^{z_4} S_{\mathrm{even}}(z)dz\right]} & 0 \\ 0 & e^{\eta\mathcal{B}_0\left[\int_{z_3}^{z_4} S_{\mathrm{even}}(z)dz\right]} \end{pmatrix} \begin{pmatrix} \mathcal{B}_0\left[\psi^+_{z_3,\mathrm{I}_{\mathrm{mid}}}\right](z) \\ \mathcal{B}_0\left[\psi^-_{z_3,\mathrm{I}_{\mathrm{mid}}}\right](z) \end{pmatrix}. \tag{4.1.25}$$

After that, the solutions in $\mathrm{I}_{\mathrm{mid}}$ and in I_0 normalized at z_2 are connected as follows,

$$\begin{pmatrix} \mathcal{B}_0\left[\psi^+_{z_3,\mathrm{I}_{\mathrm{mid}}}\right](z) \\ \mathcal{B}_0\left[\psi^-_{z_3,\mathrm{I}_{\mathrm{mid}}}\right](z) \end{pmatrix} = \begin{pmatrix} 1 & 0 \\ i & 1 \end{pmatrix} \begin{pmatrix} \mathcal{B}_0\left[\psi^+_{z_3,\mathrm{I}_0}\right](z) \\ \mathcal{B}_0\left[\psi^-_{z_3,\mathrm{I}_0}\right](z) \end{pmatrix}. \tag{4.1.26}$$

By multiplying (4.1.24)$\sim$(4.1.26) and finally restoring the normalization of the solutions in the r.h.s. of (4.1.26) from z_3 to z_4, we obtain the connection formula from $z \to +\infty$ to the origin,

$$\begin{pmatrix} \mathcal{B}_0\left[\psi^+_{z_4,\mathrm{I}_\infty}\right](z) \\ \mathcal{B}_0\left[\psi^-_{z_4,\mathrm{I}_\infty}\right](z) \end{pmatrix} = \begin{pmatrix} 1 + e^{\eta\mathcal{B}_0\left[2\int_{z_3}^{z_4} S_{\mathrm{even}}(z)dz\right]} & -i \\ ie^{\eta\mathcal{B}_0\left[2\int_{z_3}^{z_4} S_{\mathrm{even}}(z)dz\right]} & 1 \end{pmatrix} \begin{pmatrix} \mathcal{B}_0\left[\psi^+_{z_4,\mathrm{I}_0}\right](z) \\ \mathcal{B}_0\left[\psi^-_{z_4,\mathrm{I}_0}\right](z) \end{pmatrix}. \tag{4.1.27}$$

The integral $2\int_{z_3}^{z_4} S_{\mathrm{even}}(z)dz$ is equivalent to the WKB period for the one-cycle $\gamma_{3,4}$ in Fig.4.2.

Therefore the connection formula (4.1.27) can be expressed by using the WKB period,

$$\begin{pmatrix} \mathcal{B}_0\left[\psi^+_{z_4,\mathrm{I}_\infty}\right](z) \\ \mathcal{B}_0\left[\psi^-_{z_4,\mathrm{I}_\infty}\right](z) \end{pmatrix} = \begin{pmatrix} 1+e^{\eta\mathcal{B}_0\left[\Pi_{\gamma_{3,4}}\right]} & -i \\ ie^{\eta\mathcal{B}_0\left[\Pi_{\gamma_{3,4}}\right]} & 1 \end{pmatrix} \begin{pmatrix} \mathcal{B}_0\left[\psi^+_{z_4,\mathrm{I}_0}\right](z) \\ \mathcal{B}_0\left[\psi^-_{z_4,\mathrm{I}_0}\right](z) \end{pmatrix}. \tag{4.1.28}$$

The connection formula (4.1.28) is only derived at specific values of the parameters ωL and l. Therefore we need to discuss which the parameter regions our derivation is valid. As a first step, let us consider what happen if we vary ωL from $\omega L = 13/10 - i/16$ to $\omega L = 13/10 + i\delta$ ($\delta << 1$). Fig.4.3 shows the transition of the Stokes graph. The graph $[a]$ is the same as Fig.4.2. In the graph $[b]$, the Stokes region $\mathrm{I}_{\mathrm{mid}}$ narrows but survives. For this case, we obtain same connection formula as (4.1.28) because each formula for the Borel resummation of the WKB solutions that we have used to derive (4.1.28) only depends on which two adjacent Stokes regions we connect and the orientation of the Stokes line separating them. This example indicates that we obtain same connection formula (4.1.28) if the Stokes graph has the Stokes regions $\mathrm{I}_0, \mathrm{I}_{\mathrm{mid}}, \mathrm{I}_\infty$ regardless of their area. Conversely, we do not obtain the connection formula (4.1.28) in the case of the graph $[c]$ because the Stokes segment connecting z_3 and z_4 appears and the Stokes region $\mathrm{I}_{\mathrm{mid}}$ is completely crushed. Continuing to increase the imaginary part of ωL, we obtain the graph $[d]$. The Stokes segments in $[c]$ are separated into two Stokes lines again by the saddle reduction of the Stokes graph, but their position is inverted and there is no longer the Stokes region $\mathrm{I}_{\mathrm{mid}}$.

As the example of Fig.4.3, if we continuously change the parameters ωL and l, the Stokes graph (and the triangulation of Σ mapped from the Stokes graph) may be discontinuously changed by the saddle reduction and then the derivation of (4.1.28) is no longer valid. The sign of the saddle reduction of the Stokes graph is to appear the Stokes segments as the graph $[c]$ in Fig.4.3. The set of two simple zeros which are adjacent to a same Stokes region may be connected by the Stokes line. In the case of Fig.4.2, the simple zeros z_1 and z_2, z_2 and z_4, z_3 and z_4, z_1 and z_3 may be connected each other. By definition of the Stokes line (2.2.36), the conditions that these sets of the simple zeros are connected are given by the following equations,

$$\Im\left[2\int_{z_3}^{z_4} S_0(z)\,dz\right] = \Im\left[2\int_{z_1}^{z_2} S_0(z)\,dz\right] = 0, \tag{4.1.29}$$

$$\Im\left[2\int_{z_4}^{z_2} S_0(z)\,dz\right] = \Im\left[2\int_{z_3}^{z_1} S_0(z)\,dz\right] = 0, \tag{4.1.30}$$

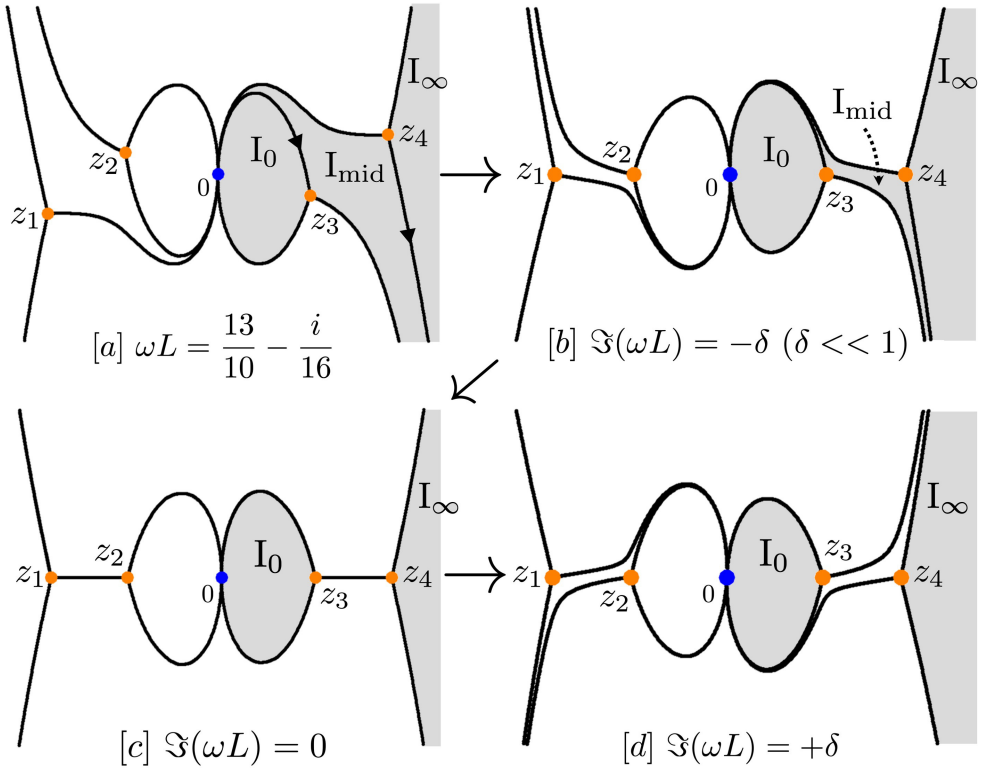

Figure 4.3: The deformation of the Stokes graph.

where we have used the parity invariance $S_0(-z) = S_0(z)$, which can be easily check from (4.1.6), and $z_1 = -z_4$, $z_2 = -z_3$. Each of the integrals can be expressed by the hypergeometric functions,

$$2\int_{z_3}^{z_4} S_0(z)\,dz = -\pi\left(1 - \frac{(l+2)^2}{2\omega^2 L^2}\right)\omega L\ {}_2F_1\left[\frac{1}{2}, \frac{1}{2}, 2, \frac{1}{2}\left(1 - \frac{(l+2)^2}{2\omega^2 L^2}\right)\right], \tag{4.1.31}$$

$$2\int_{z_4}^{z_2} S_0(z)\,dz = i\pi\left(1 + \frac{(l+2)^2}{2\omega^2 L^2}\right)\omega L\ {}_2F_1\left[\frac{1}{2}, \frac{1}{2}, 2, \frac{1}{2}\left(1 + \frac{(l+2)^2}{2\omega^2 L^2}\right)\right]. \tag{4.1.32}$$

(4.1.31) and (4.1.32) are local expressions but we can also obtain the expressions for other parameter regions by analytically continuing the hypergeometric functions. Dividing (4.1.29) and (4.1.30) by $(l+2)$ and substituting (4.1.31) and (4.1.32), we obtain the following conditions,

$$\Im\left[-\pi\left(1 - \frac{(l+2)^2}{2\omega^2 L^2}\right)\frac{\omega L}{(l+2)}\ {}_2F_1\left[\frac{1}{2}, \frac{1}{2}, 2, \frac{1}{2}\left(1 - \frac{(l+2)^2}{2\omega^2 L^2}\right)\right]\right] = 0, \tag{4.1.33}$$

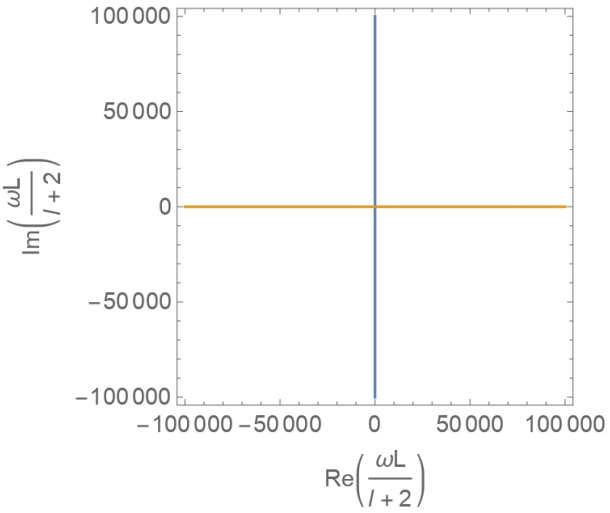

Figure 4.4: The orange line indicates the values of $\frac{\omega L}{l+2}$ satisfying (4.1.33) and the blue line indicates the values satisfying (4.1.34).

$$\Im\left[i\pi\left(1+\frac{(l+2)^2}{2\omega^2L^2}\right)\frac{\omega L}{(l+2)}\,{}_2F_1\left[\frac{1}{2},\frac{1}{2},2,\frac{1}{2}\left(1+\frac{(l+2)^2}{2\omega^2L^2}\right)\right]\right]=0. \tag{4.1.34}$$

In these expressions, there is only one parameter $\omega L/(l+2)$. Therefore we only need to check which value of $\omega L/(l+2)$ satisfies (4.1.33), (4.1.34). We can immediately find that (4.1.33) is satisfied by $\omega L/(l+2) \in \mathbb{R}$, which is consistent with the Stokes graph [c] in Fig.4.3, and (4.1.34) is satisfied by $\omega L/(l+2) \in i\mathbb{R}$. Fig.4.4 shows the points satisfying (4.1.33) or (4.1.34). In Fig.4.4, there are no points in the region $\Re(\omega L/(l+2)) > 0$ and $\Im(\omega L/(l+2)) < 0$, which includes $\omega L = \frac{13}{10} - i\frac{1}{16}$, $l = 0$. Therefore the derivation of (4.1.28) is valid for $\Re(\omega L/(l+2)) > 0$ and $\Im(\omega L/(l+2)) < 0$ region, which includes the QNMs, at least in the range depicted in Fig.4.4. We can also check arbitrary value of $\omega L/(l+2)$ by using (4.1.33) and (4.1.34).

Boundary conditions and an exact QNM condition

The quasi-normal modes for the D3-branes are the discrete set of ω at which the perturbation satisfies the following two boundary conditions [68],

(i) Only outgoing wave exists at $z \to +\infty$.

(ii) Only ingoing wave exists at $z \to 0$.

The outgoing wave at $z \to +\infty$ is the Borel resummation of the plus signed WKB solution $\mathcal{B}_0\left[\psi^+_{z_4,\mathrm{I}_\infty}\right](z)$. According to the connection formula (4.1.28), $\mathcal{B}_0\left[\psi^+_{z_4,\mathrm{I}_\infty}\right](z)$ is analytically

connected to $z \to 0$ as follows,

$$\mathcal{B}_0\left[\psi^+_{z_4,\mathrm{I}_\infty}\right](z) = \left(1 + e^{\eta\mathcal{B}_0\left[\Pi_{\gamma_{3,4}}\right]}\right)\mathcal{B}_0\left[\psi^+_{z_4,\mathrm{I}_0}\right](z) - i\mathcal{B}_0\left[\psi^-_{z_4,\mathrm{I}_0}\right](z). \tag{4.1.35}$$

The ingoing wave at $z \to 0$ is the Borel resummation of the minus signed WKB solution $\mathcal{B}_0\left[\psi^-_{z_4,\mathrm{I}_0}\right](z)$. Therefore to satisfy the boundary conditions (i) and (ii), the coefficient of $\mathcal{B}_0\left[\psi^+_{z_4,\mathrm{I}_0}\right](z)$ in the r.h.s. of (4.1.35) must to be zero,

$$1 + e^{\eta\mathcal{B}_0\left[\Pi_{\gamma_{3,4}}\right]} = 0. \tag{4.1.36}$$

Substituting $\eta = 1$ and taking the logarithm of (4.1.36), we obtain the exact condition for the QNMs,

$$\mathcal{B}_0\left[\Pi_{\gamma_{3,4}}\right] = 2\pi i\left(n + \frac{1}{2}\right), \tag{4.1.37}$$

where $n \in \mathbb{Z}_{\geq 0}$. Without considering convergence of the asymptotic series, the asymptotic expansion of the Borel resummation provides the all-order version of the Bohr-Sommerfeld condition,

$$\Pi_{\gamma_{3,4}} = 2\pi i\left(n + \frac{1}{2}\right). \tag{4.1.38}$$

In [68, 69], the r.h.s. of (4.1.38) is $2\pi n$ instead of $2\pi i\left(n + \frac{1}{2}\right)$. This mismatch comes from the difference of the definition for $S_{\mathrm{even}}(z)$. In this thesis, $S_{\mathrm{even}}(z)$ is an odd power of η. On the other hand, in [68, 69], $S_{\mathrm{even}}(z)$ is defined as an odd power of $1/\omega L$. Therefore $S_{\mathrm{even}}(z)$ in this paper is not the same ones in [68, 69].

The conditions (4.1.37) and (4.1.38) has no exponentially small terms as the exact quantization conditions for the double well potential (3.2.26), (3.2.27). From the point of view of the resurgence, it indicates there are no non-perturbative contributions to the asymptotic expansion of the QNMs for the D3-branes.

4.1.3 Computations of the QNMs for extremal D3-branes

In order to compute the QNMs from our conditions (4.1.37) and (4.1.38), we first need to evaluate the WKB period $\Pi_{\gamma_{3,4}}$. The leading term has already been given by (4.1.31). The higher order coefficients can be computed by applying the differential operator (2.2.20) to the leading term. To determine the differential operator, it is useful to transform the

Schrödinger equation (4.1.5). Under the following transformation,

$$\begin{aligned} \eta = \frac{1}{\hbar}, \quad \frac{(l+2)^2}{4} = u, \quad \Lambda = \frac{\omega L}{\sqrt{2}}, \\ z = e^{i\frac{x}{2}}, \quad \psi(z(x)) = e^{i\frac{x}{4}}\Psi(x), \end{aligned} \tag{4.1.39}$$

the Schrödinger equation (4.1.5) becomes the Mathieu differential equation,

$$\left[\hbar^2 \frac{d^2}{dx^2} - \Lambda^2 \cos(x) + u\right] \Psi(x) = 0. \tag{4.1.40}$$

(4.1.40) is also the quantum Seiberg-Witten curve for 4-dimensional $\mathcal{N} = 2$ SU(2) super Yang-Mills theory [44]. In the context of the gauge theory, u is the Coulomb moduli parameter, Λ_1 is the dynamically generated scale, and $\hbar$ is the deformation parameter in the Nekrasov-Shatashvili limit of the Ω-background. Under the transformation (4.1.39), it is shown that the WKB periods are invariant (Proposition 2.7 (b) in [25]). Therefore computing the WKB periods for (4.1.5) is equivalent to computing the WKB periods for (4.1.40). Up to 8th-order, the differential operator for the quantum Seiberg-Witten curve for 4-dimensional $\mathcal{N} = 2$ SU(2) super Yang-Mills theory is given as follows (e.g. [45]),

$$\begin{aligned} \mathcal{O}_2 &= \frac{u}{12}\frac{\partial^2}{\partial u^2} + \frac{1}{24}\frac{\partial}{\partial u}, \\ \mathcal{O}_4 &= \frac{1}{2^7}\left(\frac{28u^2}{45}\frac{\partial^4}{\partial u^4} + \frac{8u}{3}\frac{\partial^3}{\partial u^3} + \frac{5}{3}\frac{\partial^2}{\partial u^2}\right), \\ \mathcal{O}_6 &= \frac{1}{2^9}\left(\frac{124u^3}{945}\frac{\partial^6}{\partial u^6} + \frac{158u^2}{105}\frac{\partial^5}{\partial u^5} + \frac{153u}{35}\frac{\partial^4}{\partial u^4} + \frac{41}{14}\frac{\partial^3}{\partial u^3}\right), \\ \mathcal{O}_8 &= \frac{1}{2^8}\left(\frac{127u^4}{2^3\times 4725}\frac{\partial^8}{\partial u^8} + \frac{13u^3}{175}\frac{\partial^7}{\partial u^7} + \frac{517u^2}{2^4\times 63}\frac{\partial^6}{\partial u^6} + \frac{9539u}{2^3\times 945}\frac{\partial^5}{\partial u^5} + \frac{15229}{2^7\times 135}\frac{\partial^4}{\partial u^4}\right). \end{aligned} \tag{4.1.41}$$

After computing the WKB period by using the differential operator (4.1.41), we have to take the Borel resummation. To compute the Borel resummation by definition (2.2.24), we need an infinite number of the coefficients of the WKB period, but it is impossible to compute them by the differential operator technique. Instead, we use the Borel-Padé approximation,

$$\mathcal{B}_0\left[\Pi_{\gamma_{3,4}}\right] \sim \int_0^\infty e^{-\xi}\,[N/N]\,d\xi, \tag{4.1.42}$$

where $[N/N]$ indicates the diagonal Padé approximation of order N for $\Pi_{\gamma_{21}}$.

Table 4.1 shows the numerical results of the QNMs. In the results of the Exact WKB

n	l	Leaver's method	Classical WKB	Exact WKB (Borel-Padé)
0	0	$1.369686 - 0.503996i$	$\underline{\mathbf{1.36968}}2 - \underline{\mathbf{0.50399}}3i$	$\underline{\mathbf{1.369686}} - \underline{\mathbf{0.503996}}i$
	1	$2.091757 - 0.501753i$	$\underline{\mathbf{2.09175}}6 - \underline{\mathbf{0.501753}}i$	$\underline{\mathbf{2.091757}} - \underline{\mathbf{0.501753}}i$
	2	$2.806287 - 0.500981i$	$\underline{\mathbf{2.806287}} - \underline{\mathbf{0.500981}}i$	$\underline{\mathbf{2.806287}} - \underline{\mathbf{0.500981}}i$
1	0	$0.682086 - 1.559933i$	$\underline{\mathbf{0.68}}4094 - \underline{\mathbf{1.5}}65097i$	$\underline{\mathbf{0.6820}}58 - \underline{\mathbf{1.5599}}98i$
	1	$1.704812 - 1.518680i$	$\underline{\mathbf{1.70481}}2 - \underline{\mathbf{1.51867}}9i$	$\underline{\mathbf{1.704812}} - \underline{\mathbf{1.518680}}i$
	2	$2.528152 - 1.509655i$	$\underline{\mathbf{2.528152}} - \underline{\mathbf{1.509655}}i$	$\underline{\mathbf{2.528152}} - \underline{\mathbf{1.509655}}i$

Table 4.1: Numerical results of the QNMs for the D3-branes. The first column is the results of the Leaver's method. The second column is the results of the all-order QNMs condition (4.1.38), which is not taken the Borel resummation. The third column is the results of the exact QNMs condition (4.1.37) calculated by the Borel-Padé approximation.

method, we have used the diagonal Padé approximation of $N = 4$ case with 8th-order coefficients of the WKB period.

We can also obtain analytic forms of the QNMs. The coefficients of the WKB period $\Pi_{\gamma_{3,4}}$ can be expanded at $\omega L = \frac{l+2}{\sqrt{2}}$ as follows,

$$\begin{aligned}
\Pi^{(0)}_{\gamma_{3,4}} &= -2\pi\left(\omega L - \frac{l+2}{\sqrt{2}}\right) + \frac{3\pi\left(\omega L - \frac{l+2}{\sqrt{2}}\right)^2}{2\sqrt{2}(l+2)} + \cdots, \\
\Pi^{(2)}_{\gamma_{3,4}} &= \frac{\pi}{8\sqrt{2}(l+2)} - \frac{3\pi\left(\omega L - \frac{l+2}{\sqrt{2}}\right)}{64(l+2)^2} - \frac{\pi\left(\omega L - \frac{l+2}{\sqrt{2}}\right)^2}{256\sqrt{2}(l+2)^3} + \cdots, \\
\Pi^{(4)}_{\gamma_{3,4}} &= -\frac{17\pi}{2048\sqrt{2}(l+2)^3} + \frac{95\pi\left(\omega L - \frac{l+2}{\sqrt{2}}\right)}{32768(l+2)^4} + \frac{1959\pi\left(\omega L - \frac{l+2}{\sqrt{2}}\right)^2}{131072\sqrt{2}(l+2)^5} + \cdots.
\end{aligned} \tag{4.1.43}$$

Then the all-order Bohr-Sommerfeld condition (4.1.38) can be written as

$$2\pi i\left(n + \frac{1}{2}\right) = \Pi^{(0)}_{\gamma_{3,4}} + \Pi^{(2)}_{\gamma_{3,4}} + \Pi^{(4)}_{\gamma_{3,4}} + \cdots = \sum_{m=0}^{\infty} c_m \left(\omega L - \frac{l+2}{\sqrt{2}}\right)^m. \tag{4.1.44}$$

Inverting the series (4.1.44) by using the Lagrange inversion theorem, we obtain an analytic expression of the QNMs,

$$\omega_n L = \frac{l+2}{\sqrt{2}} + \frac{2\pi i\left(n + \frac{1}{2}\right) - c_0}{c_1} - \frac{c_2(2\pi i\left(n + \frac{1}{2}\right) - c_0)^2}{c_1^3} + \cdots. \tag{4.1.45}$$

In Table.4.2, we numerically compare the Leaver's method and (4.1.45), where we have used up to 8th-order coefficients of the WKB period and 16th-order of (4.1.45).

n	l	Leaver's method	(4.1.45)
0	0	$1.369686 - 0.503996i$	$\underline{\mathbf{1.36968}}2 - \underline{\mathbf{0.50399}}3i$
	1	$2.091757 - 0.501753i$	$\underline{\mathbf{2.09175}}6 - \underline{\mathbf{0.501753}}i$
	2	$2.806287 - 0.500981i$	$\underline{\mathbf{2.806287}} - \underline{\mathbf{0.500981}}i$
1	0	$0.682086 - 1.559933i$	$\underline{\mathbf{0.682}}296 - \underline{\mathbf{1.559}}289i$
	1	$1.704812 - 1.518680i$	$\underline{\mathbf{1.704812}} - \underline{\mathbf{1.51867}}9i$
	2	$2.528152 - 1.509655i$	$\underline{\mathbf{2.528152}} - \underline{\mathbf{1.509655}}i$

Table 4.2: The numerical results of (4.1.45).

In the large n limit, which corresponds to $|\omega L| \gg (l+2)$ limit, the leading order approximation (or the classical WKB approximation) is valid,

$$\Pi^{(0)}_{\gamma_{3,4}} = 2\pi i \left(n + \frac{1}{2}\right). \tag{4.1.46}$$

In this limit, the leading term of the WKB period (4.1.31) becomes

$$\Pi^{(0)}_{\gamma_{3,4}} = -\pi\omega L \; {}_2F_1\left[\frac{1}{2}, \frac{1}{2}, 2, \frac{1}{2}\right]. \tag{4.1.47}$$

Substituting (4.1.47) into (4.1.46) and rearranging the equation, we obtain the QNMs at large n,

$$\omega L = -i \frac{2\left(n + \frac{1}{2}\right)}{{}_2F_1\left[\frac{1}{2}, \frac{1}{2}, 2, \frac{1}{2}\right]}. \tag{4.1.48}$$

In some black hole geometries, it is known that the real part of the QNMs in large n limit is proportional to the entropy of the black hole (e.g. 4d Schwarzschild BH [77], 4d Schwarzschild BH and 4d Reissner-Nordström BH [78], d≥4 Schwarzschild BH and 4d Reissner-Nordström BH [79]). It is also true for the present case (4.1.48) because the extremal D3-brane metric (4.1.1) has no event horizon and therefore the entropy is zero [80].

4.2 Massless scalar perturbation to extremal M5-branes

4.2.1 E.O.M. and QNMs for scalar field in extremal M5-brane metric

The geometry of a stack of the extremal M5-branes is given by the following line element [81],

$$ds^2 = A(r)^{-1/3}\left(-dt^2 + dx_1^2 + \cdots + dx_5^2\right) + A(r)^{2/3}\left(dr^2 + r^2 d\Omega_4^2\right), \tag{4.2.1}$$

where $A(r) = 1 + \frac{R^3}{r^3}$, R is a positive real parameter, $(t, x_1, \cdots, x_5)$ are the coordinates on the M5-branes world-volume, r is the radial coordinate and $d\Omega_4^2$ is the metric on S^4 in the bulk of the M5-branes. We consider a massless scalar field Φ in this background obeying the E.O.M.:

$$\Box\Phi = \frac{1}{\sqrt{-g}}\partial_M\left(\sqrt{-g}g^{MN}\partial_N\right)\Phi = 0, \tag{4.2.2}$$

where g_{MN} $(M, N = 0, 1, \cdots, 10)$ is the metric given by (4.2.1) and $g = \det g_{MN}$. Under the separation of the variables, the solution to (4.2.2) takes the form

$$\Phi = e^{-iEt + i\boldsymbol{k}\cdot\boldsymbol{x}} r^4 \phi(r) \mathcal{Y}^l_{\boldsymbol{m}}(\boldsymbol{\theta}), \tag{4.2.3}$$

where $\mathcal{Y}^l_{\boldsymbol{m}}(\boldsymbol{\theta})$ is the spherical harmonics on S^4 obeying $\Delta_{S^4}\mathcal{Y}^l_{\boldsymbol{m}}(\boldsymbol{\theta}) = -l\,(l+3)\,\mathcal{Y}^l_{\boldsymbol{m}}(\boldsymbol{\theta})$, l and $\boldsymbol{m} = (m_1, m_2, m_3)$ are integers satisfying $|m_1| \leq m_2 \leq m_3 \leq l$ and $\boldsymbol{\theta}$ denotes the angular coordinates on S^4. The radial part $\phi(r)$ of Φ satisfies the second-order differential equation [74],

$$\left[\rho^{-4}\frac{d}{d\rho}\rho^4\frac{d}{d\rho} + 1 + \frac{(\omega R)^3}{\rho^3} - \frac{l\,(l+3)}{\rho^2}\right]\phi(\rho/\omega) = 0, \quad (\rho = \omega r) \tag{4.2.4}$$

where $\omega = \sqrt{E^2 - \boldsymbol{k}^2}$. Introducing z by $\rho = \omega R z$ and $\psi(z)$ by $\phi(\rho/\omega) = (\omega R z)^{-2}\psi(z)$, (4.2.4) becomes the Schrödinger type differential equation,

$$\left[\frac{d^2}{dz^2} - \eta^2 Q_0(z) - Q_2(z)\right]\psi(z) = 0, \tag{4.2.5}$$

with

$$Q_0(z) = -\frac{(\omega R)^2\,(z^3+1) - \left(l + \frac{3}{2}\right)^2 z}{z^3}, \quad Q_2(z) = -\frac{1}{4z^2}, \tag{4.2.6}$$

and $\eta = 1$. We keep η as a complex parameter.

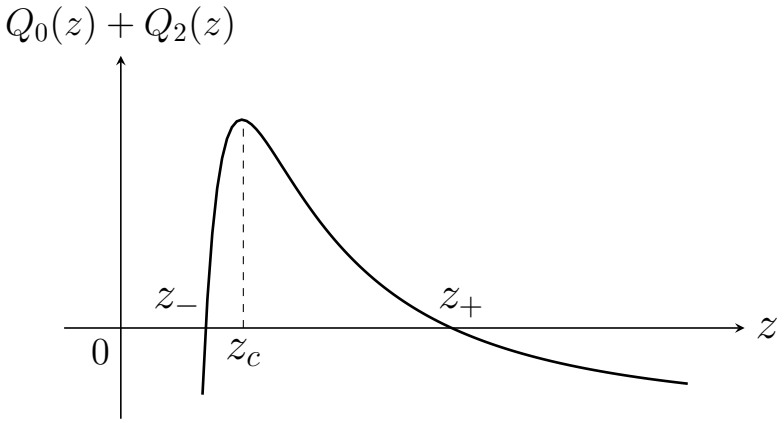

Figure 4.5: A potential graph of $Q_0(z)+Q_2(z)$.

WKB approximation for extremal D3-branes

At large l, the QNMs can be determined from the Bohr-Sommerfeld quantization condition [43],

$$\int_{z_-}^{z_+} \sqrt{Q_0(z)+Q_2(z)}dz = \pi i\left(n+\frac{1}{2}\right), \tag{4.2.7}$$

where $n \in \mathbb{Z}_{\geq 0}$ and $z_\pm$ are the turning points satisfying $Q_0(z_\pm)+Q_2(z_\pm)=0$ (Fig.4.5). At large l, the turning points close each other and the l.h.s. of (4.1.7) can be integrated by approximating $Q_0(z)+Q_2(z)$ by its expansion at the maximum point z_c (Fig.4.5). Then (4.1.7) reduces to

$$\frac{Q_0(z_c)+Q_2(z_c)}{\sqrt{2\left(Q_0''(z_c)+Q_2''(z_c)\right)}} = i\left(n+\frac{1}{2}\right). \tag{4.2.8}$$

The condition (4.2.8) can be solved perturbatively with respect to the imaginary part of ωR. Up to the linear order, one finds

$$\omega R = \frac{\sqrt[3]{2}}{\sqrt{3}}\sqrt{\left(l+\frac{3}{2}\right)^2-\frac{1}{4}} - i\frac{\sqrt[3]{2}}{\sqrt{3}}\left(n+\frac{1}{2}\right). \tag{4.2.9}$$

The formula (4.2.9) indicates that the real part of the QNMs only depends on l and the imaginary part only depends on n in the large l region.

Leaver's method for extremal M5-branes

By substituting $z = (1-x)/x$, (4.1.10) and (4.1.13) into (4.2.5), we obtain a seven-term recurrence relation

$$\begin{aligned}
&\alpha_0 f_2 + \beta_0 f_1 + \gamma_0 f_0 = 0,\\
&\alpha_1 f_3 + \beta_1 f_2 + \gamma_1 f_1 + \delta_0 f_0 = 0,\\
&\alpha_2 f_4 + \beta_2 f_3 + \gamma_2 f_2 + \delta_1 f_1 + \epsilon_0 f_0 = 0,\\
&\alpha_3 f_5 + \beta_3 f_4 + \gamma_3 f_3 + \delta_2 f_2 + \epsilon_1 f_1 + \rho_0 f_0 = 0,\\
&\alpha_{n-2} f_n + \beta_{n-2} f_{n-1} + \gamma_{n-2} f_{n-2} + \delta_{n-3} f_{n-3} + \epsilon_{n-4} f_{n-4} + \rho_{n-5} f_{n-5} + \sigma_{n-6} f_{n-6} = 0, \quad (n \geq 6),
\end{aligned} \tag{4.2.10}$$

with coefficients

$$\begin{aligned}
\alpha_n &= -\frac{1}{64}(1+n)(2+n),\\
\beta_n &= \frac{1}{16}(1+n)n,\\
\gamma_n &= \frac{1}{16}(-1+n)n + \frac{1}{4}n - in\omega R + \frac{5}{8} + \frac{3l}{4} + \frac{l^2}{4} - \frac{i\omega R}{2} - \frac{(\omega R)^2}{2},\\
\delta_n &= -\frac{1}{2}(-1+n)n - n + 4in\omega R - \frac{5}{2} - 3l - l^2 + 2i\omega R + 3(\omega R)^2,\\
\epsilon_n &= \frac{1}{4}(-1+n)n - 4in\omega R + 2 + 3l + l^2 - 2i\omega R,\\
\rho_n &= (-1+n)n + 4n + 2,\\
\sigma_n &= -(-1+n)n - 4n - 2.
\end{aligned} \tag{4.2.11}$$

(4.2.10) cannot be reduced to a three-term recurrence relation by using the gaussian elimination. Therefore we cannot use the Leaver's continuous fraction method to (4.2.5). We also tried to calculate the QNMs by computing the determinant of the coefficient matrix of the equations (4.2.10) directly, but we were not able to obtain the results with enough convergence. According to these reasons, it is thought that the Exact WKB analysis is a convenient tool to study the QNMs for the M5-branes.

4.2.2 Exact QNMs condition for extremal M5-branes

Stokes graph

First, we discuss generic properties of the Stokes graphs of the model. Let z_1, z_2, z_3 be the zeros of $Q_0(z)$ ordered as $\Re(z_1) \leq \Re(z_2) \leq \Re(z_3)$. We assume z_1, z_2, z_3 are simple zeros. The three Stokes lines then emanate from each zero. The endpoints of the Stokes lines are on either $z_1, z_2, z_3, 0, \infty$. By substituting the explicit form of $p_0(z) = \sqrt{Q_0(z)}$ into the definition of the Stokes lines (2.2.36) and dividing by the real parameter $l + \frac{3}{2}$, one finds that (2.2.36) depends on only the combination of the parameters $\omega R/\left(l + \frac{3}{2}\right)$ and η.

The Stokes graphs can be classified according to how the Stokes regions are adjacent to each other (or which triangulation of Σ the Stokes graph is mapped). If we continuously change $\theta = \arg(\eta)$, the state of the adjacent of the Stokes regions may be discontinuously changed at specific values of $\arg(\eta)$. We refer the discontinuous change of the Stokes graph as saddle reduction [25]. We specify when this saddle reduction occurs with respect to the value of $\omega R/\left(l + \frac{3}{2}\right)$ instead of $\arg(\eta)$. The sign of the saddle reduction is to appear the Stokes line that connects two zeros of $Q_0(z)$. By definition of the Stokes lines (2.2.36), the parameters at which two of z_1, z_2, z_3 are connected can be determined by the following equations,

$$\Im\left[e^{i\theta}\int_{z_1}^{z_3} p_0(z)\,dz\right] = 0, \tag{4.2.12}$$

$$\Im\left[e^{i\theta}\int_{z_2}^{z_3} p_0(z)\,dz\right] = 0, \tag{4.2.13}$$

$$\Im\left[e^{i\theta}\int_{z_1}^{z_2} p_0(z)\,dz\right] = 0. \tag{4.2.14}$$

The integrals in the square brackets are the elliptic integrals and can also be expressed by the hypergeometric function [52, 82],

$$\int_{z_1}^{z_3} p_0(z)\,dz = i\pi\left(l+\frac{3}{2}\right)\ {}_2F_1\left[-\frac{1}{6},\frac{1}{6},1,\frac{27\omega^6R^6}{4(l+\frac{3}{2})^6}\right], \tag{4.2.15}$$

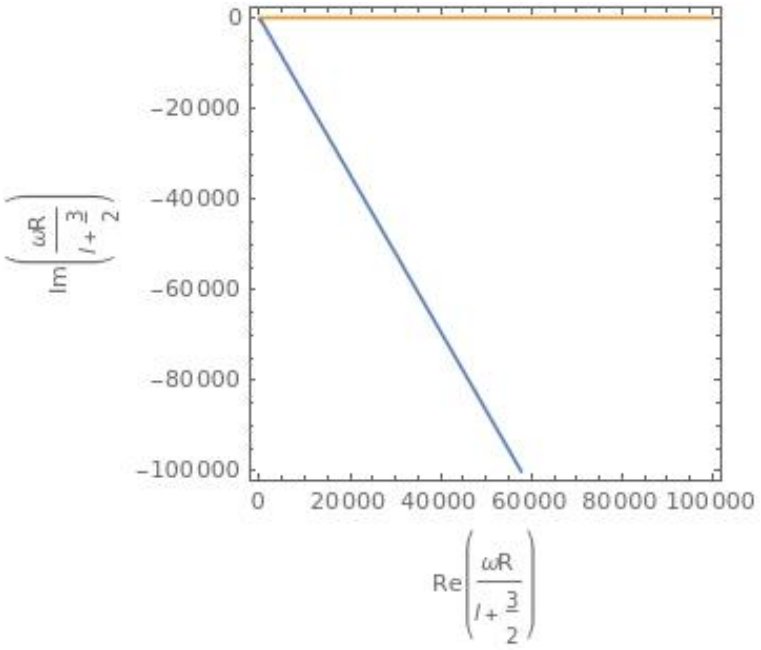

Figure 4.6: The parameters satisfying (4.2.12)∼(4.2.14) at $\arg(\eta) = 0$. The orange line indicates the value of $\omega R/\left(l+\frac{3}{2}\right)$ satisfying (4.2.13). The blue line, which is drawn on $\arg(\omega R) = -\frac{\pi}{3}$, indicates the value satisfying (4.2.14). There are no points satisfying (4.2.12).

$$\int_{z_2}^{z_3} p_0(z)\,dz = \begin{cases} -\frac{\pi\omega R\left(1-\frac{4(l+\frac{3}{2})^6}{27\omega^6R^6}\right)}{2\sqrt[3]{2}\sqrt{3}}\ {}_2F_1\left[\frac{5}{6},\frac{5}{6},2,1-\frac{4(l+\frac{3}{2})^6}{27\omega^6R^6}\right] & \left(-\frac{\pi}{6}\le\arg(\omega R)\le 0\right), \\ \int_{z_1}^{z_3} p_0(z)\,dz - e^{i\frac{\pi}{3}}\frac{\pi\omega R\left(1-\frac{4(l+\frac{3}{2})^6}{27\omega^6R^6}\right)}{2\sqrt[3]{2}\sqrt{3}}\ {}_2F_1\left[\frac{5}{6},\frac{5}{6},2,1-\frac{4(l+\frac{3}{2})^6}{27\omega^6R^6}\right] & \\ \qquad\qquad \left(-\frac{\pi}{2}\le\arg(\omega R)<-\frac{\pi}{6}\right), \end{cases} \tag{4.2.16}$$

$$\int_{z_1}^{z_2} p_0(z)\,dz = -\int_{z_2}^{z_3} p_0(z)\,dz + \int_{z_1}^{z_3} p_0(z)\,dz. \tag{4.2.17}$$

These are local expressions but we can also compute each integral for other parameter regions by analytically continuing the hypergeometric function. By substituting (4.2.15)∼(4.2.17) into (4.2.12)∼(4.2.14), we can determine the values of the parameters occurring the saddle reduction. Fig.4.6 shows the values of $\omega R/\left(l+\frac{3}{2}\right)$ satisfying (4.2.12)∼(4.2.14) at $\arg(\eta) = 0$ in a range. Fig.4.6 indicates that the Stokes line connecting z_1 and z_2 appears at $\arg(\omega R) = -\frac{\pi}{3}$. Therefore the state of the adjacent of the Stokes regions is discontinuously changed between $-\frac{\pi}{3} < \arg(\omega R) < 0$ and $-\frac{\pi}{2} \le \arg(\omega R) < -\frac{\pi}{3}$.

Let us see examples of the Stokes graphs. Fig.4.7 shows the Stokes graph for $\arg(\eta) = 0$ and $\omega R/\left(l+\frac{3}{2}\right) = \frac{2}{3} - i\frac{2}{30}$, which is in the region $-\frac{\pi}{3} < \arg(\omega R) < 0$. For $\arg(\eta) = 0$ and $-\frac{\pi}{3} < \arg(\omega R) < 0$, the Stokes regions are adjacent each other in the same way as Fig.4.7

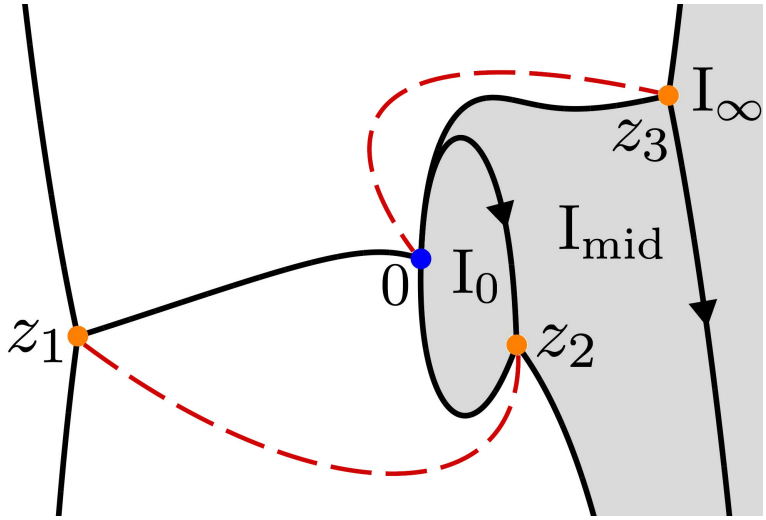

Figure 4.7: The Stokes graph for $\arg(\eta) = 0$ with $\omega R/\left(l+\frac{3}{2}\right) = \frac{2}{3} - i\frac{2}{30}$. The sheet of Σ is taken so that $P_{\mathrm{even}}(z)dz$ has the positive sign. The orange points z_1, z_2, z_3 are the zeros of $Q_0(z)$. The blue point is the origin. The red dashed lines are the branch cuts. The black lines are the Stokes lines and the black arrows show the orientation (for the negative orientation, the arrow points to the zeros of $Q_0(z)$ along the Stokes line, and for the positive orientation, the arrow points to the singular point). The stokes lines going out of the frame flow at $z = \infty$. The gray regions named I_∞, $\mathrm{I}_{\mathrm{mid}}$, I_0 are Stokes regions.

(for example, the Stokes region I_∞ is adjacent to $\mathrm{I}_{\mathrm{mid}}$, and $\mathrm{I}_{\mathrm{mid}}$ is adjacent to I_0.).

Fig.4.8 shows the saddle reduction at $\arg(\omega R) = -\frac{\pi}{3}$ with $|\omega R/\left(l+\frac{3}{2}\right)| = |\frac{2}{3} - i\frac{2}{30}|$. In the graph [a], the state of the adjacent of the Stokes regions does not change from Fig.4.7 (the Stokes region I_∞ is adjacent to $\mathrm{I}_{\mathrm{mid}}$, and $\mathrm{I}_{\mathrm{mid}}$ is adjacent to I_0). In the graph [b], two Stokes lines emanating from z_1 and z_2 overlap and become one Stokes line connecting z_1 and z_2. Continuing to decrease $\arg(\omega R)$, we obtain the graph [c] and [d]. In these cases, the Stokes line connecting z_1 and z_2 in [b] separates again but their positions invert. The new Stokes region $\tilde{\mathrm{I}}_{\mathrm{mid}}$ then appears between $\mathrm{I}_{\mathrm{mid}}$ and I_0. For $\arg(\eta) = 0$ and $-\frac{\pi}{2} \leq \arg(\omega R) < -\frac{\pi}{3}$, the Stokes regions are adjacent each other in the same way as [c] and [d] in Fig.4.8.

Connection problem

We solve the connection problem of the Borel resummed WKB solutions for $\arg(\eta) = 0$ from $z = \infty$ to the origin based on the Stokes graphs.

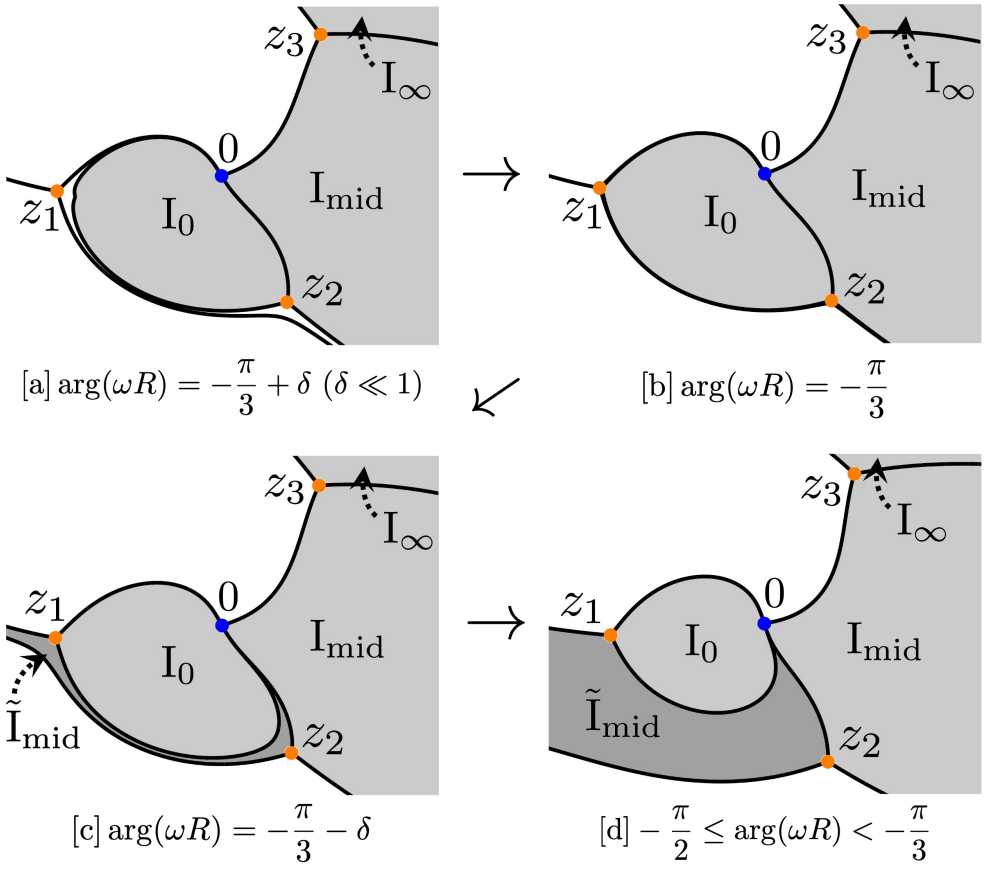

Figure 4.8: The saddle reduction of the Stokes graph.

Connection problem for $-\frac{\pi}{3} < \arg(\omega R) < 0$

For $-\frac{\pi}{3} < \arg(\omega R) < 0$, we obtain the Stokes graph of the type Fig.4.7. The connection problem from infinity to the origin is solved by computing the connection of the solutions from the Stokes region I_∞ to $\mathrm{I}_{\mathrm{mid}}$ and $\mathrm{I}_{\mathrm{mid}}$ to I_0. Between I_∞ and $\mathrm{I}_{\mathrm{mid}}$, there is a Stokes line emanating from z_3 and having the positive orientation. Then it is shown that the Borel resummed WKB solutions in the regions I_∞ and $\mathrm{I}_{\mathrm{mid}}$ are connected by the following connection formula,

$$\begin{pmatrix} \mathcal{B}_0\left[\psi^+_{z_3,\mathrm{I}_\infty}\right](z) \\ \mathcal{B}_0\left[\psi^-_{z_3,\mathrm{I}_\infty}\right](z) \end{pmatrix} = \begin{pmatrix} 1 & -i \\ 0 & 1 \end{pmatrix} \begin{pmatrix} \mathcal{B}_0\left[\psi^+_{z_3,\mathrm{I}_{\mathrm{mid}}}\right](z) \\ \mathcal{B}_0\left[\psi^-_{z_3,\mathrm{I}_{\mathrm{mid}}}\right](z) \end{pmatrix}, \tag{4.2.18}$$

where we have denoted the solutions in I_∞ as $\psi^{\pm}_{z_3,\mathrm{I}_\infty}(z)$ ($\pm$ in the superscript is the sign of $\pm P_{\mathrm{even}}(z)dz$ and z_3 in the subscript is the normalization point), and the solutions in $\mathrm{I}_{\mathrm{mid}}$ in the same way. Next, between $\mathrm{I}_{\mathrm{mid}}$ and I_0, there is a Stokes line emanating from z_2 and having the negative orientation. In order to apply the connection formula, we need to

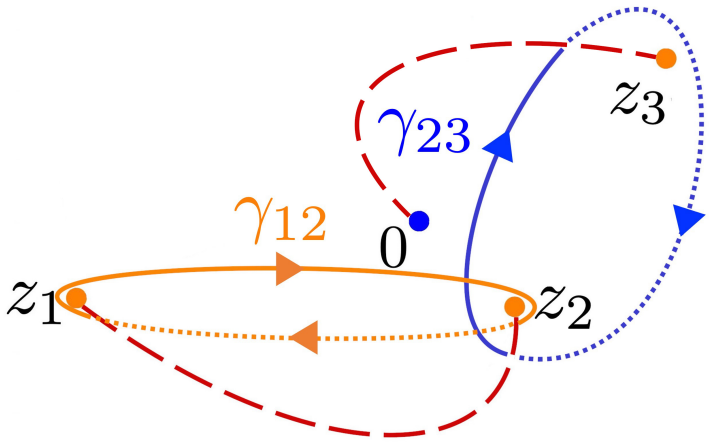

Figure 4.9: The one-cycles on Σ. The red dashed lines are the branch cuts. The solid segment in each cycle lies on the sheet of Σ on where $P_{\rm even}(z)dz$ has the positive sign. The dashed segment in each cycle lies on the sheet of Σ on where $P_{\rm even}(z)dz$ has the negative sign. The arrows on the cycles indicate the orientation.

change the normalization of the solutions,

$$\begin{pmatrix} \mathcal{B}_0\left[\psi^+_{z_3,\mathrm{I}_{\rm mid}}\right](z) \\ \mathcal{B}_0\left[\psi^-_{z_3,\mathrm{I}_{\rm mid}}\right](z) \end{pmatrix} = \begin{pmatrix} e^{-\eta\mathcal{B}_0\left[\int_{z_2}^{z_3} P_{\rm even}(z)dz\right]} & 0 \\ 0 & e^{\eta\mathcal{B}_0\left[\int_{z_2}^{z_3} P_{\rm even}(z)dz\right]} \end{pmatrix} \begin{pmatrix} \mathcal{B}_0\left[\psi^+_{z_2,\mathrm{I}_{\rm mid}}\right](z) \\ \mathcal{B}_0\left[\psi^-_{z_2,\mathrm{I}_{\rm mid}}\right](z) \end{pmatrix}, \tag{4.2.19}$$

where we have used the property that the Borel resummation commutes with addition and multiplication (2.2.27). After changing the normalization, the solutions in $\mathrm{I}_{\rm mid}$ and I_0 are connected as follows,

$$\begin{pmatrix} \mathcal{B}_0\left[\psi^+_{z_2,\mathrm{I}_{\rm mid}}\right](z) \\ \mathcal{B}_0\left[\psi^-_{z_2,\mathrm{I}_{\rm mid}}\right](z) \end{pmatrix} = \begin{pmatrix} 1 & 0 \\ i & 1 \end{pmatrix} \begin{pmatrix} \mathcal{B}_0\left[\psi^+_{z_2,\mathrm{I}_0}\right](z) \\ \mathcal{B}_0\left[\psi^-_{z_2,\mathrm{I}_0}\right](z) \end{pmatrix}. \tag{4.2.20}$$

By multiplying (4.2.18)$\sim$(4.2.20) and finally restoring the normalization of $\psi^{\pm}_{z_2,\mathrm{I}_0}$ in the r.h.s. of (4.2.20) from z_2 to z_3, we obtain the solution of the connection problem for $-\frac{\pi}{3} < \arg(\omega R) < 0$,

$$\begin{pmatrix} \mathcal{B}_0\left[\psi^+_{z_3,\mathrm{I}_\infty}\right](z) \\ \mathcal{B}_0\left[\psi^-_{z_3,\mathrm{I}_\infty}\right](z) \end{pmatrix} = \begin{pmatrix} 1+e^{\eta\mathcal{B}_0\left[2\int_{z_2}^{z_3} P_{\rm even}(z)dz\right]} & -i \\ ie^{\eta\mathcal{B}_0\left[2\int_{z_2}^{z_3} P_{\rm even}(z)dz\right]} & 1 \end{pmatrix} \begin{pmatrix} \mathcal{B}_0\left[\psi^+_{z_3,\mathrm{I}_0}\right](z) \\ \mathcal{B}_0\left[\psi^-_{z_3,\mathrm{I}_0}\right](z) \end{pmatrix}. \tag{4.2.21}$$

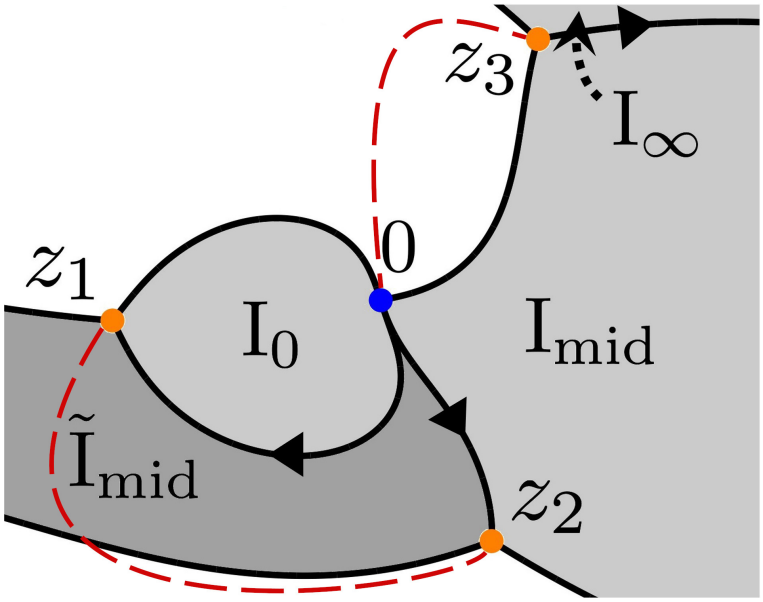

Figure 4.10: The Stokes graph for $\arg(\eta) = 0$ and $-\frac{\pi}{2} \leq \arg(\omega R) < -\frac{\pi}{3}$.

The integral $2\int_{z_2}^{z_3} P_{\mathrm{even}}(z)dz$ is equivalent to the WKB period for the one-cycle γ_{23} in Fig.4.9. Therefore (4.2.21) can be expressed in terms of the WKB period,

$$\begin{pmatrix} \mathcal{B}_0\left[\psi^+_{z_3,\mathrm{I}_\infty}\right](z) \\ \mathcal{B}_0\left[\psi^-_{z_3,\mathrm{I}_\infty}\right](z) \end{pmatrix} = \begin{pmatrix} 1+e^{\eta\mathcal{B}_0[\Pi_{\gamma_{23}}]} & -i \\ ie^{\eta\mathcal{B}_0[\Pi_{\gamma_{23}}]} & 1 \end{pmatrix} \begin{pmatrix} \mathcal{B}_0\left[\psi^+_{z_3,\mathrm{I}_0}\right](z) \\ \mathcal{B}_0\left[\psi^-_{z_3,\mathrm{I}_0}\right](z) \end{pmatrix}. \tag{4.2.22}$$

Connection problem for $-\frac{\pi}{2} \leq \arg(\omega R) < -\frac{\pi}{3}$

For $-\frac{\pi}{2} \leq \arg(\omega R) < -\frac{\pi}{3}$, we obtain the Stokes graph of the type [c] and [d] in Fig.4.8. The orientation of the Stokes lines and the branch cuts on Σ is drawn in Fig.4.10.

We will solve the connection problem of the Borel resummed WKB solutions from infinity to the origin. Around $z = 0$, the exponential factor of the WKB solutions (2.2.13) can be approximated as

$$\int S_0(z)dz = i\int \sqrt{\frac{(\omega R)^2(z^3+1) - \left(l+\frac{3}{2}\right)^2 z}{z^3}}dz \sim i\omega R\int z^{-\frac{3}{2}}dz = -2i\omega R z^{-\frac{1}{2}}. \tag{4.2.23}$$

Therefore, the WKB solutions around the origin behave as

$$\psi^\pm \sim e^{\mp 2i\frac{\omega R}{\sqrt{z}}}. \tag{4.2.24}$$

When $\arg(z) = 2\arg(\omega R)$, ψ^- becomes the pure ingoing wave at the origin. For $-\frac{\pi}{2} \leq$

$\arg(\omega R) < -\frac{\pi}{3}$, we take the solution in the region I_0 in Fig.4.10 so that the boundary condition at the origin is satisfied. Similarly, around $z = \infty$, we obtain

$$\int S_0(z)dz \sim i\omega R \int dz = i\omega R z, \tag{4.2.25}$$

and

$$\psi^{\pm} \sim e^{\pm i\omega R z}. \tag{4.2.26}$$

When $\arg(z) = -\arg(\omega R)$, ψ^+ becomes the pure outgoing wave at infinity. For $-\frac{\pi}{2} \leq \arg(\omega R) < -\frac{\pi}{3}$, we take the solution in the region I_∞ in Fig.4.10 so that the boundary condition at infinity is satisfied.

The connection problem from infinity to the origin is solved by computing the connection of the solutions from I_∞ to $\mathrm{I}_{\mathrm{mid}}$, $\mathrm{I}_{\mathrm{mid}}$ to $\tilde{\mathrm{I}}_{\mathrm{mid}}$, and $\tilde{\mathrm{I}}_{\mathrm{mid}}$ to I_0 successively. The connection formula from I_∞ to $\mathrm{I}_{\mathrm{mid}}$ is same as (4.2.18). Changing the normalization of the solutions from z_3 to z_2 has also already given by (4.2.19). The connection formula from $\mathrm{I}_{\mathrm{mid}}$ to $\tilde{\mathrm{I}}_{\mathrm{mid}}$ is given by (4.2.20) with replacing I_0 in the r.h.s. to $\tilde{\mathrm{I}}_{\mathrm{mid}}$,

$$\begin{pmatrix} \mathcal{B}_0\left[\psi^+_{z_2,\mathrm{I}_{\mathrm{mid}}}\right](z) \\ \mathcal{B}_0\left[\psi^-_{z_2,\mathrm{I}_{\mathrm{mid}}}\right](z) \end{pmatrix} = \begin{pmatrix} 1 & 0 \\ i & 1 \end{pmatrix} \begin{pmatrix} \mathcal{B}_0\left[\psi^+_{z_2,\tilde{\mathrm{I}}_{\mathrm{mid}}}\right](z) \\ \mathcal{B}_0\left[\psi^-_{z_2,\tilde{\mathrm{I}}_{\mathrm{mid}}}\right](z) \end{pmatrix}. \tag{4.2.27}$$

To compute the connection from $\tilde{\mathrm{I}}_{\mathrm{mid}}$ to I_0, we need to change the normalization of the solutions from z_2 to z_1,

$$\begin{pmatrix} \mathcal{B}_0\left[\psi^+_{z_2,\tilde{\mathrm{I}}_{\mathrm{mid}}}\right](z) \\ \mathcal{B}_0\left[\psi^-_{z_2,\tilde{\mathrm{I}}_{\mathrm{mid}}}\right](z) \end{pmatrix} = \begin{pmatrix} e^{-\eta\mathcal{B}_0\left[\int_{z_1}^{z_2} P_{\mathrm{even}}(z)dz\right]} & 0 \\ 0 & e^{\eta\mathcal{B}_0\left[\int_{z_1}^{z_2} P_{\mathrm{even}}(z)dz\right]} \end{pmatrix} \begin{pmatrix} \mathcal{B}_0\left[\psi^+_{z_1,\tilde{\mathrm{I}}_{\mathrm{mid}}}\right](z) \\ \mathcal{B}_0\left[\psi^-_{z_1,\tilde{\mathrm{I}}_{\mathrm{mid}}}\right](z) \end{pmatrix}. \tag{4.2.28}$$

Between $\tilde{\mathrm{I}}_{\mathrm{mid}}$ and I_0, there is a Stokes line emanating from z_1 and having the negative orientation. Then the solutions are connected by the following formula,

$$\begin{pmatrix} \mathcal{B}_0\left[\psi^+_{z_1,\tilde{\mathrm{I}}_{\mathrm{mid}}}\right](z) \\ \mathcal{B}_0\left[\psi^-_{z_1,\tilde{\mathrm{I}}_{\mathrm{mid}}}\right](z) \end{pmatrix} = \begin{pmatrix} 1 & 0 \\ i & 1 \end{pmatrix} \begin{pmatrix} \mathcal{B}_0\left[\psi^+_{z_1,\mathrm{I}_0}\right](z) \\ \mathcal{B}_0\left[\psi^-_{z_1,\mathrm{I}_0}\right](z) \end{pmatrix}. \tag{4.2.29}$$

By multiplying (4.2.18), (4.2.19), (4.2.27)∼(4.2.29) and finally restoring the normalization of $\psi^{\pm}_{z_1,\mathrm{I}_0}$ in the r.h.s. of (4.2.29) from z_1 to z_3, we obtain the solution of the connection

problem for $-\frac{\pi}{2} \leq \arg(\omega R) < -\frac{\pi}{3}$,

$$\begin{pmatrix} \mathcal{B}_0\left[\psi^+_{z_3,\mathrm{I}_\infty}\right](z) \\ \mathcal{B}_0\left[\psi^-_{z_3,\mathrm{I}_\infty}\right](z) \end{pmatrix} = \begin{pmatrix} 1+\left(1+e^{\eta\mathcal{B}_0\left[2\int_{z_1}^{z_2}P_{\mathrm{even}}(z)dz\right]}\right)e^{\eta\mathcal{B}_0\left[2\int_{z_2}^{z_3}P_{\mathrm{even}}(z)dz\right]} & -i \\ i\left(1+e^{\eta\mathcal{B}_0\left[2\int_{z_1}^{z_2}P_{\mathrm{even}}(z)dz\right]}\right)e^{\eta\mathcal{B}_0\left[2\int_{z_2}^{z_3}P_{\mathrm{even}}(z)dz\right]} & 1 \end{pmatrix} \begin{pmatrix} \mathcal{B}_0\left[\psi^+_{z_3,\mathrm{I}_0}\right](z) \\ \mathcal{B}_0\left[\psi^-_{z_3,\mathrm{I}_0}\right](z) \end{pmatrix}. \tag{4.2.30}$$

The integrals $2\int_{z_2}^{z_3}P_{\mathrm{even}}(z)dz$ and $2\int_{z_1}^{z_2}P_{\mathrm{even}}(z)dz$ are equivalent to the WKB periods for the one-cycles γ_{23} and γ_{12} in Fig.4.9, respectively. Therefore (4.2.30) can be expressed in terms of the WKB periods,

$$\begin{pmatrix} \mathcal{B}_0\left[\psi^+_{z_3,\mathrm{I}_\infty}\right](z) \\ \mathcal{B}_0\left[\psi^-_{z_3,\mathrm{I}_\infty}\right](z) \end{pmatrix} = \begin{pmatrix} 1+\left(1+e^{\eta\mathcal{B}_0\left[\Pi_{\gamma_{12}}\right]}\right)e^{\eta\mathcal{B}_0\left[\Pi_{\gamma_{23}}\right]} & -i \\ i\left(1+e^{\eta\mathcal{B}_0\left[\Pi_{\gamma_{12}}\right]}\right)e^{\eta\mathcal{B}_0\left[\Pi_{\gamma_{23}}\right]} & 1 \end{pmatrix} \begin{pmatrix} \mathcal{B}_0\left[\psi^+_{z_3,\mathrm{I}_0}\right](z) \\ \mathcal{B}_0\left[\psi^-_{z_3,\mathrm{I}_0}\right](z) \end{pmatrix}. \tag{4.2.31}$$

Boundary conditions and exact QNM conditions

We impose the boundary conditions (i) only outgoing wave exists at $z \to +\infty$ and (ii) only ingoing wave exists at $z \to 0$ on the Borel resummed WKB solutions. The outgoing wave at $z \to +\infty$ is $\mathcal{B}_0\left[\psi^+_{z_3,\mathrm{I}_\infty}\right](z)$. According to the connection formulae (4.2.22) and (4.2.31), $\mathcal{B}_0\left[\psi^+_{z_3,\mathrm{I}_\infty}\right](z)$ is connected to the origin as follows,

$$\mathcal{B}_0\left[\psi^+_{z_3,\mathrm{I}_\infty}\right](z) = \begin{cases} \left(1+e^{\eta\mathcal{B}_0\left[\Pi_{\gamma_{23}}\right]}\right)\mathcal{B}_0\left[\psi^+_{z_3,\mathrm{I}_0}\right](z) - i\mathcal{B}_0\left[\psi^-_{z_3,\mathrm{I}_0}\right](z) & \left(-\frac{\pi}{3} < \arg(\omega R) < 0\right), \\ \left(1+\left(1+e^{\eta\mathcal{B}_0\left[\Pi_{\gamma_{12}}\right]}\right)e^{\eta\mathcal{B}_0\left[\Pi_{\gamma_{23}}\right]}\right)\mathcal{B}_0\left[\psi^+_{z_3,\mathrm{I}_0}\right](z) - i\mathcal{B}_0\left[\psi^-_{z_3,\mathrm{I}_0}\right](z) & \\ & \left(-\frac{\pi}{2} \leq \arg(\omega R) < -\frac{\pi}{3}\right). \end{cases} \tag{4.2.32}$$

The ingoing wave at $z \to 0$ is $\mathcal{B}_0\left[\psi^-_{z_3,\mathrm{I}_0}\right](z)$. Therefore to satisfy the boundary conditions, the coefficients of $\mathcal{B}_0\left[\psi^+_{z_3,\mathrm{I}_0}\right](z)$ in (4.2.32) need to be zero,

$$\begin{cases} 1+e^{\eta\mathcal{B}_0\left[\Pi_{\gamma_{23}}\right]} = 0 & \left(-\frac{\pi}{3} < \arg(\omega R) < 0\right), \\ 1+\left(1+e^{\eta\mathcal{B}_0\left[\Pi_{\gamma_{12}}\right]}\right)e^{\eta\mathcal{B}_0\left[\Pi_{\gamma_{23}}\right]} = 0 & \left(-\frac{\pi}{2} \leq \arg(\omega R) < -\frac{\pi}{3}\right). \end{cases} \tag{4.2.33}$$

Taking the logarithm of (4.2.33) and substituting $\eta = 1$, we obtain the following conditions,

$$\begin{cases} \mathcal{B}_0\left[\Pi_{\gamma_{23}}\right] = 2\pi i\left(n+\frac{1}{2}\right) & \left(-\frac{\pi}{3} < \arg(\omega R) < 0\right), \\ \mathcal{B}_0\left[\Pi_{\gamma_{23}}\right] + \log\left(1+e^{\mathcal{B}_0\left[\Pi_{\gamma_{12}}\right]}\right) = 2\pi i\left(n+\frac{1}{2}\right) & \left(-\frac{\pi}{2} \leq \arg(\omega R) < -\frac{\pi}{3}\right), \end{cases} \tag{4.2.34}$$

where $n \in \mathbb{Z}_{\geq 0}$. The conditions (4.2.34) are satisfied by discrete sets of ω, which are the quasi-normal modes for the massless scalar perturbation in the extremal M5-brane metric. Without considering convergence of the asymptotic series, the asymptotic expansion of (4.2.34) provides the following conditions,

$$\begin{cases} \Pi_{\gamma_{23}} = 2\pi i \left(n + \frac{1}{2}\right) & \left(-\frac{\pi}{3} < \arg(\omega R) < 0\right), \\ \Pi_{\gamma_{23}} + \log\left(1 + e^{\Pi_{\gamma_{12}}}\right) = 2\pi i \left(n + \frac{1}{2}\right) & \left(-\frac{\pi}{2} \leq \arg(\omega R) < -\frac{\pi}{3}\right). \end{cases} \tag{4.2.35}$$

The first condition of (4.2.35) is the all-order extension of the Bohr-Sommerfeld condition (4.1.7).

We present some comments for (4.2.33)∼(4.2.35) from the point of view of the resurgence. First, the two QNMs conditions are continuous. Let us see the transition of the Stokes graph with rotating $\arg(\omega R)$ and $\arg(\eta)$ (Fig.4.11). From the graph [a] to [b] in Fig.4.11, $\arg(\eta)$ is rotated from $\arg(\eta) = 0$ to $\arg(\eta) = -\delta$ while $\arg(\omega R) = -\pi/3 + \delta$ is fixed. At an argument $\arg(\eta) = -\varphi$ $(-\delta < -\varphi < 0)$, the Stokes line connecting z_1 and z_2 appears and the saddle reduction happens. Then the Borel transformation of the WKB period $\Pi_{\gamma_{23}}$, whose one-cycle γ_{23} intersects with the Stokes line connecting z_1 and z_2, has a singularity on the complex ξ-plane in the direction $\arg(\xi) = +\varphi$. If we rotate $\arg(\eta)$ as crossing $\arg(\eta) = -\varphi$, the integration contour of the Borel resummation for $\Pi_{\gamma_{23}}$ collides with the singularity on the complex ξ-plane. To ensure the analyticity in η of the Borel resummation, we must take the contribution from the integration contour encircling the singularity into account. Then it is shown that the WKB period is connected as follows (theorem 2.5.1 of [23], and theorem 3.4 of [25]),

$$e^{\eta\mathcal{B}_{-\varphi-}\left[\Pi_{\gamma_{23}}\right]} = \left(1 + e^{\eta\mathcal{B}_{-\varphi}\left[\Pi_{\gamma_{12}}\right]}\right) e^{\eta\mathcal{B}_{-\varphi+}\left[\Pi_{\gamma_{23}}\right]}. \tag{4.2.36}$$

From the graph [b] to [c] in Fig.4.11, $\arg(\omega R)$ is rotated from $\arg(\omega R) = -\pi/3 + \delta$ to $\arg(\omega R) = -\pi/3 - \delta$ while $\arg(\eta) = -\delta$ is fixed. Finally from the graph [c] to [d], $\arg(\eta)$ is rotated from $\arg(\eta) = -\delta$ to $\arg(\eta) = 0$ while $\arg(\omega R) = -\pi/3 - \delta$ is fixed. During [b] to [d], the saddle reduction does not happen and therefore the r.h.s. of (4.2.36) does not change discontinuously. In summary, Fig.4.11 indicates $e^{\eta\mathcal{B}_0\left[\Pi_{\gamma_{23}}\right]}$ for $-\frac{\pi}{3} < \arg(\omega R) < 0$ and $\left(1 + e^{\eta\mathcal{B}_0\left[\Pi_{\gamma_{12}}\right]}\right) e^{\eta\mathcal{B}_0\left[\Pi_{\gamma_{23}}\right]}$ for $-\frac{\pi}{2} \leq \arg(\omega R) < -\frac{\pi}{3}$ with $\arg(\eta) = 0$ are continuous. Therefore the two conditions in (4.2.33) are also continuous.

Next comment is about the non-perturbative property of the QNMs. Calculating the QNMs from the conditions (4.2.33)∼(4.2.35), one finds the term $e^{\eta\mathcal{B}_0\left[\Pi_{\gamma_{12}}\right]}$ in the conditions

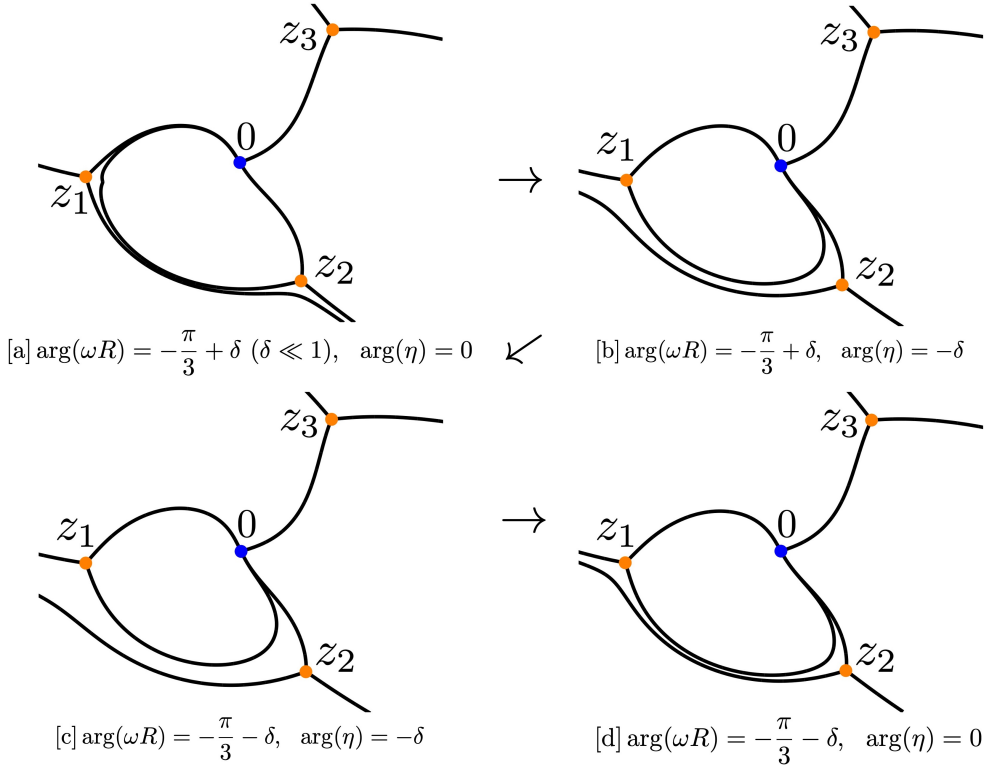

Figure 4.11: The transition of the Stokes graph with rotating $\arg(\omega R)$ and $\arg(\eta)$. The graph [a], [d] are same as [a], [d] in Fig.4.8, respectively.

for $-\frac{\pi}{2} \leq \arg(\omega R) < -\frac{\pi}{3}$ is exponentially small. We can also find this type of exponentially small terms in the study of the energy quantization conditions for resurgent quantum mechanics (e.g. [27, 31, 71–73]). In these cases, the exponentially small terms arise from the tunnel effect and produce the instanton contributions to the asymptotic expansion of the energy eigenvalues. The conditions (4.2.33)∼(4.2.35) imply that the QNMs in the region $-\frac{\pi}{2} \leq \arg(\omega R) < -\frac{\pi}{3}$ have such an instanton contribution.

Following the argument for the non-perturbative property, the continuation for the QNMs conditions (4.2.36) can be seen as that the discontinuity of the perturbative part is leading the non-perturbative part of the QNMs.

4.2.3 Computations of the QNMs for extremal M5-branes

In this section, we will numerically and analytically compute the QNMs by using the conditions (4.2.33)∼(4.2.35). We first compute the WKB periods. The leading order contributions of the WKB periods are given by two times (4.2.15)∼(4.2.17). To compute the higher order contributions, it is useful to transform the equation (4.2.5). Under the following

transformations,

$$\begin{aligned} \eta = \frac{1}{\hbar}, \quad \left(l + \frac{3}{2}\right)^2 = u, \quad \omega R = i\frac{\Lambda_1}{2}, \\ z = (\sqrt{\Lambda_1}/2)e^{ix}, \quad \psi(z(x)) = (\sqrt{\Lambda_1}/2)^{(1/2)} e^{i\frac{x}{2}} \Psi(x), \end{aligned} \tag{4.2.37}$$

the equation (4.2.5) becomes as follows,

$$\left[\hbar^2 \frac{d^2}{dx^2} + u + \frac{1}{16}\Lambda_1^3 e^{2ix} + \frac{1}{2}\Lambda_1^{\frac{3}{2}} e^{-ix}\right] \Psi(x) = 0. \tag{4.2.38}$$

(4.2.38) is the quantum Seiberg-Witten curve for 4-dimensional $\mathcal{N} = 2$ SU(2) supersymmetric QCD with a massless fundamental matter [46]. In the context of the gauge theory, u is the Coulomb moduli parameter, Λ_1 is the dynamically generated scale, and $\hbar$ is the deformation parameter in the Nekrasov-Shatashvili limit of the Ω-background. (4.2.37) is a new example of the Seiberg-Witten/gravity correspondence [67–69]. Under the transformation (4.2.37), it is shown that the WKB periods are invariant (Proposition 2.7 (b) in [25]). Therefore computing the WKB periods for (4.2.5) is equivalent to computing the WKB periods for the quantum Seiberg-Witten curve (4.2.38). The higher-order contributions of the WKB periods for the quantum Seiberg-Witten curve can be computed by applying differential operators with respect to u to the leading order contributions [46],

$$\Pi_\gamma^{(2n)} = \mathcal{O}_{2n} \Pi_\gamma^{(0)}. \tag{4.2.39}$$

Up to 4th-order, the differential operators are given as follows,

$$\begin{aligned} \mathcal{O}_2 &= \frac{1}{12}\left(2u\frac{\partial^2}{\partial u^2} + \frac{\partial}{\partial u}\right), \\ \mathcal{O}_4 &= \frac{1}{1440}\left(28u^2\frac{\partial^4}{\partial u^4} + 124u\frac{\partial^3}{\partial u^3} + 81\frac{\partial^2}{\partial u^2}\right). \end{aligned} \tag{4.2.40}$$

After computing the WKB periods, we take the Borel resummation of them. In this paper, we use the Borel-Padé approximation,

$$\mathcal{B}_0\left[\Pi_\gamma\right] \sim \int_0^\infty e^{-\xi}\left[N/N\right] d\xi, \tag{4.2.41}$$

where $[N/N]$ is the diagonal Padé approximation of order N for the Borel transformation of the WKB periods.

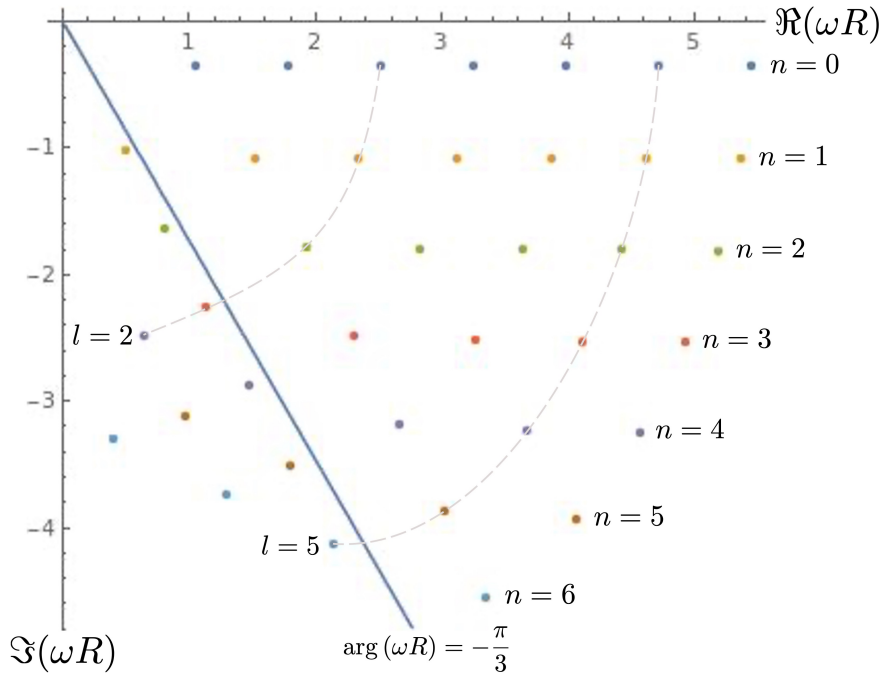

Figure 4.12: The numerical values of the QNMs calculated from the exact conditions (4.2.34). The upper right points from the line at $\arg(\omega R) = -\frac{\pi}{3}$ are calculated by the condition for $-\frac{\pi}{3} < \arg(\omega R) < 0$ of (4.2.34), and the lower left points are calculated by the condition for $-\frac{\pi}{2} \leq \arg(\omega R) < -\frac{\pi}{3}$.

Fig.4.12 shows the numerical values of the QNMs calculated from the exact conditions (4.2.34), where we have used up to 4th-order of the WKB periods and the diagonal Padé approximation of order 2. In Fig.4.12, the QNMs for $l < n$ are located in $\arg(\omega R) < -\frac{\pi}{3}$ region. With fixed l, the imaginary part of the QNMs becomes small as n increases. The polarization modes with $\boldsymbol{k} = 0$ of the scalar field then get to decay at $t \to +\infty$ quickly. We also compare the results of (4.2.34) with the large l expression (4.2.9) in Table.4.3. At $n = 1$ and $l = 0$, the argument of the numerical result of (4.2.34) is smaller than $-\frac{\pi}{3}$ while the argument of the result of (4.2.9) is larger than $-\frac{\pi}{3}$. This result indicates that we need to use the second condition in (4.2.34) to calculate the QNMs in $\arg(\omega R) < -\frac{\pi}{3}$ region (or $l < n$ region).

Fig.4.13 shows the real part of the QNMs with $l = 5$ calculated from the exact conditions. The behavior of the real part of QNMs changes between $\arg(\omega R) > -\frac{\pi}{3}$ and $\arg(\omega R) < -\frac{\pi}{3}$. The QNMs with other l show the same behavior. We can find similar behavior of the real part of the QNMs in the case of Kerr-BH [83], where the QNMs are numerically calculated by using the general Heun function. We expect that the change of the behavior of the QNMs

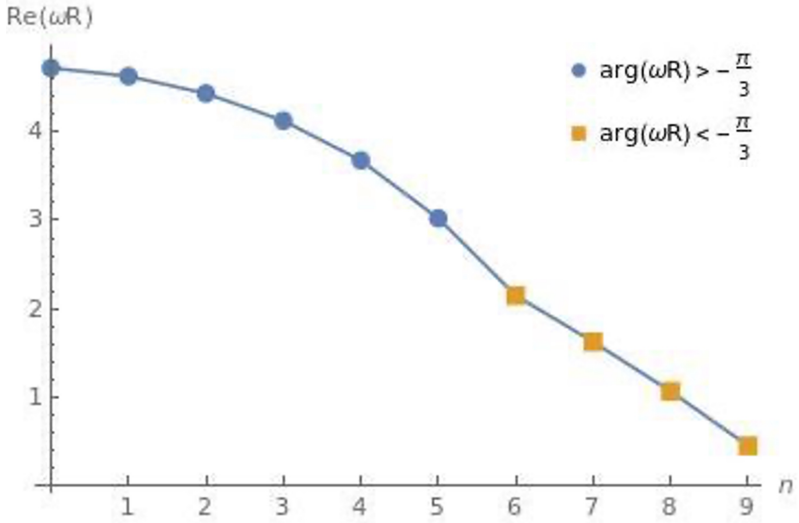

Figure 4.13: The real part of the QNMs with $l = 5$. The blue points are calculated by the condition for $-\frac{\pi}{3} < \arg(\omega R) < 0$ of (4.2.34), and the orange points are calculated by the condition for $-\frac{\pi}{2} \leq \arg(\omega R) < -\frac{\pi}{3}$.

for Kerr-BH can also be explained by the change of the exact conditions.

By using the Padé approximation, one can numerically check the singularity of the Borel transformation of the WKB period. For example, at $\omega R = \exp\left(-i\frac{\pi}{3} + i\frac{1}{100}\right)$ and $l = 0$, we find that the diagonal Padé approximation of order 2 for the Borel transformation of $\Pi_{\gamma_{23}}$ with 4th-order coefficients has a singularity at $\xi = 1.797240 + 0.320820i$.

Analytic expressions of the QNMs can also be obtained in parts. For $-\frac{\pi}{6} \leq \arg(\omega R) \leq 0$, the coefficients of the WKB period $\Pi^{(n)}_{\gamma_{23}}$ can be expanded at $\omega R = \frac{\sqrt[3]{2}\left(l+\frac{3}{2}\right)}{\sqrt{3}}$,

$$
\begin{aligned}
\Pi^{(0)}_{\gamma_{23}} &= -2^{2/3}\sqrt{3}\pi\left(\omega R - \frac{\sqrt[3]{2}\left(l+\frac{3}{2}\right)}{\sqrt{3}}\right) + \frac{5\pi\left(\omega R - \frac{\sqrt[3]{2}\left(l+\frac{3}{2}\right)}{\sqrt{3}}\right)^2}{2^{5/3}\left(l+\frac{3}{2}\right)} + \cdots, \\
\Pi^{(2)}_{\gamma_{23}} &= \frac{5\pi}{72\left(l+\frac{3}{2}\right)} - \frac{25\pi\left(\omega R - \frac{\sqrt[3]{2}\left(l+\frac{3}{2}\right)}{\sqrt{3}}\right)}{288\left(\sqrt[3]{2}\sqrt{3}\left(l+\frac{3}{2}\right)^2\right)} - \frac{325\pi\left(\omega R - \frac{\sqrt[3]{2}\left(l+\frac{3}{2}\right)}{\sqrt{3}}\right)^2}{10368\left(2^{2/3}\left(l+\frac{3}{2}\right)^3\right)} + \cdots, \\
\Pi^{(4)}_{\gamma_{23}} &= -\frac{2471\pi}{746496\left(l+\frac{3}{2}\right)^3} + \frac{33565\pi\left(\omega R - \frac{\sqrt[3]{2}\left(l+\frac{3}{2}\right)}{\sqrt{3}}\right)}{5971968\sqrt[3]{2}\sqrt{3}\left(l+\frac{3}{2}\right)^4} + \frac{1560503\pi\left(\omega R - \frac{\sqrt[3]{2}\left(l+\frac{3}{2}\right)}{\sqrt{3}}\right)^2}{71663616\left(2^{2/3}\left(l+\frac{3}{2}\right)^5\right)} + \cdots.
\end{aligned}
\tag{4.2.42}
$$

n	l	(4.2.34)	$-\frac{\pi}{3} < \arg(\omega R)$	(4.2.9)	$-\frac{\pi}{3} < \arg(\omega R)$
0	0	$1.057134 - 0.365624i$	True	$1.028721 - 0.363707i$	True
	1	$1.798272 - 0.364387i$	True	$1.781797 - 0.363707i$	True
	2	$2.531500 - 0.364053i$	True	$2.519842 - 0.363707i$	True
1	0	$0.506956 - 1.023014i$	False	$1.028721 - 1.091123i$	True
	1	$1.535914 - 1.086901i$	True	$1.781797 - 1.091123i$	True
	2	$2.351632 - 1.089620i$	True	$2.519842 - 1.091123i$	True

Table 4.3: Numerical results of the exact conditions (4.2.34) and the large l expression (4.2.9). The fourth column indicates which the numerical values of the third column satisfy $-\frac{\pi}{3} < \arg(\omega R)$ or not, and the sixth column indicates which the numerical values of the fifth column satisfy $-\frac{\pi}{3} < \arg(\omega R)$ or not.

Then the first condition of (4.2.35) can be expressed as,

$$2\pi i\left(n+\frac{1}{2}\right) = \Pi^{(0)}_{\gamma_{23}} + \Pi^{(2)}_{\gamma_{23}} + \Pi^{(4)}_{\gamma_{23}} + \cdots = \sum_{m=0}^{\infty} c_m \left(\omega R - \frac{\sqrt[3]{2}\left(l+\frac{3}{2}\right)}{\sqrt{3}}\right)^m . \tag{4.2.43}$$

Applying the Lagrange inversion theorem to (4.2.43), we obtain an analytic form of the QNMs for $-\frac{\pi}{6} \leq \arg(\omega R) \leq 0$,

$$\omega_n R = \frac{\sqrt[3]{2}\left(l+\frac{3}{2}\right)}{\sqrt{3}} + \frac{2\pi i\left(n+\frac{1}{2}\right) - c_0}{c_1} - \frac{c_2(2\pi i\left(n+\frac{1}{2}\right) - c_0)^2}{c_1^3} + \cdots . \tag{4.2.44}$$

Table.4.4 shows some numerical values of the QNMs calculated by the first condition in (4.2.34) and (4.2.44), where we have used up to 4th-order of the WKB period and 8-th order of (4.2.44).

To obtain an analytic form of the QNMs for $\arg(\omega R) < -\frac{\pi}{6}$ as (4.2.44), we also need to expand (4.2.15). But the expansion of (4.2.15) at $\omega R = \frac{\sqrt[3]{2}\left(l+\frac{3}{2}\right)}{\sqrt{3}}$ has the logarithm term $\log\left(\omega R - \frac{\sqrt[3]{2}\left(l+\frac{3}{2}\right)}{\sqrt{3}}\right)$ and therefore we cannot compute the inverse series. We need another computational method to obtain an analytic form for $\arg(\omega R) < -\frac{\pi}{6}$.

In the large n limit, which corresponds to $|\omega R| \gg (l+\frac{3}{2})$ limit, the leading order approximation is valid,

$$\begin{cases} \Pi^{(0)}_{\gamma_{23}} = 2\pi i\left(n+\frac{1}{2}\right) & \left(-\frac{\pi}{3} < \arg(\omega R) < 0\right), \\ \Pi^{(0)}_{\gamma_{23}} + \log\left(1+e^{\Pi^{(0)}_{\gamma_{12}}}\right) = 2\pi i\left(n+\frac{1}{2}\right) & \left(-\frac{\pi}{2} \leq \arg(\omega R) < -\frac{\pi}{3}\right). \end{cases} \tag{4.2.45}$$

n	l	(4.2.34)	(4.2.44)	$-\frac{\pi}{6} \leq \arg(\omega R)$
0	0	$1.057134 - 0.365624i$	$\underline{\mathbf{1.0571}}03 - \underline{\mathbf{0.365624}}i$	True
	1	$1.798272 - 0.364387i$	$\underline{\mathbf{1.79827}}0 - \underline{\mathbf{0.364387}}i$	True
	2	$2.531500 - 0.364053i$	$\underline{\mathbf{2.531500}} - \underline{\mathbf{0.364053}}i$	True
1	1	$1.535914 - 1.086901i$	$\underline{\mathbf{1.53}}6070 - \underline{\mathbf{1.08}}7184i$	False
	2	$2.351632 - 1.089620i$	$\underline{\mathbf{2.35163}}8 - \underline{\mathbf{1.0896}}38i$	True

Table 4.4: Numerical results of the first condition in (4.2.34) and (4.2.44). The fifth column indicates which the numerical values of the third and fourth columns satisfy $-\frac{\pi}{6} \leq \arg(\omega R)$ or not. The result of (4.2.44) at $n = 1,\ l = 1$, which does not satisfy $-\frac{\pi}{6} \leq \arg(\omega R)$, has lower precision than the other results.

In addition, we can neglect the exponentially small term $e^{\Pi^{(0)}_{\gamma_{12}}}$ as we neglect the tunnel effect at the large energy classical limit in quantum mechanics. Then two conditions in (4.2.45) reduce to a single condition,

$$\Pi^{(0)}_{\gamma_{23}} = 2\pi i \left(n + \frac{1}{2}\right). \tag{4.2.46}$$

At $|\omega R| \gg (l + \frac{3}{2})$, the potential function $Q_0(z)$ is approximated as $Q_0(z) = -(\omega R)^2 \frac{z^3+1}{z^3}$. The solutions to $Q_0(z) = 0$ then become $z_1 = -1,\ z_2 = e^{-i\frac{\pi}{3}},\ z_3 = e^{i\frac{\pi}{3}}$. Now $\Pi^{(0)}_{\gamma_{23}}$ can be expressed as

$$\Pi^{(0)}_{\gamma_{23}} = 2i\omega R \int_{e^{-i\frac{\pi}{3}}}^{e^{i\frac{\pi}{3}}} \sqrt{\frac{z^3+1}{z^3}} dz = -\frac{\pi\omega R}{\sqrt[3]{2}\sqrt{3}}\ {}_2F_1\left[\frac{5}{6}, \frac{5}{6}, 2, 1\right]. \tag{4.2.47}$$

Substituting (4.2.47) into (4.2.46), we find that the QNM at large n is pure imaginary,

$$\omega R = -i \frac{2\sqrt[3]{2}\sqrt{3}}{{}_2F_1\left[\frac{5}{6}, \frac{5}{6}, 2, 1\right]} \left(n + \frac{1}{2}\right). \tag{4.2.48}$$

In some black hole metrics, it is known that the real part of the QNMs at large n is proportional to the entropy of the black hole (e.g. [40, 77–79]). The entropy of the extremal M5-brane metric (4.2.1) is zero because it has no event horizon. It is consistent with the real part of (4.2.48) is zero.

Summary

In this chapter, we have studied the QNMs spectral problem for the massless scalar fields in the extremal D3/M5-branes background by using the Exact WKB analysis. We have

derived the exact QNMs conditions written in terms of the Borel resummed WKB periods. The QNMs computed from the exact conditions are consistent with the classical WKB approximation and the Leaver's method. We have also found the transformation of the E.O.M. for the massless scalar fields to the quantum Seiberg-Witten curves for 4-dimensional $\mathcal{N} = 2$ SU(2) supersymmetric gauge theories. For the M5-branes case, the exact conditions have shown that the discontinuity of the perturbative part of the QNMs leads the non-perturbative part of themselves.

Chapter 5

TBA equations for quantum mechanics

In this chapter, we review the TBA equations governing the Borel resummed WKB periods for arbitrary polynomial potentials and Central-Centrifugal potentials. The discontinuity and the classical limit of the WKB periods form the Riemann-Hilbert problem and the TBA equations are given as a solution to the problem. Combining with the exact energy quantization condition, we show that the TBA equations calculate the spectrum exactly. This review chapter is based on [28, 47].

5.1 Arbitrary polynomial potentials

5.1.1 Discontinuity of WKB periods for arbitrary polynomial potentials

We consider the Schrödinger equation on the Riemann sphere $\mathbb{C}^* = \mathbb{C} \cup \{\infty\}$ with arbitrary polynomial potentials with degree $r+1$,

$$\left[\frac{d^2}{dz^2} - \eta^2 Q_0(z)\right] \psi(z) = 0, \tag{5.1.1}$$

with

$$Q_0(z) = V(z) - E = \sum_{n=0}^{r+1} a_n z^n - E, \tag{5.1.2}$$

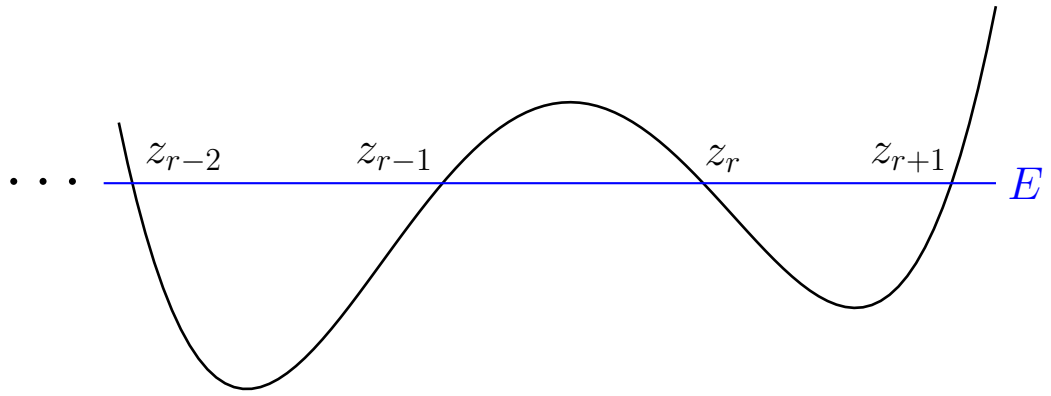

Figure 5.1: An example of the potential $V(z)$ on the real z-axis.

where we take a_n as a real parameter and fix $a_{r+1} = 1$. The WKB curve for (5.1.1) is a hypergeometric curve describing a Riemann surface with genus $g = [r/2]$.

Let us consider the parameter region in the moduli space of the WKB curve where all the simple zeros are real. We name the simple zeros so that

$$z_1 < z_2 < \cdots < z_{r+1}. \tag{5.1.3}$$

Fig.5.1 shows an example of the potential graph on the real z-axis and the simple zeros. On the real z-axis, r intervals appear,

$$[z_i, z_{i+1}], \quad i = 1, 2, \cdots, r. \tag{5.1.4}$$

The intervals for $i = r, r-2, r-4, \cdots$ are the classically allowed intervals, and for $i = r-1, r-3, r-5, \cdots$ are the classically forbidden intervals. We denote $\gamma_{i,i+1}$ as the one-cycle encircling the interval $[z_i, z_{i+1}]$. We also choose the branch cuts and the orientation of the one-cycles so that

$$m_{i,i+1} := i\Pi^{(0)}_{\gamma_{i,i+1}} = i \oint_{\gamma_{i,i+1}} S_0(z)dz \quad \text{(for the classically allowed intervals)} \tag{5.1.5}$$

and

$$m_{i,i+1} := -\Pi^{(0)}_{\gamma_{i,i+1}} = - \oint_{\gamma_{i,i+1}} S_0(z)dz \quad \text{(for the classically forbidden intervals)} \tag{5.1.6}$$

are real and positive.

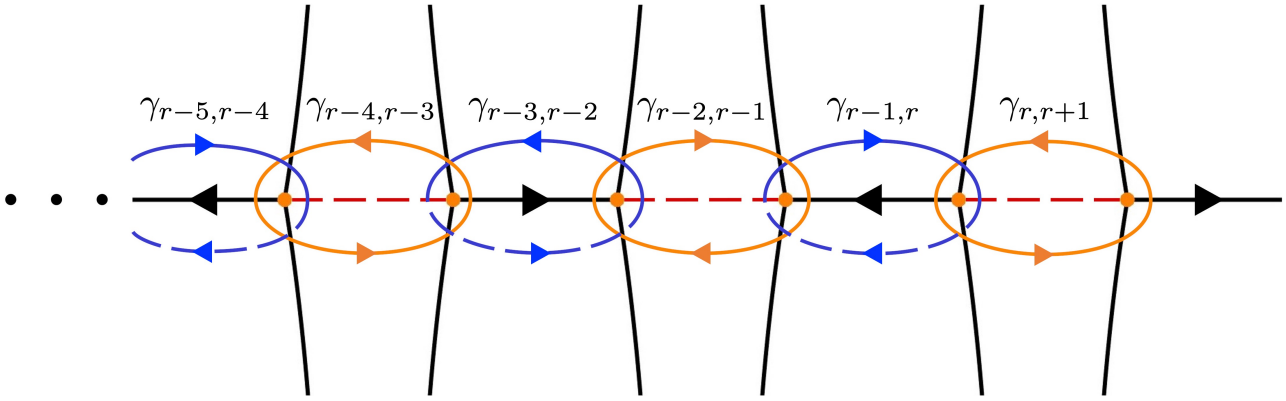

Figure 5.2: The Stokes graph at $\arg(\eta) = 0$ for arbitrary polynomial potentials with all the simple zeros are real.

For $\arg(\eta) = 0$, the Stokes graph is given by Fig.5.2. Because of the definition of the Stokes lines (2.2.36) and (5.1.6), the Stokes segments lie on the classically forbidden intervals. Then, by the Delabaere-Pham formula (2.2.50), the WKB periods for the classically forbidden intervals have no discontinuity for the direction $\arg(\eta) = 0$ and the WKB period for the classically allowed intervals have the following discontinuity,

$$e^{\eta\mathcal{B}_{0-}\left[\Pi_{\gamma_{i,i+1}}\right]} = e^{\eta\mathcal{B}_{0+}\left[\Pi_{\gamma_{i,i+1}}\right]}\left(1+e^{\eta\mathcal{B}_0\left[\Pi_{\gamma_{i-1,i}}\right]}\right)\left(1+e^{\eta\mathcal{B}_0\left[\Pi_{\gamma_{i+1,i+2}}\right]}\right), \quad (i = r, r-2, \cdots) \tag{5.1.7}$$

where we define $e^{\eta\mathcal{B}_\varphi\left[\Pi_{\gamma_{0,1}}\right]} = e^{\eta\mathcal{B}_\varphi\left[\Pi_{\gamma_{r+1,r+2}}\right]} = 0$.

For $\arg(\eta) = \pi$, we obtain the Stokes graph Fig.5.2 with opposite orientation because, by the definition of the Stokes lines (2.2.36) and their orientation (2.2.37),

$$\Im\left[e^{i\pi}\int_{z_*}^{z} S_0\left(z'\right)dz'\right] = -\Im\left[\int_{z_*}^{z} S_0\left(z'\right)dz'\right] = 0 \Leftrightarrow \Im\left[\int_{z_*}^{z} S_0\left(z'\right)dz'\right] = 0, \tag{5.1.8}$$

and

$$\Re\left[e^{i\pi}\int_{z_*}^{z} S_0\left(z'\right)dz'\right] = -\Re\left[\int_{z_*}^{z} S_0\left(z'\right)dz'\right]. \tag{5.1.9}$$

Therefore, by the Delabaere-Pham formula (2.2.50), the WKB periods for the classically forbidden intervals have no discontinuity for the direction $\arg(\eta) = \pi$ and the WKB period for the classically allowed intervals have the following discontinuity,

$$e^{\eta\mathcal{B}_{\pi-}\left[\Pi_{\gamma_{i,i+1}}\right]} = e^{\eta\mathcal{B}_{\pi+}\left[\Pi_{\gamma_{i,i+1}}\right]}\left(1+e^{-\eta\mathcal{B}_\pi\left[\Pi_{\gamma_{i-1,i}}\right]}\right)^{-1}\left(1+e^{-\eta\mathcal{B}_\pi\left[\Pi_{\gamma_{i+1,i+2}}\right]}\right)^{-1}. \quad (i = r, r-2, \cdots) \tag{5.1.10}$$

The Stokes graph also has the Stokes segments in the direction $\arg(\eta) = \pm\pi/2$ because the Stokes lines are drawn on the point satisfying the following equation,

$$\Im\left[e^{i\pm\frac{\pi}{2}}\int_{z_*}^{z} S_0\left(z'\right)dz'\right] = \pm\Im\left[i\int_{z_*}^{z} S_0\left(z'\right)dz'\right] = 0, \tag{5.1.11}$$

and it is shown that the classically allowed intervals satisfy this condition by (5.1.5). Therefore, in the direction $\arg(\eta) = \pm\pi/2$, the WKB periods for the classically allowed intervals have no discontinuity and the WKB periods for the classically forbidden intervals have the discontinuity, which is determined by the Delabaere-Pham formula (2.2.50). By the definition of the orientation of the Stokes lines (2.2.37) and (5.1.5), the discontinuity of the WKB periods for the classically forbidden intervals is given as follows,

$$e^{\eta\mathcal{B}_{\pm\frac{\pi}{2}-}\left[\Pi_{\gamma_{i,i+1}}\right]} = e^{\eta\mathcal{B}_{\pm\frac{\pi}{2}+}\left[\Pi_{\gamma_{i,i+1}}\right]}\left(1+e^{\mp\eta\mathcal{B}_{\pm\frac{\pi}{2}}\left[\Pi_{\gamma_{i-1,i}}\right]}\right)^{\pm 1}\left(1+e^{\mp\eta\mathcal{B}_{\pm\frac{\pi}{2}}\left[\Pi_{\gamma_{i+1,i+2}}\right]}\right)^{\pm 1}. \ (i = r-1, r-3, \cdots) \tag{5.1.12}$$

5.1.2 TBA equations for arbitrary polynomial potentials

The discontinuity formulae of the WKB periods (5.1.7), (5.1.10), (5.1.12) can be put into a uniform expression by introducing function $\epsilon_{i,i+1}(\theta)$ as follows,

$$\begin{aligned}
&\epsilon_{i,i+1}(\theta - i\frac{\pi}{2} + i\varphi) = \eta\mathcal{B}_{\varphi}\left[\Pi_{\gamma_{i,i+1}}\right], \quad (i = r, r-2, \cdots)\\
&\epsilon_{i,i+1}(\theta + i\varphi) = -\eta\mathcal{B}_{\varphi}\left[\Pi_{\gamma_{i,i+1}}\right], \qquad (i = r-1, r-3, \cdots)
\end{aligned} \tag{5.1.13}$$

where θ is defined by

$$e^{\theta+i\varphi} = \eta. \tag{5.1.14}$$

The discontinuity formulae are then put together into one,

$$\lim_{\delta\to 0}\left[\epsilon_{i,i+1}\left(\theta \pm i\frac{\pi}{2} + i\delta\right) - \epsilon_{i,i+1}\left(\theta \pm i\frac{\pi}{2} - i\delta\right)\right] = \pm\left[L_{i-1,i}(\theta) + L_{i+1,i+2}(\theta)\right], \ (i = 1, 2, \cdots, r) \tag{5.1.15}$$

where

$$L_{i,i+1}(\theta) := \log\left(1 + e^{-\epsilon_{i,i+1}(\theta)}\right). \tag{5.1.16}$$

The function $\epsilon_{i,i+1}(\theta)$ has the following asymptotic behavior,

$$\epsilon_{i,i+1}(\theta) = m_{i,i+1}e^{\theta} + \mathcal{O}(e^{-\theta}), \quad \theta \to \infty \tag{5.1.17}$$

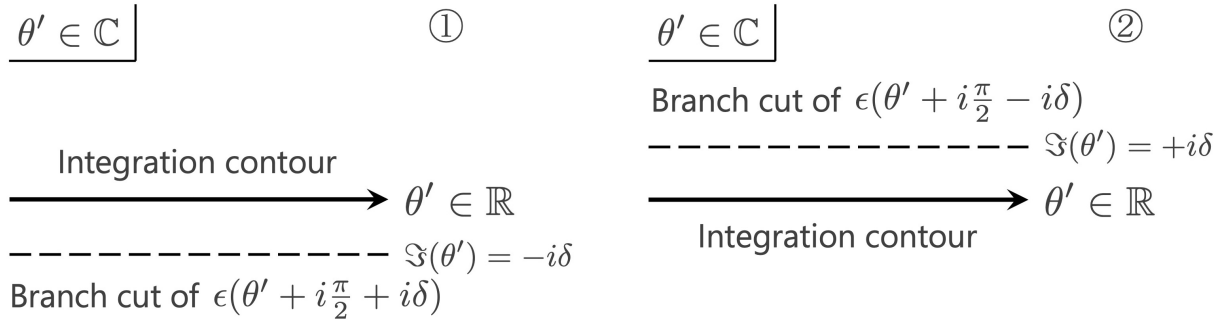

Figure 5.3: ① The integration contour of the first term of the l.h.s. of (5.1.18). ② The integration contour of the second term of the l.h.s. of (5.1.18).

because $\theta \to \infty$ expansion of $\epsilon_{i,i+1}(\theta)$ is equivalent to $\eta \to \infty$ expansion of the Borel resummation of the WKB period.

Now we derive the TBA equations for the function $\epsilon_{i,i+1}(\theta)$ by using the discontinuity (5.1.15) and the asymptotic behavior (5.1.17) following the method in [28]. Taking the convolution of the plus signed equation of (5.1.15) with $K(\theta) = 1/(2\pi\cosh(\theta))$, we obtain

$$\lim_{\delta\to 0}\left[\int_{\mathbb{R}} \frac{\epsilon_{i,i+1}\left(\theta' + i\frac{\pi}{2} + i\delta\right)}{\cosh(\theta-\theta')}\frac{d\theta'}{2\pi} - \int_{\mathbb{R}} \frac{\epsilon_{i,i+1}\left(\theta' + i\frac{\pi}{2} - i\delta\right)}{\cosh(\theta-\theta')}\frac{d\theta'}{2\pi}\right] = \int_{\mathbb{R}} \frac{L_{i-1,i}(\theta') + L_{i+1,i+2}(\theta')}{\cosh(\theta-\theta')}\frac{d\theta'}{2\pi}. \tag{5.1.18}$$

The integration contour of the l.h.s. of (5.1.18) on the complex θ'-plane is drawn in Fig.5.3. For the first term of the l.h.s. of (5.1.18), the integrand has the branch cut at $\Im(\theta') = -i\delta$ (① in Fig.5.3). Taking the limit $\delta \to 0$, the branch cut approaches to the real-axis from below and therefore we need to deform the integration contour to the slightly above. Similarly, the integrand of the second term of the l.h.s. of (5.1.18) has the branch cut at $\Im(\theta') = +i\delta$ (② in Fig.5.3) and we need to deform the integration contour to the slightly below under the limit $\delta \to 0$. We denote the resulting integrals as follows,

$$\begin{aligned}&\lim_{\delta\to 0}\left[\int_{\mathbb{R}} \frac{\epsilon_{i,i+1}\left(\theta' + i\frac{\pi}{2} + i\delta\right)}{\cosh(\theta-\theta')}\frac{d\theta'}{2\pi} - \int_{\mathbb{R}} \frac{\epsilon_{i,i+1}\left(\theta' + i\frac{\pi}{2} - i\delta\right)}{\cosh(\theta-\theta')}\frac{d\theta'}{2\pi}\right] \\ &= \int_{-\infty+i0}^{+\infty+i0} \frac{\epsilon_{i,i+1}\left(\theta' + i\frac{\pi}{2}\right)}{\cosh(\theta-\theta')}\frac{d\theta'}{2\pi} - \int_{-\infty-i0}^{+\infty-i0} \frac{\epsilon_{i,i+1}\left(\theta' + i\frac{\pi}{2}\right)}{\cosh(\theta-\theta')}\frac{d\theta'}{2\pi}.\end{aligned} \tag{5.1.19}$$

The integration contour of the first term in the second line of (5.1.19) is drawn in Fig.5.4 as C_1. The integration contour C_1 can be deformed as the sum of the contours $C_2+C_3+C_4+C_5$, where the contour C_5 arises from the pole of $1/\cosh(\theta-\theta')$. The integral along C_5 can be

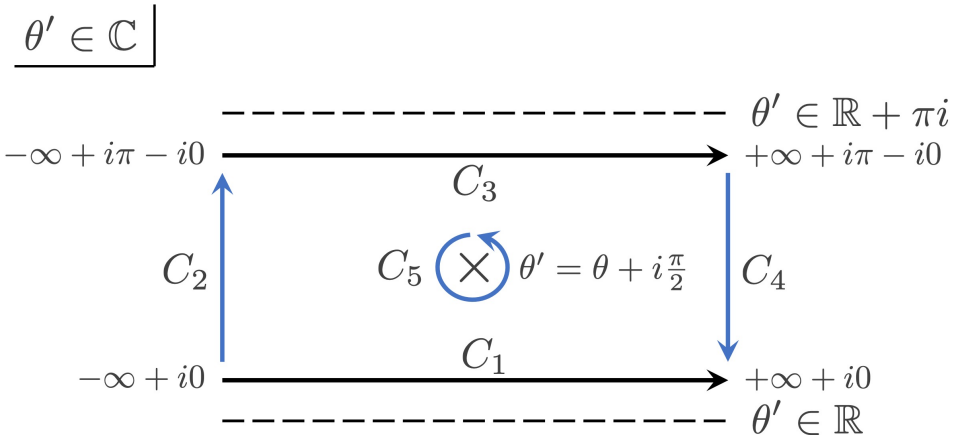

Figure 5.4: A deformation of the integration contour of the first term in the second line of (5.1.19). The dashed lines are the branch cut of $\epsilon_{i,i+1}\left(\theta' + i\frac{\pi}{2}\right)$.

evaluate as

$$\oint_{C_5} \frac{\epsilon_{i,i+1}\left(\theta' + i\frac{\pi}{2}\right)}{\cosh\left(\theta - \theta'\right)} \frac{d\theta'}{2\pi} = i\mathrm{Res}_{\theta'=\theta+i\frac{\pi}{2}} \left[\frac{\epsilon_{i,i+1}\left(\theta' + i\frac{\pi}{2}\right)}{\cosh\left(\theta - \theta'\right)}\right] = \epsilon_{i,i+1}\left(\theta + i\pi\right) = -\epsilon_{i,i+1}\left(\theta\right). \tag{5.1.20}$$

For C_3, we obtain

$$\begin{aligned} \int_{C_3} \frac{\epsilon_{i,i+1}\left(\theta' + i\frac{\pi}{2}\right)}{\cosh\left(\theta - \theta'\right)} \frac{d\theta'}{2\pi} &= \int_{-\infty+i\pi-i0}^{+\infty+i\pi-i0} \frac{\epsilon_{i,i+1}\left(\theta' + i\frac{\pi}{2}\right)}{\cosh\left(\theta - \theta'\right)} \frac{d\theta'}{2\pi} \\ &= -\int_{-\infty-i0}^{+\infty-i0} \frac{\epsilon_{i,i+1}\left(\theta' - i\frac{\pi}{2}\right)}{\cosh\left(\theta - \theta'\right)} \frac{d\theta'}{2\pi} \\ &= \int_{-\infty-i0}^{+\infty-i0} \frac{\epsilon_{i,i+1}\left(\theta' + i\frac{\pi}{2}\right)}{\cosh\left(\theta - \theta'\right)} \frac{d\theta'}{2\pi}, \end{aligned} \tag{5.1.21}$$

where we have used the shift $\theta' \to \theta' - i\pi$ in the second line and $\epsilon_{i,i+1}\left(\theta' - i\frac{\pi}{2}\right) = -\epsilon_{i,i+1}\left(\theta' + i\frac{\pi}{2}\right)$ in the third line. This result shows that the integral along C_3 is canceled by the second term in the second line of (5.1.19). The integral along C_4 can be evaluated by using the asymptotic behavior (5.1.17) as follows,

$$\int_{C_4} \frac{\epsilon_{i,i+1}\left(\theta' + i\frac{\pi}{2}\right)}{\cosh\left(\theta - \theta'\right)} \frac{d\theta'}{2\pi} = \frac{m_{i,i+1}}{\pi} \int_{+\infty+i\pi}^{+\infty} \frac{e^{\theta'+i\frac{\pi}{2}}}{e^{\theta'-\theta}} d\theta' = i\frac{m_{i,i+1}}{\pi} e^{\theta}(-i\pi) = m_{i,i+1}e^{\theta}. \tag{5.1.22}$$

On the other hand, in order to evaluate the integral along C_2, we assume the following boundary condition,

$$\lim_{\theta' \to -\infty} \frac{\epsilon_{i,i+1}\left(\theta' + i\frac{\pi}{2}\right)}{\cosh\left(\theta - \theta'\right)} = 0. \tag{5.1.23}$$

Then the integral along C_2 becomes zero. In summary, we obtain

$$-\epsilon_{i,i+1}(\theta) + m_{i,i+1}e^{\theta} = \int_{\mathbb{R}} \frac{L_{i-1,i}(\theta')}{\cosh(\theta-\theta')}\frac{d\theta'}{2\pi} + \int_{\mathbb{R}} \frac{L_{i+1,i+2}(\theta')}{\cosh(\theta-\theta')}\frac{d\theta'}{2\pi}. \tag{5.1.24}$$

Organizing this equation, we obtain the TBA equations for arbitrary polynomial potentials [28],

$$\epsilon_{i,i+1}(\theta) = m_{i,i+1}e^{\theta} - \int_{\mathbb{R}} \frac{L_{i-1,i}(\theta')}{\cosh(\theta-\theta')}\frac{d\theta'}{2\pi} - \int_{\mathbb{R}} \frac{L_{i+1,i+2}(\theta')}{\cosh(\theta-\theta')}\frac{d\theta'}{2\pi}. \quad (i = 1, 2, \cdots, r) \tag{5.1.25}$$

The large θ expansion of the TBA equations provides the all-order asymptotic expansion of $\epsilon_{i,i+1}(\theta)$,

$$\epsilon_{i,i+1}(\theta) = m_{i,i+1}e^{\theta} + \sum_{n\geq 1} m_{i,i+1}^{(2n)} e^{(1-2n)\theta}, \quad \theta \to \infty \tag{5.1.26}$$

where

$$m_{i,i+1}^{(2n)} = \frac{(-1)^n}{\pi}\int_{\mathbb{R}} e^{(2n-1)\theta}\left(L_{i-1,i}(\theta) + L_{i+1,i+2}(\theta)\right)d\theta. \tag{5.1.27}$$

(5.1.27) is related to the coefficients of the WKB periods by the following equations,

$$\begin{aligned} m_{i,i+1}^{(2n)} &= (-1)^n i\Pi_{\gamma_{i,i+1}}^{(2n)}, \quad (i = r, r-2, \cdots) \\ m_{i,i+1}^{(2n)} &= -\Pi_{\gamma_{i,i+1}}^{(2n)}, \quad (i = r-1, r-3, \cdots) \end{aligned} \tag{5.1.28}$$

because $\theta \to \infty$ expansion of $\epsilon_{i,i+1}(\theta)$ is equivalent to $\eta \to \infty$ expansion of the Borel resummation of the WKB period.

5.2 Example: Double-well potential

5.2.1 TBA equations for double-well potential

As an example of the general result (5.1.25), we pick up the system of the double-well potential (3.2.1), which corresponds to $r = 3$ and $a_3 = a_1 = 0$ case of (5.1.1). The parameter region so that all the simple zeros are real is the energy region of the below the potential barrier $0 < E < \frac{\kappa^2}{4}$ (see Fig.3.2).

The TBA equations are given as follows,

$$\begin{aligned}\epsilon_{2,3}(\theta) &= m_{2,3}e^{\theta} - 2\int_{\mathbb{R}} \frac{L_{3,4}(\theta')}{\cosh(\theta-\theta')}\frac{d\theta'}{2\pi},\\ \epsilon_{3,4}(\theta) &= m_{3,4}e^{\theta} - \int_{\mathbb{R}} \frac{L_{2,3}(\theta')}{\cosh(\theta-\theta')}\frac{d\theta'}{2\pi},\end{aligned} \tag{5.2.1}$$

where we have used the identity (3.2.14). For the double-well potential, the leading terms of the WKB periods $m_{i,i+1}$ can be expressed in terms of the elliptic integrals [1] [28, 84],

$$m_{2,3} = -\Pi^{(0)}_{\gamma_{2,3}} = \frac{4}{3}z_4^3\left[\left(2-k^2\right)E(1-k^2) - k^2K(1-k^2)\right], \tag{5.2.3}$$

$$m_{3,4} = i\Pi^{(0)}_{\gamma_{3,4}} = \frac{2}{3}z_4^3\left[\left(2-k^2\right)E(k^2) - 2\left(1-k^2\right)K(k^2)\right], \tag{5.2.4}$$

where k is the elliptic moduli given by

$$k = \sqrt{1-\frac{z_3^2}{z_4^2}} = \sqrt{\frac{4\sqrt{E}}{2\sqrt{E}+\kappa}}. \tag{5.2.5}$$

The TBA equations (5.2.1) are valid for the below the potential barrier, but we can also obtain the integral equations for the above the potential barrier by considering the wall-crossing of the TBA equations [28, 30, 85].

We can calculate the coefficients of the WKB periods through the equation (5.1.28). Table.5.1 shows the numerical values of the coefficients of the WKB periods calculated by the TBA equations and compare with the differential operator method (2.2.20). For (3.2.1), the second and fourth order of the differential operator is given as follows [28],

$$\mathcal{O}_2 = b_1^{(2)}\partial_{u_1} + b_3^{(2)}\partial_{u_3}, \tag{5.2.6}$$

$$\mathcal{O}_4 = b_1^{(4)}\partial_{u_1} + b_3^{(4)}\partial_{u_3}, \tag{5.2.7}$$

[1] Here we have used the notation of the elliptic integrals so that

$$E(x) = \text{EllipticE[x]}, \quad K(x) = \text{EllipticK[x]}, \tag{5.2.2}$$

in Mathematica code.

n	$(-1)^n i\Pi^{(2n)}_{\gamma_{3,4}}$	$m^{(2n)}_{3,4}$	$-\Pi^{(2n)}_{\gamma_{2,3}}$	$m^{(2n)}_{2,3}$
1	-0.08707917	$-\underline{\mathbf{0.08707912}}$	-0.52131451	$-\underline{\mathbf{0.52131}}366$
2	0.00666021	$\underline{\mathbf{0.00666}}019$	0.84901435	$\underline{\mathbf{0.84901}}001$

Table 5.1: The numerical results of the coefficients of the WKB periods with $E = 1$, $\kappa = 4$. The calculation of the TBA equations is done by Fourier discretization with 2^{18} points and a cutoff of the integrals $(-L, L)$ where $L = 100\,(1 - 1/2^{18})$.

where the coefficients are given as,

$$\begin{aligned} b_1^{(2)} &= \frac{4\,(u_1^4 + 16u_1^2u_3 + 48u_3^2)}{3\Delta}, \\ b_3^{(2)} &= \frac{-16u_1^3u_3 - 64u_1u_3^2}{3\Delta}, \end{aligned} \tag{5.2.8}$$

$$\begin{aligned} b_1^{(4)} &= \frac{2}{45\Delta^3}(1792u_1^{13} + 40800u_1^{11}u_3 + 390528u_1^9u_3^2 + 1555456u_1^7u_3^3 + 405504u_1^5u_3^4 \\ &\quad - 12656640u_1^3u_3^5 - 23101440u_1u_3^6), \\ b_3^{(4)} &= \frac{1}{45\Delta^3}(1792u_1^{12}u_3 + 38784u_1^{10}u_3^2 + 708096u_1^8u_3^3 + 5582848u_1^6u_3^4 + 16957440u_1^4u_3^5 \\ &\quad + 10321920u_1^2u_3^6 - 21626880u_3^7), \end{aligned} \tag{5.2.9}$$

with

$$\Delta := -16u_1^4u_3 - 128u_1^2u_3^2 - 256u_3^3, \tag{5.2.10}$$

and $u_1 = \kappa, u_3 = E - \frac{\kappa^2}{4}$.

5.2.2 Exact quantization condition for double-well potential and TBA equations

Combining the TBA equations (5.2.1) with the exact quantization condition (3.2.27), we can calculate the energy spectrum. In terms of the TBA equations, one can find that the median resummation is given as the principal value of the singular integral:

$$\begin{aligned} i\eta\mathcal{B}_{0,\mathrm{med}}\left[\Pi_{\gamma_{3,4}}\right] &= \frac{i\eta}{2}\left(\mathcal{B}_{0,+}\left[\Pi_{\gamma_{3,4}}\right] + \mathcal{B}_{0,-}\left[\Pi_{\gamma_{3,4}}\right]\right) \\ &= \lim_{\delta\to+0}\frac{i\eta}{2}\left(\epsilon_{3,4}\left(\theta - i\frac{\pi}{2} + i\delta\right) + \epsilon_{3,4}\left(\theta - i\frac{\pi}{2} - i\delta\right)\right) \\ &= m_{3,4}e^{\theta} + \mathrm{P}\int_{\mathbb{R}}\frac{2L_{2,3}(\theta)}{\sinh\left(\theta - \theta'\right)}\frac{d\theta'}{2\pi}, \end{aligned} \tag{5.2.11}$$

n	Energy	η
0	2.289649	1.000014
1	2.752077	1.000014

Table 5.2: The second column is the energy spectrum at $\kappa = 4, \eta = 1$ calculated by solving the Schrödinger equation (3.2.1) numerically. The third column is the solutions to the exact quantization condition (3.2.27) with respect to η calculated by the TBA equations.

where

$$\mathrm{P}\int_{\mathbb{R}} \frac{2L_2(\theta)}{\sinh(\theta-\theta')}\frac{d\theta'}{2\pi} := \lim_{\delta\to 0}\int_{\mathbb{R}} \frac{2L_{2,3}(\theta')\sinh(\theta-\theta')\cos\delta}{\sinh^2(\theta-\theta')\cos^2(\delta)+\cosh^2(\theta-\theta')\sin^2(\delta)}\frac{d\theta'}{2\pi}. \quad (5.2.12)$$

As a consistency check, we first calculate the energy spectrum at $\kappa = 4, \eta = 1$ by solving the Schrödinger equation (3.2.1) numerically, and then calculate the solution η, which must be one, to the exact quantization condition (3.2.27) substituted the energy spectrum. Table.5.2 shows the numerical results.

5.3 Central and centrifugal potentials

5.3.1 Discontinuity of WKB periods for central and centrifugal potentials

We generalize the result for arbitrary polynomial potentials in the presence of central and centrifugal potentials. Let us consider the following Schrödinger equation on the Riemann sphere $\mathbb{C}^* = \mathbb{C} \cup \{\infty\}$,

$$\left[\frac{d^2}{dz^2} - \eta^2 Q_0(z) - Q_2(z)\right]\psi(z) = 0, \quad (5.3.1)$$

with

$$Q_0(z) = V(z) - E = \sum_{n=-1}^{r+1} a_n z^n - E, \quad Q_2(z) = \frac{l(l+1)}{z^2}, \quad (-1 \le l \le 0) \quad (5.3.2)$$

where we take a_n as a real parameter and fix $a_{r+1} = 1$. For this equation, there is the simple pole at $z = 0$ on the WKB curve. We consider the parameter region in the moduli space where all the simple zeros are real and positive. We name the simple zeros so that

$$0 < z_1 < z_2 < \cdots < z_{r+2}. \quad (5.3.3)$$

The intervals $[z_i, z_{i+1}]$ for $i = r+1, r-1, r-3, \cdots$ are the classically allowed intervals, and for $i = r, r-2, r-4, \cdots$ are the classically forbidden intervals. We denote $\gamma_{i,i+1}$ as the one-cycle encircling the interval $[z_i, z_{i+1}]$. We also choose the branch cuts and the orientation of the one-cycles so that (5.1.5 and (5.1.6) are real and positive.

By the restriction that all the simple zeros are real and positive, if the interval $[z_1, z_2]$ is classically forbidden, then a_{-1} must be negative so that the interval $[0, z_1]$ is classically allowed, and if the interval $[z_1, z_2]$ is classically allowed, then a_{-1} must be positive so that the interval $[0, z_1]$ is classically forbidden. We define $\hat{\gamma}$ as the one-cycle encircling $[0, z_1]$ and $\hat{m}$ as when $[0, z_1]$ is classically allowed,

$$\hat{m} := i\Pi_{\hat{\gamma}}^{(0)} = i \oint_{\hat{\gamma}} S_0(z) dz, \tag{5.3.4}$$

and when $[0, z_1]$ is classically forbidden,

$$\hat{m} := -\Pi_{\hat{\gamma}}^{(0)} = - \oint_{\hat{\gamma}} S_0(z) dz. \tag{5.3.5}$$

We also choose the branch cut and the orientation of $\hat{\gamma}$ so that $\hat{m}$ is real and positive.

The discontinuity formulae of the WKB periods depend on which $[0, z_1]$ is classically allowed or forbidden. For $[0, z_1]$ is classically allowed case, we obtain the same discontinuity formulae as (5.1.7) at $\arg(\eta) = 0$ and (5.1.10) at $\arg(\eta) = \pi$ for any classically allowed cycle $\hat{\gamma}, \gamma_{i,i+1}$ $(i = r+1, r-1, \cdots, 2)$. On the other hand, at $\arg(\eta) = \pm\pi/2$, the discontinuity formulae of the WKB periods for $\gamma_{i,i+1} (i = r, r-2, \cdots, 3)$ are same as (5.1.12) but the formula for $\gamma_{1,2}$ is modified as follows,

$$e^{\eta\mathcal{B}_{\pm\frac{\pi}{2}-}[\Pi_{\gamma_{1,2}}]} = e^{\eta\mathcal{B}_{\pm\frac{\pi}{2}+}[\Pi_{\gamma_{1,2}}]} \left(1 - (e^{2\pi i l} + e^{-2\pi i l}) e^{\mp\eta\mathcal{B}_{\pm\frac{\pi}{2}}[\Pi_{\hat{\gamma}}]} + e^{\mp 2\eta\mathcal{B}_{\pm\frac{\pi}{2}}[\Pi_{\hat{\gamma}}]}\right)^{\pm 1} \left(1 + e^{\mp\eta\mathcal{B}_{\pm\frac{\pi}{2}}[\Pi_{\gamma_{2,3}}]}\right)^{\pm 1}, \tag{5.3.6}$$

because, at $\arg(\eta) = \pm\pi/2$, $\gamma_{1,2}$ intersects with the Stokes segment connecting the simple zero and the simple pole and then the discontinuity formula is given by (2.2.51). Similarly, for $[0, z_1]$ is classically forbidden case, we obtain the same discontinuity formula as (5.1.12) at $\arg(\eta) = \pm\pi/2$ for any classically forbidden cycle $\hat{\gamma}, \gamma_{i,i+1}$ $(i = r, r-2, \cdots, 2)$. And at $\arg(\eta) = 0, \pi$, the discontinuity formulae of the WKB periods for $\gamma_{i,i+1} (i = r+1, r-1, \cdots, 3)$

are same as (5.1.7) and (5.1.10) but the formula for $\gamma_{1,2}$ is modified as follows,

$$e^{\eta\mathcal{B}_{\varphi-}\left[\Pi_{\gamma_{1,2}}\right]} = e^{\eta\mathcal{B}_{\varphi+}\left[\Pi_{\gamma_{1,2}}\right]}\left(1-(e^{2\pi il}+e^{-2\pi il})e^{\mp\eta\mathcal{B}_{\varphi}\left[\Pi_{\hat{\gamma}}\right]}+e^{\mp 2\eta\mathcal{B}_{\varphi}\left[\Pi_{\hat{\gamma}}\right]}\right)^{\pm 1}\left(1+e^{\mp\eta\mathcal{B}_{\varphi}\left[\Pi_{\gamma_{2,3}}\right]}\right)^{\pm 1}, \tag{5.3.7}$$

where $\varphi = 0, \pi$.

5.3.2 TBA equations for central and centrifugal potentials

We introduce the epsilon function as follows,

$$\begin{aligned}\epsilon_{i,i+1}(\theta - i\frac{\pi}{2} + i\varphi) &= \eta\mathcal{B}_{\varphi}\left[\Pi_{\gamma_{i,i+1}}\right], \quad (i = r+1, r-1, \cdots)\\ \epsilon_{i,i+1}(\theta + i\varphi) &= -\eta\mathcal{B}_{\varphi}\left[\Pi_{\gamma_{i,i+1}}\right], \qquad (i = r, r-2, \cdots)\end{aligned} \tag{5.3.8}$$

and

$$\begin{aligned}\hat{\epsilon}(\theta - i\frac{\pi}{2} + i\varphi) &= \eta\mathcal{B}_{\varphi}\left[\Pi_{\hat{\gamma}}\right] \quad \text{for } [0, z_1] \text{ is classically allowed case,}\\ \hat{\epsilon}(\theta + i\varphi) &= -\eta\mathcal{B}_{\varphi}\left[\Pi_{\hat{\gamma}}\right] \qquad \text{for } [0, z_1] \text{ is classically forbidden case.}\end{aligned} \tag{5.3.9}$$

Then the discontinuity formulae for the central and centrifugal potentials can be expressed in simpler form,

$$\begin{aligned}\lim_{\delta\to 0}\left[\epsilon_{i,i+1}\left(\theta \pm i\frac{\pi}{2} + i\delta\right) - \epsilon_{i,i+1}\left(\theta \pm i\frac{\pi}{2} - i\delta\right)\right] &= \pm\left[L_{i-1,i}(\theta) + L_{i+1,i+2}(\theta)\right], \quad (i = 2, \cdots, r+1)\\ \lim_{\delta\to 0}\left[\epsilon_{1,2}\left(\theta \pm i\frac{\pi}{2} + i\delta\right) - \epsilon_{1,2}\left(\theta \pm i\frac{\pi}{2} - i\delta\right)\right] &= \pm\left[\hat{L}(\theta) + L_{2,3}(\theta)\right],\\ \lim_{\delta\to 0}\left[\hat{\epsilon}\left(\theta \pm i\frac{\pi}{2} + i\delta\right) - \hat{\epsilon}\left(\theta \pm i\frac{\pi}{2} - i\delta\right)\right] &= \pm L_{1,2}(\theta),\end{aligned} \tag{5.3.10}$$

where $L_{i,i+1}(\theta)$ is defined in (5.1.16) and

$$\hat{L}(\theta) := \log\left(1-(e^{2\pi il}+e^{-2\pi il})e^{-\hat{\epsilon}(\theta)}+e^{-2\hat{\epsilon}(\theta)}\right). \tag{5.3.11}$$

Taking the convolution of (5.3.10) with $K(\theta) = 1/\left(2\pi\cosh(\theta)\right)$ and using the asymptotic behavior of the epsilon function as we have derived (5.1.25), we obtain the TBA equations

for the central and centrifugal potentials [47],

$$\begin{aligned}
\epsilon_{i,i+1}(\theta) &= m_{i,i+1}e^{\theta} - \int_{\mathbb{R}} \frac{L_{i-1,i}(\theta')}{\cosh(\theta-\theta')}\frac{d\theta'}{2\pi} - \int_{\mathbb{R}} \frac{L_{i+1,i+2}(\theta')}{\cosh(\theta-\theta')}\frac{d\theta'}{2\pi}, \quad (i=2,\cdots,r+1)\\
\epsilon_{1,2}(\theta) &= m_{1,2}e^{\theta} - \int_{\mathbb{R}} \frac{\hat{L}(\theta')}{\cosh(\theta-\theta')}\frac{d\theta'}{2\pi} - \int_{\mathbb{R}} \frac{L_{2,3}(\theta')}{\cosh(\theta-\theta')}\frac{d\theta'}{2\pi},\\
\hat{\epsilon}(\theta) &= \hat{m}e^{\theta} - \int_{\mathbb{R}} \frac{L_{1,2}(\theta')}{\cosh(\theta-\theta')}\frac{d\theta'}{2\pi}.
\end{aligned} \tag{5.3.12}$$

The large θ expansion of the TBA equations provides the all-order asymptotic expansion of $\epsilon_{i,i+1}(\theta), \hat{\epsilon}(\theta)$,

$$\begin{aligned}
\epsilon_{i,i+1}(\theta) &= m_{i,i+1}e^{\theta} + \sum_{n\geq 1} m_{i,i+1}^{(2n)} e^{(1-2n)\theta},\\
\hat{\epsilon}(\theta) &= m_{i,i+1}e^{\theta} + \sum_{n\geq 1} \hat{m}^{(2n)} e^{(1-2n)\theta},
\end{aligned} \tag{5.3.13}$$

where

$$\begin{aligned}
m_{i,i+1}^{(2n)} &= \frac{(-1)^n}{\pi}\int_{\mathbb{R}} e^{(2n-1)\theta}\left(L_{i-1,i}(\theta)+L_{i+1,i+2}(\theta)\right)d\theta, \quad (i=2,\cdots,r+1)\\
m_{1,2}^{(2n)} &= \frac{(-1)^n}{\pi}\int_{\mathbb{R}} e^{(2n-1)\theta}\left(\hat{L}(\theta)+L_{2,3}(\theta)\right)d\theta,\\
\hat{m}^{(2n)} &= \frac{(-1)^n}{\pi}\int_{\mathbb{R}} e^{(2n-1)\theta}L_{1,2}(\theta)d\theta.
\end{aligned} \tag{5.3.14}$$

(5.3.14) is related to the coefficients of the WKB periods by the following equations,

$$\begin{aligned}
m_{i,i+1}^{(2n)} &= (-1)^n i\Pi_{\gamma_{i,i+1}}^{(2n)}, \quad (i=r+1,r-1,\cdots)\\
m_{i,i+1}^{(2n)} &= -\Pi_{\gamma_{i,i+1}}^{(2n)}, \quad (i=r,r-2,\cdots)
\end{aligned} \tag{5.3.15}$$

and

$$\begin{aligned}
\hat{m}^{(2n)} &= (-1)^n i\Pi_{\hat{\gamma}}^{(2n)} \quad \text{for } [0,z_1] \text{ is classically allowed case},\\
\hat{m}^{(2n)} &= -\Pi_{\hat{\gamma}}^{(2n)} \qquad \text{for } [0,z_1] \text{ is classically forbidden case}.
\end{aligned} \tag{5.3.16}$$

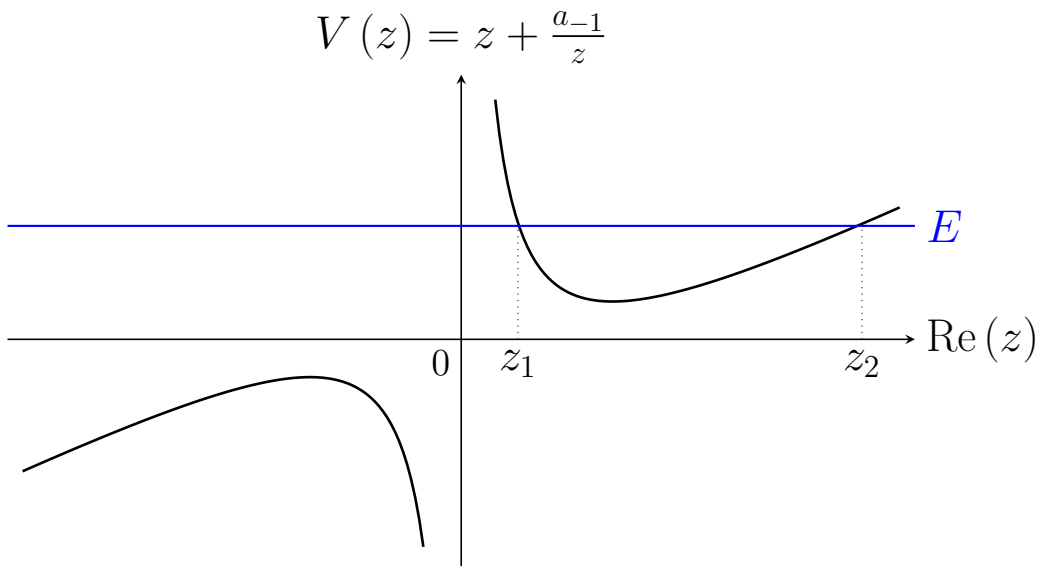

Figure 5.5: The potential $V(z)$ on the real z-axis.

5.4 Example: Central force and linear perturbation

As an example of (5.3.12), we consider the system of the central force with linear perturbation,

$$\left[\frac{d^2}{dz^2} - \eta^2 Q_0(z) - Q_2(z)\right]\psi(z) = 0, \tag{5.4.1}$$

with

$$Q_0(z) = V(z) - E = z - E + \frac{a_{-1}}{z}, \quad Q_2(z) = \frac{l(l+1)}{z^2}. \tag{5.4.2}$$

For this equation, there are two simple zeros z_1, z_2. The interval $[z_1, z_2]$ is classically allowed and a_{-1} must be positive so that the interval $[0, z_1]$ is classically forbidden. The potential on the real z-axis is drawn in Fig.5.5.

The TBA equations are given as follows,

$$\begin{aligned} \epsilon_{1,2}(\theta) &= m_{1,2}e^{\theta} - \int_{\mathbb{R}} \frac{\hat{L}(\theta')}{\cosh(\theta - \theta')}\frac{d\theta'}{2\pi}, \\ \hat{\epsilon}(\theta) &= \hat{m}e^{\theta} - \int_{\mathbb{R}} \frac{L_{1,2}(\theta')}{\cosh(\theta - \theta')}\frac{d\theta'}{2\pi}. \end{aligned} \tag{5.4.3}$$

For the case (5.4.1), the leading terms of the WKB periods can be expressed in term of the

n	$(-1)^n i\Pi^{(2n)}_{\gamma_{1,2}}$	$m^{(2n)}_{1,2}$	$-\Pi^{(2n)}_{\hat{\gamma}}$	$\hat{m}^{(2n)}$
1	-0.29605493	$-\underline{\mathbf{0.29605493}}$	-0.11667229	$-\underline{\mathbf{0.11667229}}$
2	0.15808446	$\underline{\mathbf{0.15808446}}$	0.01972364	$\underline{\mathbf{0.01972364}}$

Table 5.3: The numerical results of the coefficients of the WKB periods for $E = 3, a_{-1} = 1, l = -2/5$. The calculation of the TBA equations is done by Fourier discretization with 2^{18} points and a cutoff of the integrals $(-L, L)$ where $L = 100\,(1 - 1/2^{18})$.

hypergeometric function [2] [47],

$$m_{1,2} = i\Pi^{(0)}_{\gamma_{1,2}} = \frac{(z_1 - z_2)^2}{\sqrt{z_1}} \frac{\Gamma(\frac{1}{2})\Gamma(\frac{3}{2})}{\Gamma(3)}\ {}_2F_1\left[\frac{1}{2}, \frac{3}{2}, 3, \frac{z_1 - z_2}{z_1}\right], \tag{5.4.5}$$

$$\hat{m} = -\Pi^{(0)}_{\hat{\gamma}} = -\frac{1}{2} z_1 \sqrt{z_2} \frac{\Gamma(-\frac{1}{2})\Gamma(\frac{1}{2})}{\Gamma(2)}\ {}_2F_1\left[-\frac{1}{2}, \frac{1}{2}, 2, \frac{z_1}{z_2}\right]. \tag{5.4.6}$$

We can also calculate the coefficients of the WKB periods through the equation (5.3.15). Table.5.3 shows the numerical values of the coefficients of the WKB periods calculated by the TBA equations and compare with the differential operator method (2.2.20). For (5.4.1), the second and fourth order of the differential operator is given as follows [47],

$$\mathcal{O}_2 = -\frac{1}{12} \sum_{k=0}^{1} u_k\,(2-k)\,(-k-3)\,\partial_{u_{k+1}}\partial_{u_2} + \frac{l\,(l+1)}{u_2} u_0 \partial_{u_1}, \tag{5.4.7}$$

$$\begin{aligned}
\mathcal{O}_4 = {} & \frac{7}{1440}\left[-\frac{13\times 4}{3} u_2 u_0 \partial^4_{u_2} + \frac{32u_1}{3}\sum_{k=0}^{1}(-5k+11)\,u_k \partial_{u_{k+1}}\partial^3_{u_2}\right] \\
& + \frac{1}{768}\left[-64\times 3 u_0 \partial^3_{u_2} + \frac{128u_1}{u_2}\sum_{k=0}^{1}(-3k+7)\,u_k\partial_{u_{k+1}}\partial^2_{u_2}\right] \\
& - \frac{l\,(l+1)}{12}\left[-6u_0\partial_{u_2} + \frac{4u_1}{u_2}\sum_{k=0}^{1}(-3k+7)\,u_k\partial_{u_{k+1}}\right]\partial^2_{u_2} \\
& - \frac{l\,(l+1)\,(1-l\,(l+1))}{6u_2}\left[-5u_0\partial_{u_2} + \frac{4u_1}{u_2}\sum_{k=0}^{1}(-k+3)\,u_k\partial_{u_{k+1}}\right]\partial_{u_2},
\end{aligned} \tag{5.4.8}$$

with $u_0 = 1, u_1 = -E, u_2 = a_1$.

[2] Here we have used the notation of the hypergeometric function so that

$${}_2F_1\,[a, b, c, z] = \text{Hypergeometric2F1}\,[\text{a}, \text{b}, \text{c}, \text{z}], \tag{5.4.4}$$

in Mathematica code.

Summary

In this chapter, we have derived the TBA equations governing the Borel resummed WKB periods for arbitrary polynomial potentials and central-centrifugal potentials. We have determined the discontinuity of the Borel resummed WKB periods in the whole of the complex η-plane by using the Delabaere-Pham formula. The TBA equations are derived so that the discontinuity and the asymptotic behavior of the Borel resummed WKB periods are satisfied. The WKB periods calculated from the TBA equations are consistent with the differential operators results. Combining the exact energy quantization condition for the double-well potential, we have checked that the TBA equations provide the spectrum exactly.

Chapter 6

TBA equations for quantum Seiberg-Witten curves

In this chapter, we derive the TBA equations for the quantum Seiberg-Witten curves of 4-dimensional $\mathcal{N} = 2$ SU(2) $N_f = 0, 2$ supersymmetric gauge theories. The TBA equations determine the mass of the BPS particles in the low-energy effective theory of the models exactly. The TBA equations show that the effective central charge of the underlying CFT is proportional to the one-loop beta function of the gauge theory. We also show that the TBA equations for 4-dimensional $\mathcal{N} = 2$ SU(2) $N_f = 0$ theory determine the QNMs for the extremal D3-branes by combining with the exact condition. This chapter is based on the author's papers [65, 66].

6.1 Review of quantum Seiberg-Witten curve

6.1.1 Seiberg-Witten curve for SU(2)

The Seiberg-Witten curve for $\mathcal{N} = 2$ SU(2) gauge theory with $N_f = 0, \cdots, 4$ fundamental hypermultiplets on 4-dimensional Minkowski space is the following algebraic curve,

$$K(p) - \frac{\bar{\Lambda}}{2}\left(K_+(p)e^{iz} + K_-(p)e^{-iz}\right) = 0, \tag{6.1.1}$$

where $\bar{\Lambda} = \Lambda_{N_f}^{2-\frac{N_f}{2}}$ with $\Lambda_{N_f} \in \mathbb{C}$ being the dynamically generated scale for $N_f \leq 3$ and $\bar{\Lambda} = e^{\pi i \tau_{\rm UV}}$ with $\tau_{\rm UV}$ being the UV coupling constant [86, 87]. $K(p)$ and $K_\pm(p)$ are given as

follows,

$$K(p) = \begin{cases} p^2 - u, & N_f = 0, 1, \\ p^2 - u + \frac{\Lambda_2^2}{8}, & N_f = 2, \\ p^2 - u + \frac{\Lambda_3}{4}\left(p + \frac{m_1+m_2+m_3}{2}\right), & N_f = 3, \\ (1 + \frac{e^{2\pi i \tau_{\rm UV}}}{2})p^2 - u + \frac{e^{2\pi i \tau_{\rm UV}}}{4} p \sum_{i=1}^4 m_i + \frac{e^{2\pi i \tau_{\rm UV}}}{8} p \sum_{i<j}^4 m_i m_j, & N_f = 4, \end{cases} \tag{6.1.2}$$

$$K_+(p) = \prod_{i=1}^{N_+}(p + m_i), \quad K_-(p) = \prod_{i=N_++1}^{N_f}(p + m_i), \tag{6.1.3}$$

where $u \in \mathbb{C}$ is the Coulomb moduli parameter and $m_1, \cdots, m_{N_f} \in \mathbb{C}$ are the bare masses of the hypermultiplets, N_+ is an integer satisfying $1 \leq N_+ \leq N_f$. The curve (6.1.1) defines a Riemann surface with genus one. Let α and β be a canonical one-cycles on the Riemann surface, they generates periods we denote as

$$a_\alpha = \oint_\alpha p(z)dz, \quad a_\beta = \oint_\beta p(z)dz, \tag{6.1.4}$$

where $p(z)$ is the solution to (6.1.1). a_α and a_β are called Seiberg-Witten periods. The Seiberg-Witten periods gives the renormalized masses $M_{\rm BPS}$ of the BPS particles in the low-energy effective theory of the $\mathcal{N} = 2$ gauge theory as [49, 50]

$$M_{\rm BPS} = \sqrt{2}|Z| = \sqrt{2}|n_e a_\alpha + n_m a_\beta|, \tag{6.1.5}$$

where $n_e, n_m \in \mathbb{Z}$ are the electric and magnetic changes of the BPS particles and Z is the central charge of the $\mathcal{N} = 2$ supersymmetry algebra [88].

6.1.2 Ω-deformation and quantum Seiberg-Witten curve

$\mathcal{N} = 2$ SU(2) gauge theory with $N_f = 0, \cdots, 4$ fundamental hypermultiplets on the Ω-background is the theory constructed from the dimensional reduction of $\mathcal{N} = 1$ supersymmetric gauge theories on $\mathbb{R}^{1,3} \times \mathbb{T}^2$, where the metric is given by the following line element [56],

$$ds_6^2 = \eta_{\mu\nu}(dx^\mu + \Omega_n{}^\mu{}_\rho x^\rho dx^n)(dx^\nu + \Omega_m{}^\nu{}_\rho x^\rho dx^m) - (dx^4)^2 - (dx^5)^2, \tag{6.1.6}$$

with $\mu, \nu, \rho = 0, 1, 2, 3$ and $n, m = 4, 5$. x^4 and x^5 are the coordinates on $\mathbb{T}^2$:

$$x^4 \sim x^4 + 2\pi R_4, \quad x^5 \sim x^5 + 2\pi R_5, \tag{6.1.7}$$

where R_4 and R_5 are the radius of the compactification. $\Omega_n{}^{\mu}{}_{\rho}$ is the matrix given by

$$\frac{1}{\sqrt{2}}\left(\Omega_4^{\mu\nu} + i\Omega_5^{\mu\nu}\right) = \frac{1}{\sqrt{2}}\begin{pmatrix} 0 & \epsilon_1 & 0 & 0 \\ -\epsilon_1 & 0 & 0 & 0 \\ 0 & 0 & 0 & \epsilon_2 \\ 0 & 0 & -\epsilon_2 & 0 \end{pmatrix}, \tag{6.1.8}$$

$$\frac{1}{\sqrt{2}}\left(\Omega_4^{\mu\nu} - i\Omega_5^{\mu\nu}\right) = \frac{1}{\sqrt{2}}\begin{pmatrix} 0 & \bar{\epsilon}_1 & 0 & 0 \\ -\bar{\epsilon_1} & 0 & 0 & 0 \\ 0 & 0 & 0 & \bar{\epsilon_2} \\ 0 & 0 & -\bar{\epsilon_2} & 0 \end{pmatrix}, \tag{6.1.9}$$

where $\epsilon_1, \epsilon_2 \in \mathbb{C}$. In the limit $R_4, R_5 \to 0$, we obtain 4-dimensional $\mathcal{N} = 2$ gauge theory on the Ω-background parametrized by the deformation parameters ϵ_1, ϵ_2.

$\epsilon_2 \to 0$ limit is called Nekrasov-Shatashvili limit [57]. In the Nekrasov-Shatashvili limit, the Seiberg-Witten periods receive the deformation parametrized by ϵ_1. The deformed Seiberg-Witten periods is called quantum period. In [44], it was argued that the ϵ_1 expansion of the quantum periods for $\mathcal{N} = 2$ SU(2) $N_f = 0$ theory are identical to the WKB periods for the differential equation that is obtained by replacing p in the Seiberg-Witten curve (6.1.1) with the differential operator $-i\epsilon_1 \frac{d}{dz}$. This identification is generalized to the theory with matters [46]. The differential equation obtained by the replacement $p \to -i\epsilon_1 \frac{d}{dz}$ is called quantum Seiberg-Witten curves.

The Borel resummed WKB periods for the quantum Seiberg-Witten curves determine the quantum periods exactly. In the following section, we will derive the TBA equations governing the Borel resummed WKB periods for the quantum Seiberg-Witten curves of $\mathcal{N} = 2$ $SU(2)$ gauge theory with $N_f = 0, 2$.

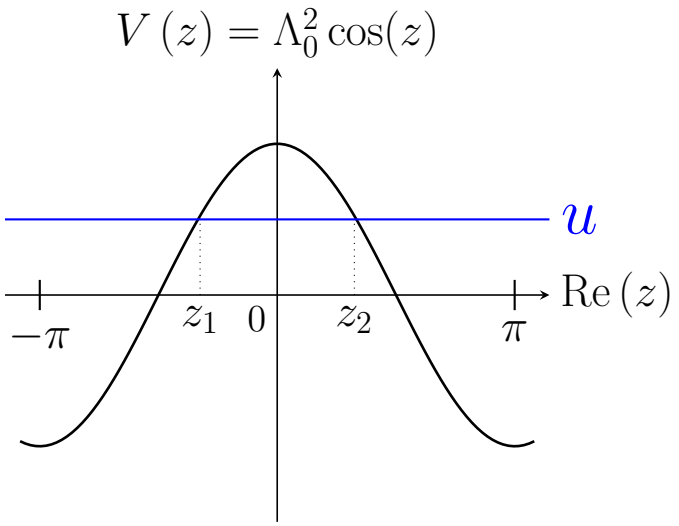

Figure 6.1: The potential $V(z)$ on the real z-axis in $z \in [-\pi, \pi]$. $z_1 = -z_2$ and z_2 are the simple zeros of $Q_0(z)$.

6.2 $\mathcal{N} = 2$ $SU(2)$ Super Yang-Mills theory

6.2.1 Discontinuity of WKB periods for $\mathcal{N} = 2$ $SU(2)$ SYM

The quantum Seiberg-Witten curve for 4-dimensional $\mathcal{N} = 2$ $SU(2)$ Super Yang-Mills theory is the Mathieu equation [44],

$$\left[\frac{d^2}{dz^2} - \eta^2 Q_0(z)\right] \psi(z) = 0, \tag{6.2.1}$$

with

$$Q_0(z) = V(z) - u = \Lambda_0^2 \cos(z) - u, \tag{6.2.2}$$

where Λ_0 is the dynamically generated scale, $u \in \mathbb{C}$ is the Coulomb moduli parameter and $\eta = 1/\epsilon_1$ is the deformation parameter in the Nekrasov-Shatashvili limit of the Ω-background.

We apply the Exact WKB analysis to (6.2.1) on the Riemann sphere composed by the cylinder $\mathbb{C}/\langle z \sim z + 2\pi \rangle$ with the compactification $\mathbb{C}^* = (\mathbb{C}/\langle z \sim z + 2\pi \rangle) \cup \{\pm i\infty\}$. In the following analysis, we restrict to the parameter as $-\Lambda_0^2 < u < \Lambda_0^2$, which is in the strong coupling region of 4-dimensional $\mathcal{N} = 2$ $SU(2)$ Super Yang-Mills theory. In this regime, the simple zeros of $Q_0(z)$ are real. The potential graph on the real z-axis is given by Fig.6.1.

The Stokes graph at $\arg(\eta) = 0$ is drawn in Fig.6.2. On the WKB curve, there are

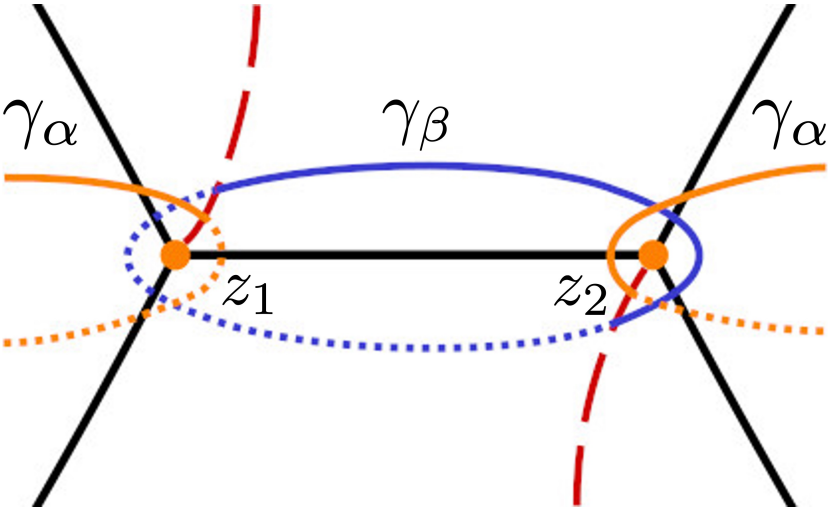

Figure 6.2: The Stokes graph at $\arg(\eta) = 0$ for the quantum Seiberg-Witten curve of 4-dimensional $\mathcal{N} = 2$ $SU(2)$ Super Yang-Mills theory in $z \in [-\pi, \pi]$. The branch cut emanating from z_1 is connected to $+i\infty$ and the branch cut emanating from z_2 is connected to $-i\infty$.

two one-cycles γ_β, which encircles the classically forbidden interval on the real z-axis (see Fig.6.1), and γ_α, which encircles the classically allowed interval. We choose the branch cuts and the orientation of the one-cycles so that

$$m_\beta := -\Pi^{(0)}_{\gamma_\beta} = -\oint_{\gamma_\beta} S_0(z)dz \tag{6.2.3}$$

and

$$m_\alpha := i\Pi^{(0)}_{\gamma_\alpha} = i\oint_{\gamma_\alpha} S_0(z)dz \tag{6.2.4}$$

are real and positive. m_β and m_α can be expressed by using the hypergeometric function (4.1.31) and (4.1.32) through the transformation of the parameters and the coodtinate (4.1.39).

The discontinuity formulae for the WKB periods can be determined by using the analogy of arbitrary polynomial potentials case in sec.5.1. In the present case, the WKB period for γ_β has no discontinuity for $\arg(\eta) = 0$, and the WKB period for γ_α has the following discontinuity,

$$e^{\eta\mathcal{B}_{0-}[\Pi_{\gamma_\alpha}]} = e^{\eta\mathcal{B}_{0+}[\Pi_{\gamma_\alpha}]}\left(1 + e^{\eta\mathcal{B}_0[\Pi_{\gamma_\beta}]}\right)^2, \tag{6.2.5}$$

where there is the index 2 in the r.h.s. of (6.2.5) because the one-cycle γ_α intersects with γ_β two times (see Fig.6.2). Similarly, the WKB period for γ_α also has the discontinuity at

$\arg(\eta) = \pi$ as follows,

$$e^{\eta\mathcal{B}_{\pi-}[\Pi_{\gamma_\alpha}]} = e^{\eta\mathcal{B}_{\pi+}[\Pi_{\gamma_\alpha}]}\left(1+e^{\eta\mathcal{B}_{\pi}\left[\Pi_{\gamma_\beta}\right]}\right)^{-2}. \tag{6.2.6}$$

For the direction $\arg(\eta) = \pm\pi/2$, the WKB period for the classically allowed cycle γ_α has no discontinuity, and the WKB period for the classically forbidden cycle γ_β has the discontinuity,

$$e^{\eta\mathcal{B}_{\pm\frac{\pi}{2}-}\left[\Pi_{\gamma_\beta}\right]} = e^{\eta\mathcal{B}_{\pm\frac{\pi}{2}+}\left[\Pi_{\gamma_\beta}\right]}\left(1+e^{\mp\eta\mathcal{B}_{\pm\frac{\pi}{2}}[\Pi_{\gamma_\alpha}]}\right)^{\pm 2}. \tag{6.2.7}$$

6.2.2 TBA equations for $\mathcal{N}=2$ $SU(2)$ SYM

As (5.1.13), we introduce the epsilon functions as follows,

$$\begin{aligned}\epsilon_\alpha(\theta - i\frac{\pi}{2} + i\varphi) &= \eta\mathcal{B}_\varphi\left[\Pi_{\gamma_\alpha}\right],\\ \epsilon_\beta(\theta + i\varphi) &= -\eta\mathcal{B}_\varphi\left[\Pi_{\gamma_\beta}\right].\end{aligned} \tag{6.2.8}$$

Then the discontinuity formulae (6.2.5)$\sim$(6.2.7) can be written as,

$$\begin{aligned}\lim_{\delta\to 0}\left[\epsilon_\alpha\left(\theta \pm i\frac{\pi}{2} + i\delta\right) - \epsilon_\alpha\left(\theta \pm i\frac{\pi}{2} - i\delta\right)\right] &= \pm 2L_\beta(\theta),\\ \lim_{\delta\to 0}\left[\epsilon_\beta\left(\theta \pm i\frac{\pi}{2} + i\delta\right) - \epsilon_\beta\left(\theta \pm i\frac{\pi}{2} - i\delta\right)\right] &= \pm 2L_\alpha(\theta),\end{aligned} \tag{6.2.9}$$

where

$$L_\alpha(\theta) := \log\left(1+e^{-\epsilon_\alpha(\theta)}\right), \quad L_\beta(\theta) := \log\left(1+e^{-\epsilon_\beta(\theta)}\right). \tag{6.2.10}$$

Taking the convolution of (6.2.9) with $K(\theta) = 1/\left(2\pi\cosh(\theta)\right)$ and using the asymptotic behavior of the epsilon function as we have derived (5.1.25), we obtain the TBA equations for 4-dimensional $\mathcal{N}=2$ $SU(2)$ Super Yang-Mills theory [65],

$$\begin{aligned}\epsilon_\alpha(\theta) &= m_\alpha e^\theta - 2\int_{\mathbb{R}}\frac{L_\beta(\theta')}{\cosh\left(\theta-\theta'\right)}\frac{d\theta'}{2\pi},\\ \epsilon_\beta(\theta) &= m_\beta e^\theta - 2\int_{\mathbb{R}}\frac{L_\alpha(\theta')}{\cosh\left(\theta-\theta'\right)}\frac{d\theta'}{2\pi}.\end{aligned} \tag{6.2.11}$$

The TBA equations (6.2.11) coincide with the "conformal limit" of the TBA equations describing the geometry of the moduli space of 4-dimensional $\mathcal{N}=2$ $SU(2)$ Super Yang-Mills theory on $\mathbb{R}^3\times S^1$ [89–91]. We derived the TBA equations by using the discontinuity formulae of the WKB periods, but they can also be derived by using the functional relation

of the wronskian for subdominant asymptotic solutions [92], which method is called the ODE/IM correspondence.

At $u = 0$, we have

$$m_\alpha = m_\beta =: m. \tag{6.2.12}$$

Substituting this identification into (6.2.11) and calculating the TBA equations, one also finds

$$\epsilon_\alpha(\theta) = \epsilon_\beta(\theta) =: \epsilon(\theta). \tag{6.2.13}$$

Therefore two TBA equations (6.2.11) collapse to one,

$$\epsilon(\theta) = me^\theta - 2\int_{\mathbb{R}} \frac{L(\theta')}{\cosh(\theta - \theta')} \frac{d\theta'}{2\pi}, \tag{6.2.14}$$

where

$$L(\theta) = \log\left(1 + e^{-\epsilon(\theta)}\right). \tag{6.2.15}$$

The TBA equation (6.2.14) coinsides with the massless Sinh-Gordon TBA equation, which is the conformal limit of the TBA equation for the Sinh-Gordon model [93]. The TBA equation (6.2.14) is also studied in the context of the ODE/IM correspondence for the generalized Mathieu equation [94].

So far we have derived the TBA equations for $-\Lambda_0^2 < u < \Lambda_0^2$. But we can extend the TBA equations for complex u as far as u belongs to the minimal chamber [89, 91]. On the complex u-plane, the minimal chamber coincide with the inside of the marginal stability curve [51]. The marginal stability curve is a real co-dimension one curve in u-plane which runs through the points $u = \pm\Lambda_0^2$. In the inside of the marginal stability curve, the TBA equations are written as follows [85]:

$$m_\alpha = |m_\alpha| e^{i\phi_\alpha}, \quad m_\beta = |m_\beta| e^{i\phi_\beta}, \tag{6.2.16}$$

$$\begin{aligned} \tilde{\epsilon}_\alpha(\theta) &= |m_\alpha| e^\theta - 2\int_{\mathbb{R}} \frac{\log\left(1 + e^{-\tilde{\epsilon}_\beta(\theta')}\right)}{\cosh(\theta - \theta' + i\phi_\beta - i\phi_\alpha)} \frac{d\theta'}{2\pi}, \\ \tilde{\epsilon}_\beta(\theta) &= |m_\beta| e^\theta - 2\int_{\mathbb{R}} \frac{\log\left(1 + e^{-\tilde{\epsilon}_\alpha(\theta')}\right)}{\cosh(\theta - \theta' + i\phi_\alpha - i\phi_\beta)} \frac{d\theta'}{2\pi}, \end{aligned} \tag{6.2.17}$$

where

$$\tilde{\epsilon}_\alpha(\theta) := \epsilon_\alpha(\theta - i\phi_\alpha), \quad \tilde{\epsilon}_\beta(\theta) := \epsilon_\beta(\theta - i\phi_\beta), \tag{6.2.18}$$

and $|\phi_\alpha - \phi_\beta| < \frac{\pi}{2}$. The integral equations for the outside of the marginal stability region can

be also obtained [89, 91], but then we obtain an infinite number of the integral equations, which are no longer of the form of the TBA equations, and it is difficult to solve even numerically. In the language of the Exact WKB analysis, the appearance of an infinite number of the integral equations corresponds to the appearance of an infinite number of the quantum periods.

The number of the quantum periods is equivalent to the number of the stable BPS states in the gauge theory [70, 89]. For the pure $N = 2$ $SU(2)$ gauge theory, there are two stable BPS states in the strong coupling region and an infinite number of the states in the weak coupling region. Therefore we conclude that the TBA equations (6.2.17) is valid for the strong coupling region.

We can determine the coefficients of the WKB periods by expanding the TBA equations at $\theta \to \infty$. For (6.2.11), we obtain

$$\begin{aligned} \epsilon_\alpha(\theta) &= m_\alpha e^\theta + \sum_{n\geq 1} m_\alpha^{(2n)} e^{(1-2n)\theta}, \\ \epsilon_\beta(\theta) &= m_\beta e^\theta + \sum_{n\geq 1} m_\beta^{(2n)} e^{(1-2n)\theta}, \end{aligned} \tag{6.2.19}$$

with

$$\begin{aligned} m_\alpha^{(2n)} &= 2\frac{(-1)^n}{\pi}\int_{\mathbb{R}} e^{(2n-1)\theta} L_\beta(\theta) d\theta, \\ m_\beta^{(2n)} &= 2\frac{(-1)^n}{\pi}\int_{\mathbb{R}} e^{(2n-1)\theta} L_\alpha(\theta) d\theta. \end{aligned} \tag{6.2.20}$$

Then the coefficients of the WKB periods can be recovered as follows,

$$m_\alpha^{(2n)} = (-1)^n i \Pi_{\gamma_\alpha}^{(2n)}, \quad m_\beta^{(2n)} = -\Pi_{\gamma_\beta}^{(2n)}. \tag{6.2.21}$$

In Table.6.1, we compare some coefficients of the WKB periods, which is calculated by using the differential operators (4.1.41), and the corresponding TBA results.

6.2.3 Effective central charge and PNP-relation for $\mathcal{N} = 2$ $SU(2)$ SYM

By using the TBA equations, we can determine the effective central charge $c_{\text{eff}} = c - 24\Delta_{\min}$ of the underlying 2d CFT, where c is the central charge of the Virasoro algebra and $\Delta_{\min}$

n	$(-1)^n i\Pi^{(2n)}_{\gamma_\alpha}$	$m^{(2n)}_\alpha$	$-\Pi^{(2n)}_{\gamma_\beta}$	$m^{(2n)}_\beta$
1	-0.15993792	$-\underline{\mathbf{0.15993}}849$	-0.42667081	$-\underline{\mathbf{0.42667}}143$
2	0.00420150	$\underline{\mathbf{0.00420150}}$	0.22398998	$\underline{\mathbf{0.2239899}}9$

Table 6.1: The numerical results of the coefficients of the WKB periods ($\Lambda_0 = 1$, $u = -0.6$). The calculation of the TBA equations is done by Fourier discretization with 2^{18} points and a cutoff of the integrals $(-L, L)$ where $L = 41.837877$.

is the minimum eigenvalue of the Virasoro operator L_0. For (6.2.11), c_{eff} is given as follows [95, 96],

$$c_{\text{eff}} = \frac{6}{\pi^2}\sum_{a=\alpha,\beta} m_a \int_{\mathbb{R}} e^\theta L_a(\theta) d\theta = 2 + \frac{3}{\pi^2}\sum_{a=\alpha,\beta}\left(\epsilon^\star_a \log(1+e^{\epsilon^\star_a}) + 2\text{Li}_2(-e^{\epsilon^\star_a})\right), \tag{6.2.22}$$

where

$$\epsilon^\star_a := \lim_{\theta\to-\infty}\epsilon_a(\theta). \tag{6.2.23}$$

$\theta \to -\infty$ limit (or equivalently, $\epsilon \to \infty$ limit) of the TBA equations (6.2.11) shows that $\epsilon^\star_a$ satisfies the following equation,

$$e^{-\epsilon^\star_\alpha} = 1 + e^{-\epsilon^\star_\beta}, \quad e^{-\epsilon^\star_\beta} = 1 + e^{-\epsilon^\star_\alpha}. \tag{6.2.24}$$

In [90, 97], it is pointed out that there are no mathematically rigorous solutions to these equations. But we can formally consider that $\epsilon^\star_a \to -\infty$ are the solutions. Then we can identify the effective central charge associated with TBA equations (6.2.11),

$$c_{\text{eff}} = 2. \tag{6.2.25}$$

This result agrees with the numerical calculation of (6.2.22).

There is another way to compute the effective central charge (6.2.25) based on the coefficients of the WKB periods. By using (6.2.3), (6.2.4) and (6.2.20), the second equation of (6.2.22) can be expressed as

$$c_{\text{eff}} = \frac{6}{\pi^2}\sum_{a=\alpha,\beta} m_a \int_{\mathbb{R}} e^\theta L_a(\theta) d\theta = i\frac{3}{\pi}\left(\Pi^{(0)}_{\gamma_\alpha}\Pi^{(2)}_{\gamma_\beta} - \Pi^{(0)}_{\gamma_\beta}\Pi^{(2)}_{\gamma_\alpha}\right). \tag{6.2.26}$$

$\Pi^{(2)}_{\gamma_\alpha}$ and $\Pi^{(2)}_{\gamma_\beta}$ can be computed by using the differential operator $\mathcal{O}_2$ in (4.1.41). Note that

the leading term of the WKB periods satisfy the second-order Picard-Fuchs equation [98],

$$\frac{\partial^2}{\partial u^2}\left(\Pi^{(0)}_{\gamma_\alpha}, \Pi^{(0)}_{\gamma_\beta}\right) = \frac{-1}{4(u+1)(u-1)}\left(\Pi^{(0)}_{\gamma_\alpha}, \Pi^{(0)}_{\gamma_\beta}\right), \tag{6.2.27}$$

the last equation (6.2.26) can be rewrite as follows,

$$i\frac{3}{\pi}\left(\Pi^{(0)}_{\gamma_\alpha}\Pi^{(2)}_{\gamma_\beta} - \Pi^{(0)}_{\gamma_\beta}\Pi^{(2)}_{\gamma_\alpha}\right) = \frac{i}{8\pi}\left(\Pi^{(0)}_{\gamma_\alpha}\frac{\partial}{\partial u}\Pi^{(0)}_{\gamma_\beta} - \Pi^{(0)}_{\gamma_\beta}\frac{\partial}{\partial u}\Pi^{(0)}_{\gamma_\alpha}\right). \tag{6.2.28}$$

From the wronskian relation of the leading terms of the WKB periods [99],

$$\Pi^{(0)}_{\gamma_\alpha}\frac{\partial}{\partial u}\Pi^{(0)}_{\gamma_\beta} - \Pi^{(0)}_{\gamma_\beta}\frac{\partial}{\partial u}\Pi^{(0)}_{\gamma_\alpha} = -16\pi i \tag{6.2.29}$$

we finally obtain

$$\frac{i}{8\pi}\left(\Pi^{(0)}_{\gamma_\alpha}\frac{\partial}{\partial u}\Pi^{(0)}_{\gamma_\beta} - \Pi^{(0)}_{\gamma_\beta}\frac{\partial}{\partial u}\Pi^{(0)}_{\gamma_\alpha}\right) = 2. \tag{6.2.30}$$

And therefore $c_{\text{eff}} = 2$. This relational expression between the WKB periods for classically allowed cycle and classically forbidden cycle is called the PNP-relation.

In [100, 101], it is shown that the l.h.s of (6.2.30) is proportional to the coefficient of the one-loop beta function for the 4-dimensional $\mathcal{N} = 2$ $SU(2)$ Super Yang-Mills theory. Therefore (6.2.26) indicates that the quantum collection to the beta function for the 4d gauge theory is governed by the effective central charge of the 2d CFT.

6.2.4 QNMs for D3-branes and TBA equations

Combining the TBA equations (6.2.17) with the exact QNMs condition for the D3-branes (4.1.36), we can calculate the QNMs that do not violate the condition $|\phi_\alpha - \phi_\beta| < \frac{\pi}{2}$. As a consistency check, we first calculate the QNMs by using the Leaver's method, and then calculate the solution η, which must be one, to the exact QNMs condition (4.1.36) substituted the QNMs. The numerical results are shown in Table.6.2. Table.6.2 implies the condition $|\phi_\alpha - \phi_\beta| < \frac{\pi}{2}$ is satisfied by the QNMs that the absolute value of the imaginary part is larger than the real part.

n	l	Leaver's method	η
1	0	$0.682086 - 1.559933i$	1.000190
2	1	$0.449645 - 2.627530i$	1.000114
	2	$1.873956 - 2.544763i$	1.000038

Table 6.2: The third column is the QNMs calculated by the Leaver's method. The fourth column is the solutions to the exact QNMs condition (4.1.36) with respect to η calculated by the TBA equations.

6.3 $\mathcal{N} = 2$ $SU(2)$ $N_f = 2$ SQCD with flavor symmetry

6.3.1 Discontinuity of WKB periods for $\mathcal{N} = 2$ $SU(2)$ $N_f = 2$ SQCD

The quantum Seiberg-Witten curve for 4-dimensional $\mathcal{N} = 2$ $SU(2)$ SQCD with two fundamental hypermultiplets is the following differential equation [46],

$$\left[\frac{d^2}{dz^2} - \eta^2 Q_0(z)\right]\psi(z) = 0, \tag{6.3.1}$$

with

$$Q_0(z) = V(z) - u = -\frac{\Lambda_2}{2}\left(m_1 e^{iz} + m_2 e^{-iz}\right) - \frac{\Lambda_2^2}{8}\cos(2z) - u, \tag{6.3.2}$$

where Λ_2 is the dynamically generated scale, $u \in \mathbb{C}$ is the Coulomb moduli parameter, $m_1, m_2 \in \mathbb{C}$ are the bare masses of the hypermultiplets and $\eta = 1/\epsilon_1$ is the deformation parameter in the Nekrasov-Shatashvili limit of the Ω-background.

We apply the Exact WKB analysis to (6.3.1) on the Riemann sphere composed by the cylinder $\mathbb{C}/\langle z \sim z + 2\pi\rangle$ with the compactification $\mathbb{C}^* = (\mathbb{C}/\langle z \sim z + 2\pi\rangle) \cup \{\pm i\infty\}$. In the following analysis, we consider the case that the hypermultiplets have a same mass $m_1 = m_2 = m$ and $m, u, \Lambda_2 \in \mathbb{R}$. Then $Q_0(z)$ is a real-valued function of the real z-axis,

$$Q_0(z) = V(z) - u = -\Lambda_2 m\cos(z) - \frac{\Lambda_2^2}{8}\cos(2z) - u. \tag{6.3.3}$$

Restricting the parameters to $-\frac{\Lambda_2}{2} < m < \frac{\Lambda_2}{2}$ and $\Lambda_2|m| - \frac{\Lambda_2^2}{8} < u < m^2 + \frac{\Lambda_2^2}{8}$, the simple zeros of $Q_0(z)$ become real. The potential graph on the real z-axis is drawn in Fig.6.3. In the context of the gauge theory, the restriction of u corresponds to the strong coupling region.

The Stokes graph at $\arg(\eta) = 0$ is drawn in Fig.6.4. There are four one-cycles $\gamma_\beta, \gamma_{\tilde{\beta}}$, which encircle the classically forbidden intervals on the real z-axis (Fig.6.3), and $\gamma_\alpha, \gamma_{\tilde{\alpha}}$,

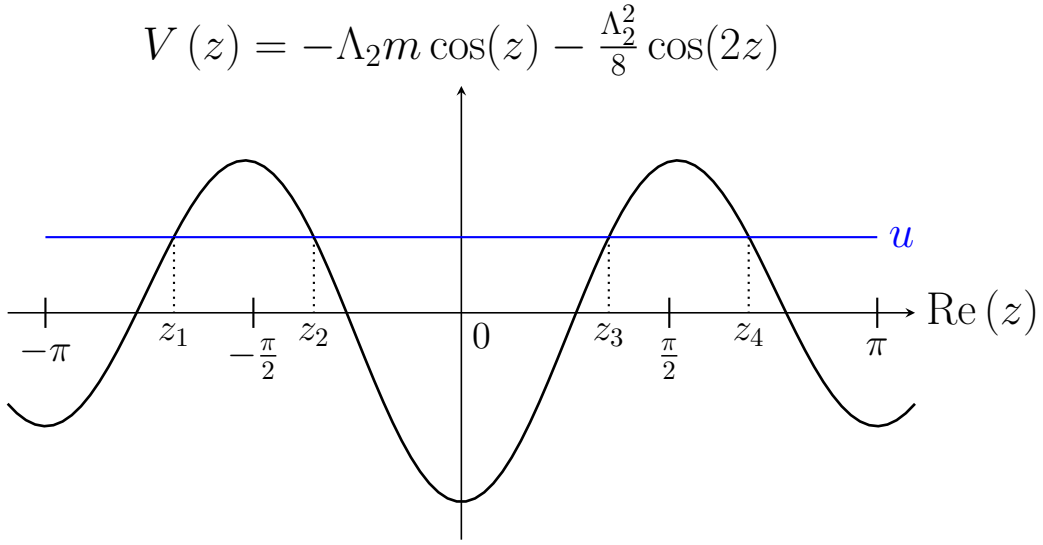

Figure 6.3: The potential on the real z-axis in $z \in [-\pi, \pi]$. $z_1 = -z_4, z_2 = -z_3, z_3, z_4$ are the simple zeros of $Q_0(z)$.

which encircle the classically allowed intervals on the real z-axis. We choose the branch cuts and the orientation of the one-cycles so that

$$m_\beta := -\Pi^{(0)}_{\gamma_\beta} = -\oint_{\gamma_\beta} S_0(z)dz, \quad m_{\tilde{\beta}} := -\Pi^{(0)}_{\gamma_{\tilde{\beta}}} = -\oint_{\gamma_{\tilde{\beta}}} S_0(z)dz, \tag{6.3.4}$$

and

$$m_\alpha := i\Pi^{(0)}_{\gamma_\alpha} = i\oint_{\gamma_\alpha} S_0(z)dz, \quad m_{\tilde{\alpha}} := i\Pi^{(0)}_{\gamma_{\tilde{\alpha}}} = i\oint_{\gamma_{\tilde{\alpha}}} S_0(z)dz \tag{6.3.5}$$

are real and positive. Because of the higher order coefficient $S_n(z)$ $(n \geq 1)$ is holomorphic at $z = \pm i\infty$ (Proposition 2.8. in [25]), the WKB periods satisfy the following relations,

$$\Pi_\beta = \Pi_{\tilde{\beta}} + 2\pi i \mathrm{Res}_{z=+i\infty} S_0(z) - 2\pi i \mathrm{Res}_{z=-i\infty} S_0(z), \tag{6.3.6}$$

$$\Pi_\alpha = \Pi_{\tilde{\alpha}} + 2\pi i \mathrm{Res}_{z=+i\infty} S_0(z) + 2\pi i \mathrm{Res}_{z=-i\infty} S_0(z). \tag{6.3.7}$$

For $m_1 = m_2 = m$ case, we obtain $2\pi i \mathrm{Res}_{z=\pm i\infty} S_0(z) = 2\pi m$ [70] and therefore

$$\Pi_\beta = \Pi_{\tilde{\beta}}, \tag{6.3.8}$$

$$\Pi_\alpha = \Pi_{\tilde{\alpha}} + 4\pi m. \tag{6.3.9}$$

As the pure SU(2) case, for the direction $\arg(\eta) = 0, \pi$, the WKB periods for $\gamma_\beta, \gamma_{\tilde{\beta}}$ have

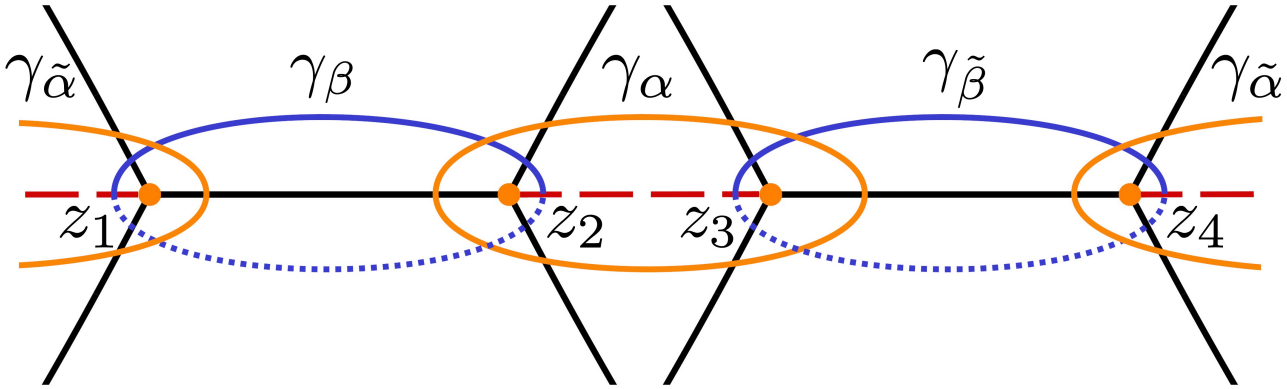

Figure 6.4: The Stokes graph at $\arg(\eta) = 0$ for the quantum Seiberg-Witten curve of 4-dimensional $\mathcal{N} = 2$ $SU(2)$ $N_f = 2$ SQCD with flavor symmetry in $z \in [-\pi, \pi]$.

no discontinuity and for $\gamma_\alpha, \gamma_{\tilde{\alpha}}$ have the following discontinuity,

$$e^{\eta\mathcal{B}_{0-}[\Pi_{\gamma_\alpha}]} = e^{\eta\mathcal{B}_{0+}[\Pi_{\gamma_\alpha}]}\left(1+e^{\eta\mathcal{B}_0\left[\Pi_{\gamma_\beta}\right]}\right)\left(1+e^{\eta\mathcal{B}_0\left[\Pi_{\gamma_{\tilde{\beta}}}\right]}\right), \tag{6.3.10}$$

$$e^{\eta\mathcal{B}_{0-}\left[\Pi_{\gamma_{\tilde{\alpha}}}\right]} = e^{\eta\mathcal{B}_{0+}\left[\Pi_{\gamma_{\tilde{\alpha}}}\right]}\left(1+e^{\eta\mathcal{B}_0\left[\Pi_{\gamma_\beta}\right]}\right)\left(1+e^{\eta\mathcal{B}_0\left[\Pi_{\gamma_{\tilde{\beta}}}\right]}\right), \tag{6.3.11}$$

$$e^{\eta\mathcal{B}_{\pi-}[\Pi_{\gamma_\alpha}]} = e^{\eta\mathcal{B}_{\pi+}[\Pi_{\gamma_\alpha}]}\left(1+e^{-\eta\mathcal{B}_\pi\left[\Pi_{\gamma_\beta}\right]}\right)\left(1+e^{-\eta\mathcal{B}_\pi\left[\Pi_{\gamma_{\tilde{\beta}}}\right]}\right), \tag{6.3.12}$$

$$e^{\eta\mathcal{B}_{\pi-}\left[\Pi_{\gamma_{\tilde{\alpha}}}\right]} = e^{\eta\mathcal{B}_{\pi+}\left[\Pi_{\gamma_{\tilde{\alpha}}}\right]}\left(1+e^{-\eta\mathcal{B}_\pi\left[\Pi_{\gamma_\beta}\right]}\right)\left(1+e^{-\eta\mathcal{B}_\pi\left[\Pi_{\gamma_{\tilde{\beta}}}\right]}\right). \tag{6.3.13}$$

Similarly, for the direction $\arg(\eta) = \pm\pi/2$, the WKB periods for $\gamma_\alpha, \gamma_{\tilde{\alpha}}$ have no discontinuity and for $\gamma_\beta, \gamma_{\tilde{\beta}}$ have the following discontinuity,

$$e^{\eta\mathcal{B}_{\pm\frac{\pi}{2}-}\left[\Pi_{\gamma_\beta}\right]} = e^{\eta\mathcal{B}_{\pm\frac{\pi}{2}+}\left[\Pi_{\gamma_\beta}\right]}\left(1+e^{\mp\eta\mathcal{B}_{\pm\frac{\pi}{2}}[\Pi_{\gamma_\alpha}]}\right)^{\pm}\left(1+e^{\mp\eta\mathcal{B}_{\pm\frac{\pi}{2}}\left[\Pi_{\gamma_{\tilde{\alpha}}}\right]}\right)^{\pm}, \tag{6.3.14}$$

$$e^{\eta\mathcal{B}_{\pm\frac{\pi}{2}-}\left[\Pi_{\gamma_{\tilde{\beta}}}\right]} = e^{\eta\mathcal{B}_{\pm\frac{\pi}{2}+}\left[\Pi_{\gamma_{\tilde{\beta}}}\right]}\left(1+e^{\mp\eta\mathcal{B}_{\pm\frac{\pi}{2}}[\Pi_{\gamma_\alpha}]}\right)^{\pm}\left(1+e^{\mp\eta\mathcal{B}_{\pm\frac{\pi}{2}}\left[\Pi_{\gamma_{\tilde{\alpha}}}\right]}\right)^{\pm}. \tag{6.3.15}$$

6.3.2 TBA equations for $\mathcal{N} = 2$ $SU(2)$ $N_f = 2$ SQCD

We introduce the epsilon functions as follows,

$$\begin{aligned}
&\epsilon_\alpha(\theta - i\frac{\pi}{2} + i\varphi) = \eta\mathcal{B}_\varphi\left[\Pi_{\gamma_\alpha}\right], \quad \epsilon_{\tilde{\alpha}}(\theta - i\frac{\pi}{2} + i\varphi) = \eta\mathcal{B}_\varphi\left[\Pi_{\gamma_{\tilde{\alpha}}}\right], \\
&\epsilon_\beta(\theta + i\varphi) = -\eta\mathcal{B}_\varphi\left[\Pi_{\gamma_\beta}\right], \quad \epsilon_{\tilde{\beta}}(\theta + i\varphi) = -\eta\mathcal{B}_\varphi\left[\Pi_{\gamma_{\tilde{\beta}}}\right].
\end{aligned} \tag{6.3.16}$$

Then the discontinuity formulae (6.3.10)∼(6.3.15) can be written as follows,

$$\begin{aligned}
\lim_{\delta\to 0}\left[\epsilon_\alpha\left(\theta \pm i\frac{\pi}{2}+i\delta\right)-\epsilon_\alpha\left(\theta \pm i\frac{\pi}{2}-i\delta\right)\right] &= \pm\left[L_\beta(\theta)+L_{\tilde\beta}(\theta)\right],\\
\lim_{\delta\to 0}\left[\epsilon_{\tilde\alpha}\left(\theta \pm i\frac{\pi}{2}+i\delta\right)-\epsilon_{\tilde\alpha}\left(\theta \pm i\frac{\pi}{2}-i\delta\right)\right] &= \pm\left[L_\beta(\theta)+L_{\tilde\beta}(\theta)\right],\\
\lim_{\delta\to 0}\left[\epsilon_\beta\left(\theta \pm i\frac{\pi}{2}+i\delta\right)-\epsilon_\beta\left(\theta \pm i\frac{\pi}{2}-i\delta\right)\right] &= \pm\left[L_\alpha(\theta)+L_{\tilde\alpha}(\theta)\right],\\
\lim_{\delta\to 0}\left[\epsilon_{\tilde\beta}\left(\theta \pm i\frac{\pi}{2}+i\delta\right)-\epsilon_{\tilde\beta}\left(\theta \pm i\frac{\pi}{2}-i\delta\right)\right] &= \pm\left[L_\alpha(\theta)+L_{\tilde\alpha}(\theta)\right],
\end{aligned} \tag{6.3.17}$$

where

$$\begin{aligned}
L_\alpha(\theta) &:= \log\left(1+e^{-\epsilon_\alpha(\theta)}\right), \quad L_{\tilde\alpha}(\theta) := \log\left(1+e^{-\epsilon_{\tilde\alpha}(\theta)}\right),\\
L_\beta(\theta) &:= \log\left(1+e^{-\epsilon_\beta(\theta)}\right), \quad L_{\tilde\beta}(\theta) := \log\left(1+e^{-\epsilon_{\tilde\beta}(\theta)}\right).
\end{aligned} \tag{6.3.18}$$

Taking the convolution of (6.3.17) with $K(\theta) = 1/\left(2\pi\cosh(\theta)\right)$ and using the asymptotic behavior of the epsilon function as we have derived (5.1.25), we obtain the TBA equations for 4-dimensional $\mathcal{N}=2$ $SU(2)$ $N_f=2$ SQCD with flavor symmetry [66],

$$\begin{aligned}
\epsilon_\alpha(\theta) &= m_\alpha e^\theta - \int_{\mathbb{R}}\frac{L_\beta(\theta')}{\cosh\left(\theta-\theta'\right)}\frac{d\theta'}{2\pi} - \int_{\mathbb{R}}\frac{L_{\tilde\beta}(\theta')}{\cosh\left(\theta-\theta'\right)}\frac{d\theta'}{2\pi},\\
\epsilon_{\tilde\alpha}(\theta) &= m_{\tilde\alpha} e^\theta - \int_{\mathbb{R}}\frac{L_\beta(\theta')}{\cosh\left(\theta-\theta'\right)}\frac{d\theta'}{2\pi} - \int_{\mathbb{R}}\frac{L_{\tilde\beta}(\theta')}{\cosh\left(\theta-\theta'\right)}\frac{d\theta'}{2\pi},\\
\epsilon_\beta(\theta) &= m_\beta e^\theta - \int_{\mathbb{R}}\frac{L_\alpha(\theta')}{\cosh\left(\theta-\theta'\right)}\frac{d\theta'}{2\pi} - \int_{\mathbb{R}}\frac{L_{\tilde\alpha}(\theta')}{\cosh\left(\theta-\theta'\right)}\frac{d\theta'}{2\pi},\\
\epsilon_{\tilde\beta}(\theta) &= m_{\tilde\beta} e^\theta - \int_{\mathbb{R}}\frac{L_\alpha(\theta')}{\cosh\left(\theta-\theta'\right)}\frac{d\theta'}{2\pi} - \int_{\mathbb{R}}\frac{L_{\tilde\alpha}(\theta')}{\cosh\left(\theta-\theta'\right)}\frac{d\theta'}{2\pi}.
\end{aligned} \tag{6.3.19}$$

The identification (6.3.8) leads $\epsilon_\beta(\theta) = \epsilon_{\tilde\beta}(\theta)$ and the TBA equations can be collapsed to three,

$$\begin{aligned}
\epsilon_\alpha(\theta) &= m_\alpha e^\theta - 2\int_{\mathbb{R}}\frac{L_\beta(\theta')}{\cosh\left(\theta-\theta'\right)}\frac{d\theta'}{2\pi},\\
\epsilon_{\tilde\alpha}(\theta) &= m_{\tilde\alpha} e^\theta - 2\int_{\mathbb{R}}\frac{L_\beta(\theta')}{\cosh\left(\theta-\theta'\right)}\frac{d\theta'}{2\pi},\\
\epsilon_\beta(\theta) &= m_\beta e^\theta - \int_{\mathbb{R}}\frac{L_\alpha(\theta')}{\cosh\left(\theta-\theta'\right)}\frac{d\theta'}{2\pi} - \int_{\mathbb{R}}\frac{L_{\tilde\alpha}(\theta')}{\cosh\left(\theta-\theta'\right)}\frac{d\theta'}{2\pi}.
\end{aligned} \tag{6.3.20}$$

So far we only consider the special parameter region, but we can also derive the TBA equations for a pure imaginary region ($m, \Lambda_2 \in i\mathbb{R}$) and an anti-same mass region ($m_1 = -m_2$) in the same way.

For general parameter region, we need to analytically continue the TBA equations [85]. After analytically continuing (6.3.19), we obtain the following equations,

$$m_\alpha = |m_\alpha| e^{i\phi_\alpha}, \quad m_{\tilde{\alpha}} = |m_{\tilde{\alpha}}| e^{i\phi_{\tilde{\alpha}}}, \quad m_\beta = |m_\beta| e^{i\phi_\beta}, \quad m_{\tilde{\beta}} = |m_{\tilde{\beta}}| e^{i\phi_{\tilde{\beta}}}, \tag{6.3.21}$$

$$\begin{aligned}
\tilde{\epsilon}_\alpha(\theta) &= |m_\alpha| e^\theta - \int_{\mathbb{R}} \frac{\log\left(1+e^{-\tilde{\epsilon}_\beta(\theta')}\right)}{\cosh(\theta-\theta'+i\phi_\beta-i\phi_\alpha)} \frac{d\theta'}{2\pi} - \int_{\mathbb{R}} \frac{\log\left(1+e^{-\tilde{\epsilon}_{\tilde{\beta}}(\theta')}\right)}{\cosh(\theta-\theta'+i\phi_{\tilde{\beta}}-i\phi_\alpha)} \frac{d\theta'}{2\pi}, \\
\tilde{\epsilon}_{\tilde{\alpha}}(\theta) &= |m_{\tilde{\alpha}}| e^\theta - \int_{\mathbb{R}} \frac{\log\left(1+e^{-\tilde{\epsilon}_\beta(\theta')}\right)}{\cosh(\theta-\theta'+i\phi_\beta-i\phi_{\tilde{\alpha}})} \frac{d\theta'}{2\pi} - \int_{\mathbb{R}} \frac{\log\left(1+e^{-\tilde{\epsilon}_{\tilde{\beta}}(\theta')}\right)}{\cosh(\theta-\theta'+i\phi_{\tilde{\beta}}-i\phi_{\tilde{\alpha}})} \frac{d\theta'}{2\pi}, \\
\tilde{\epsilon}_\beta(\theta) &= |m_\beta| e^\theta - \int_{\mathbb{R}} \frac{\log\left(1+e^{-\tilde{\epsilon}_\alpha(\theta')}\right)}{\cosh(\theta-\theta'+i\phi_\alpha-i\phi_\beta)} \frac{d\theta'}{2\pi} - \int_{\mathbb{R}} \frac{\log\left(1+e^{-\tilde{\epsilon}_{\tilde{\alpha}}(\theta')}\right)}{\cosh(\theta-\theta'+i\phi_{\tilde{\alpha}}-i\phi_\beta)} \frac{d\theta'}{2\pi}, \\
\tilde{\epsilon}_{\tilde{\beta}}(\theta) &= |m_{\tilde{\beta}}| e^\theta - \int_{\mathbb{R}} \frac{\log\left(1+e^{-\tilde{\epsilon}_\alpha(\theta')}\right)}{\cosh(\theta-\theta'+i\phi_\alpha-i\phi_{\tilde{\beta}})} \frac{d\theta'}{2\pi} - \int_{\mathbb{R}} \frac{\log\left(1+e^{-\tilde{\epsilon}_{\tilde{\alpha}}(\theta')}\right)}{\cosh(\theta-\theta'+i\phi_{\tilde{\alpha}}-i\phi_{\tilde{\beta}})} \frac{d\theta'}{2\pi},
\end{aligned} \tag{6.3.22}$$

where

$$\tilde{\epsilon}_\alpha(\theta) := \epsilon_\alpha(\theta - i\phi_\alpha), \quad \tilde{\epsilon}_{\tilde{\alpha}}(\theta) := \epsilon_{\tilde{\alpha}}(\theta - i\phi_{\tilde{\alpha}}), \quad \tilde{\epsilon}_\beta(\theta) := \epsilon_\beta(\theta - i\phi_\beta), \quad \tilde{\epsilon}_{\tilde{\beta}}(\theta) := \epsilon_{\tilde{\beta}}(\theta - i\phi_{\tilde{\beta}}), \tag{6.3.23}$$

and the absolute values of the difference of the two of $\phi_\alpha, \phi_\beta, \phi_{\tilde{\alpha}}, \phi_{\tilde{\beta}}$ are less than $\frac{\pi}{2}$ (e.g. $|\phi_\alpha - \phi_\beta| < \frac{\pi}{2}$). For the larger than $\frac{\pi}{2}$ case, the residue of the pole deforms the TBA equations and typically we find an infinite number of the integral equations.

For the $N = 2$ $SU(2)$ $N_f = 2$ SQCD, there are four stable BPS states in the strong coupling region and an infinite number of the states in the weak coupling region. According to [70, 89], we conclude that the TBA equations (6.3.22) is valid for the strong coupling region.

In principle, we can also derive the TBA equations for $m_1 \neq m_2$ by computing the discontinuity of the WKB periods. But in this case $Q_0(z)$ is not a real-valued function on the real z-axis and there is no way to analytically determine the directions of the discontinuity as the same-mass case. This difficulty also exists for 4-dimensional $N = 2$ $SU(2)$ $N_f = 1, 3, 4$ SQCD. However, the number of the stable BPS states for the $N = 2$ $SU(2)$ $N_f = 2$ SQCD with $m_1 \neq m_2$ is the same for the same-mass case. Therefore we conjecture that the TBA equations (6.3.22) is also valid for the $m_1 \neq m_2$ case.

Now we discuss the TBA equations at some special points in the moduli space. In the massless case $m = 0$, (6.3.9) leads to $\Pi_\alpha = \Pi_{\tilde{\alpha}}$ or equivalently $\epsilon_\alpha(\theta) = \epsilon_{\tilde{\alpha}}(\theta)$ and the TBA

equations can be collapsed to two,

$$\begin{aligned}\epsilon_\alpha(\theta) &= m_\alpha e^\theta - 2\int_{\mathbb{R}} \frac{L_\beta(\theta')}{\cosh(\theta-\theta')}\frac{d\theta'}{2\pi},\\ \epsilon_\beta(\theta) &= m_\beta e^\theta - 2\int_{\mathbb{R}} \frac{L_\alpha(\theta')}{\cosh(\theta-\theta')}\frac{d\theta'}{2\pi}.\end{aligned} \tag{6.3.24}$$

(6.3.24) agrees with the TBA equations for 4-dimensional $N = 2$ $SU(2)$ SYM given in (6.2.11). This agreement is compatible with that the quantum SW curve for $N = 2$ $SU(2)$ $N_f = 2$ SQCD (6.3.1) becomes the one for $N = 2$ $SU(2)$ SYM in the massless case. We also obtain the TBA equations (6.3.24) in the decoupling limit ($m \to \infty$ and $\Lambda_2 \to 0$ while $m\Lambda_2$ being fixes), which turns the $N_f = 2$ SQCD into the SYM, because in this limit the quantum SW curve (6.3.1) becomes the one for $N = 2$ $SU(2)$ SYM.

The point $m = \frac{\Lambda_2}{2}$, $u = \frac{3}{8}\Lambda^2$ is the supercomformal or Argyres-Douglas point where mutually nonlocal BPS states become massless [102]. In the limit $m \to \frac{\Lambda_2}{2}$, $u \to \frac{3}{8}\Lambda^2$ with keeping the theory in the strong coupling region, $\tilde{\alpha}$-cycle shrinks and $\Pi_{\tilde{\alpha}}$ goes to zero. If we neglect $\tilde{\alpha}$-cycle, we obtain the following TBA equations,

$$\begin{aligned}\epsilon_\alpha(\theta) &= m_\alpha e^\theta - 2\int_{\mathbb{R}} \frac{L_\beta(\theta')}{\cosh(\theta-\theta')}\frac{d\theta'}{2\pi},\\ \epsilon_\beta(\theta) &= m_\beta e^\theta - \int_{\mathbb{R}} \frac{L_\alpha(\theta')}{\cosh(\theta-\theta')}\frac{d\theta'}{2\pi}.\end{aligned} \tag{6.3.25}$$

These TBA equations agree with the ones for the double-well potential (5.2.1), which is the quantum SW curve for (A_1, A_3) AD theory. Under the universality of the AD theory [61], the quantum SW curve for (A_1, A_3) AD theory is equivalent to the $SU(2)$ $N_f = 2$ AD theory.

The large θ expansion of the TBA equations (6.3.19) provides the all-order aasymptotic expansion of the epsilon functions,

$$\begin{aligned}\epsilon_\alpha(\theta) &= m_\alpha e^\theta + \sum_{n\geq 1} m_\alpha^{(2n)} e^{(1-2n)\theta},\\ \epsilon_{\tilde{\alpha}}(\theta) &= m_\alpha e^\theta + \sum_{n\geq 1} m_{\tilde{\alpha}}^{(2n)} e^{(1-2n)\theta},\\ \epsilon_\beta(\theta) &= m_\beta e^\theta + \sum_{n\geq 1} m_\beta^{(2n)} e^{(1-2n)\theta},\\ \epsilon_{\tilde{\beta}}(\theta) &= m_\beta e^\theta + \sum_{n\geq 1} m_{\tilde{\beta}}^{(2n)} e^{(1-2n)\theta},\end{aligned} \tag{6.3.26}$$

n	$(-1)^n i\Pi^{(2n)}_{\gamma_\alpha}, (-1)^n i\Pi^{(2n)}_{\gamma_{\tilde{\alpha}}}$	$m^{(2n)}_{\alpha}, m^{(2n)}_{\tilde{\alpha}}$	$-\Pi^{(2n)}_{\gamma_\beta}, -\Pi^{(2n)}_{\gamma_{\tilde{\beta}}}$	$m^{(2n)}_{\beta}, m^{(2n)}_{\tilde{\beta}}$
1	-0.50248407	$-\underline{\mathbf{0.50248}}11$	-0.23951302	$-\underline{\mathbf{0.23951}}316$
2	0.31200029	$\underline{\mathbf{0.31200}}019$	0.01588744	$\underline{\mathbf{0.01588}}743$

Table 6.3: The numerical results of the coefficients of the quantum periods ($\Lambda_2 = 4$, $u = 1$, $m = 1/8$). The numerical calculation in the TBA equations is done by Fourier discretization with 2^{18} points and a cutoff of the integrals $(-L, L)$ where $L = 40 + \log(2\pi)$.

with

$$\begin{aligned} m^{(2n)}_{\alpha} = m^{(2n)}_{\tilde{\alpha}} &= 2\frac{(-1)^n}{\pi}\int_{\mathbb{R}} e^{(2n-1)\theta}\left[L_\beta(\theta) + L_{\tilde{\beta}}(\theta)\right]d\theta, \\ m^{(2n)}_{\beta} = m^{(2n)}_{\tilde{\beta}} &= 2\frac{(-1)^n}{\pi}\int_{\mathbb{R}} e^{(2n-1)\theta}\left[L_\alpha(\theta) + L_{\tilde{\alpha}}(\theta)\right]d\theta. \end{aligned} \tag{6.3.27}$$

The coefficients of the WKB periods can be determined from (6.3.27) as follows,

$$m^{(2n)}_{\alpha} = m^{(2n)}_{\tilde{\alpha}} = (-1)^n i\Pi^{(2n)}_{\gamma_\alpha} = (-1)^n i\Pi^{(2n)}_{\gamma_{\tilde{\alpha}}}, \quad m^{(2n)}_{\beta} = m^{(2n)}_{\tilde{\beta}} = -\Pi^{(2n)}_{\gamma_\beta} = -\Pi^{(2n)}_{\gamma_{\tilde{\beta}}}. \tag{6.3.28}$$

The identifications of the higher-order coefficients of the WKB periods (6.3.28) are agree with (6.3.8) and (6.3.9). We compare the calculation of the WKB periods using the TBA equations and the differential operator (2.2.20). For 4-dimensional $\mathcal{N} = 2$ $SU(2)$ $N_f = 2$ SQCD with flavor symmetry, the second and fourth order of the differential operator is given as follows [46],

$$\mathcal{O}_2 = \frac{1}{6}\frac{\partial}{\partial u} + \frac{1}{3}u\frac{\partial^2}{\partial u^2} + \frac{1}{4}m\frac{\partial^2}{\partial m \partial u}, \tag{6.3.29}$$

$$\mathcal{O}_4 = \frac{5}{24}\frac{\partial^2}{\partial u^2} + \frac{1}{3}u\frac{\partial^3}{\partial u^3} + \frac{7}{90}u\frac{\partial^4}{\partial u^4} + \frac{7}{60}um\frac{\partial^4}{\partial m \partial u^3} + \frac{23}{96}m\frac{\partial^3}{\partial m^2 \partial u^2} + \frac{7}{160}m^2\frac{\partial^4}{\partial m^2 \partial u^2}. \tag{6.3.30}$$

Note that there are at least first order u-derivative in each terms. Therefore we can evaluate the higher order coefficients of the WKB periods by using the u-derivative of $\Pi^{(0)}_{\gamma}$,

$$\partial_u \Pi^{(0)}_{\alpha} = \partial_u \Pi^{(0)}_{\tilde{\alpha}} = \frac{4\pi}{\Lambda_2}\left(e^{iz_1} - e^{iz_2}\right)^{-\frac{1}{2}}\left(e^{iz_4} - e^{iz_3}\right)^{-\frac{1}{2}}\ {}_2F_1\left[\frac{1}{2}, \frac{1}{2}, 1, \frac{\left(e^{iz_3} - e^{iz_2}\right)\left(e^{iz_1} - e^{iz_4}\right)}{\left(e^{iz_1} - e^{iz_2}\right)\left(e^{iz_3} - e^{iz_4}\right)}\right], \tag{6.3.31}$$

$$\partial_u \Pi^{(0)}_{\beta} = \partial_u \Pi^{(0)}_{\tilde{\beta}} = \frac{4\pi}{\Lambda_2}\left(e^{iz_2} - e^{iz_3}\right)^{-\frac{1}{2}}\left(e^{iz_1} - e^{iz_4}\right)^{-\frac{1}{2}}\ {}_2F_1\left[\frac{1}{2}, \frac{1}{2}, 1, \frac{\left(e^{iz_4} - e^{iz_3}\right)\left(e^{iz_2} - e^{iz_1}\right)}{\left(e^{iz_2} - e^{iz_3}\right)\left(e^{iz_4} - e^{iz_1}\right)}\right], \tag{6.3.32}$$

In Table.6.3, we have compared the differential operator results and the TBA results.

6.3.3 Effective central charge and PNP-relation for $\mathcal{N}=2$ $SU(2)$ $N_f=2$ SQCD

For (6.3.19), the effective central charge of the underlying 2d CFT is given as follows [95,96],

$$c_{\text{eff}} = \frac{6}{\pi^2}\sum_{a=\alpha,\tilde{\alpha},\beta,\tilde{\beta}} m_a \int_{\mathbb{R}} e^{\theta} L_a(\theta) d\theta = 4 + \frac{3}{\pi^2}\sum_{a=\alpha,\beta}\left(\epsilon_a^\star \log(1+e^{\epsilon_a^\star}) + 2\text{Li}_2(-e^{\epsilon_a^\star})\right). \quad (6.3.33)$$

where $\epsilon_a^\star$ is defined in (6.2.23). In $\theta \to -\infty$ limit, The TBA equations (6.3.19) lead

$$\begin{aligned} e^{-\epsilon_\alpha^\star} = e^{-\epsilon_{\tilde{\alpha}}^\star} &= \left(1+e^{-\epsilon_\beta^\star}\right)^{\frac{1}{2}}\left(1+e^{-\epsilon_{\tilde{\beta}}^\star}\right)^{\frac{1}{2}}, \\ e^{-\epsilon_\beta^\star} = e^{-\epsilon_{\tilde{\beta}}^\star} &= \left(1+e^{-\epsilon_\alpha^\star}\right)^{\frac{1}{2}}\left(1+e^{-\epsilon_{\tilde{\alpha}}^\star}\right)^{\frac{1}{2}}. \end{aligned} \quad (6.3.34)$$

and therefore

$$e^{-\epsilon_\alpha^\star} = 1+e^{-\epsilon_\beta^\star}, \quad e^{-\epsilon_\beta^\star} = 1+e^{-\epsilon_\alpha^\star}. \quad (6.3.35)$$

These are the same equations as (6.2.24) and we have formally regarded $\epsilon_a^\star \to -\infty$ as the solutions. By substituting the solutions into (6.3.33), we obtain

$$c_{\text{eff}} = 4. \quad (6.3.36)$$

This result also agrees with the numerical calculation.

We can also compute the effective central charge from the coefficients of the WKB periods. The large θ expansion of the TBA equations (6.3.27), (6.3.28) leads to a relational expression between c_{eff} and the WKB periods,

$$c_{\text{eff}} = i\frac{6}{\pi}\left[\Pi^{(0)}_{\gamma_\alpha}\Pi^{(2)}_{\gamma_\beta} - \Pi^{(2)}_{\gamma_\alpha}\Pi^{(0)}_{\gamma_\beta}\right] + \frac{6}{\pi^2}(m_{\tilde{\alpha}} - m_\alpha)\int_{\mathbb{R}} e^{\theta} L_{\tilde{\alpha}} d\theta. \quad (6.3.37)$$

$\Pi^{(0)}_{\gamma_\alpha}\Pi^{(2)}_{\gamma_\beta} - \Pi^{(2)}_{\gamma_\alpha}\Pi^{(0)}_{\gamma_\beta}$ can be expressed only $\Pi^{(0)}_{\gamma_\alpha}, \Pi^{(0)}_{\gamma_\beta}$ by using the differential operator $\mathcal{O}_2$ (6.3.29). After some transpositions, we get the following relation,

$$\begin{aligned} \left[\Pi^{(0)}_{\gamma_\alpha}\frac{\partial\Pi^{(0)}_{\gamma_\beta}}{\partial u} - \frac{\partial\Pi^{(0)}_{\gamma_\alpha}}{\partial u}\Pi^{(0)}_{\gamma_\beta}\right] = &-i\pi c_{\text{eff}} + 3u\left[\Pi^{(0)}_{\gamma_\alpha}\frac{\partial^2\Pi^{(0)}_{\gamma_\beta}}{\partial u^2} - \frac{\partial^2\Pi^{(0)}_{\gamma_\alpha}}{\partial u^2}\Pi^{(0)}_{\gamma_\beta}\right] \\ &+ \frac{3}{2}m\left[\Pi^{(0)}_{\gamma_\alpha}\frac{\partial^2\Pi^{(0)}_{\gamma_\beta}}{\partial m\partial u} - \frac{\partial^2\Pi^{(0)}_{\gamma_\alpha}}{\partial m\partial u}\Pi^{(0)}_{\gamma_\beta}\right] - i\frac{6}{\pi^2}(m_{\tilde{\alpha}} - m_\alpha)\int_{\mathbb{R}} e^{\theta} L_{\tilde{\alpha}} d\theta. \end{aligned} \quad (6.3.38)$$

In the massless case $m = 0$, $\Pi^{(0)}_{\gamma_\alpha}, \Pi^{(0)}_{\gamma_\beta}$ satisfies the second order Picard-Fuchs equation [46] and the second, third and forth terms in the r.h.s of (6.3.38) become zero,

$$\left[\Pi^{(0)}_{\gamma_\alpha}\frac{\partial\Pi^{(0)}_{\gamma_\beta}}{\partial u} - \frac{\partial\Pi^{(0)}_{\gamma_\alpha}}{\partial u}\Pi^{(0)}_{\gamma_\beta}\right] = -i\pi c_{\text{eff}}. \tag{6.3.39}$$

Because, at the massless point, the quantum periods agree with the ones for the pure SU(2) theory, the combination $\left[\Pi^{(0)}_{\gamma_\alpha}\frac{\partial\Pi^{(0)}_{\gamma_\beta}}{\partial u} - \frac{\partial\Pi^{(0)}_{\gamma_\alpha}}{\partial u}\Pi^{(0)}_{\gamma_\beta}\right]$ satisfies the Wronskian relation for the pure SU(2) theory [99],

$$\left[\Pi^{(0)}_{\gamma_\alpha}\frac{\partial\Pi^{(0)}_{\gamma_\beta}}{\partial u} - \frac{\partial\Pi^{(0)}_{\gamma_\alpha}}{\partial u}\Pi^{(0)}_{\gamma_\beta}\right] = -4\pi i, \tag{6.3.40}$$

where the difference from (6.2.29) comes from the difference of the normalization of the parameter $\Lambda^2 = -\frac{\Lambda_2^2}{8}$. Comparing (6.3.40) with (6.3.39), we obtain $c_{\text{eff}} = 4$.

As the pure SU(2) case, it is shown that the l.h.s of (6.3.40) is proportional to the coefficient of the one-loop beta function for the 4-dimensional $\mathcal{N} = 2$ $SU(2)$ $N_f = 2$ SQCD [100, 101]. Therefore (6.3.39) indicates that the quantum collection to the beta function for the 4d gauge theory is governed by the effective central charge of the 2d CFT.

Summary

In this chapter, we have derived the TBA equations for the quantum Seiberg-Witten curves of 4-dimensional $\mathcal{N} = 2$ SU(2) supersymmetric gauge theories with $N_f = 0, 2$ fundamental hypermultiplets. The TBA equations determine the mass of the BPS particles in the low-energy effective theories exactly. We have also computed the effective central charges of the underlying 2d CFTs from the TBA equations. We have shown that the effective central charges are proportional to the one-loop beta functions for the 4d gauge theories. The quantum Seiberg-Witten curve for $N_f = 0$ SYM agrees with the E.O.M. for the massless scalar field in the extremal D3-branes background. Combining the exact QNMs condition, we have checked that the TBA equations provide the spectrum exactly.

Chapter 7

Conclusions and Discussions

In this thesis, we have studied the QNMs spectral problems and the quantum Seiberg-Witten curves based on the Exact WKB analysis. We state the conclusions and list some open problems below.

QNMs spectral problems

In Chapter 4, we have applied the Exact WKB analysis to the QNMs spectral problem of the massless scalar perturbation to the extremal D3/M5-branes metric. We have solved the connection problems of the Borel resummed WKB solutions. Combining with the boundary conditions, we have obtained the exact conditions of the QNMs that are expressed by the Borel resummed WKB periods. Based on our exact conditions, we have numerically calculated the QNMs by using the Borel-Padé approximation and have derived analytic expressions of the QNMs in some regions. We have also shown that the radial component of the E.O.M for the massless scalar fields can be transformed to the quantum Seiberg-Witten curves for 4-dimensional $\mathcal{N} = 2$ SU(2) supersymmetric theories, which enable us to utilize the gauge theory results to compute the QNMs. For the D3-branes, we have compared the results of the exact QNMs condition with the Leaver's numerical method and they are matched. This results indicates that the Exact WKB analysis works in the study of the QNMs properly. For the M5-branes, we have obtained two exact QNMs conditions depending on the argument of the complex frequency of the scalar field. The exact conditions are connected by the Delabaere-Pham formula and have shown that the discontinuity of the perturbative part of the QNMs leads the non-perturbative part of themselves.

As future works, we are interested in to derive the exact QNMs conditions for other metrics and perturbations. Following the extremal M5-branes, we have already done some

computations for a massless scalar perturbation to the extremal M2-branes. In this case, we observed the saddle reduction of the Stokes graph like the M5-branes case. But for the M2-branes, the leading contributions of the WKB periods are integrals of a hypergeometric curve and therefore it is difficult to compute them. We are also interested in applying the Exact WKB analysis to the black hole metrics that were studied in the context of the Seiberg-Witten/gravity correspondence [67–69]. In these papers, the authors conjectured that the QNMs are calculated by only the all-order Bohr-Sommerfeld condition with suitable WKB period. The conjectures were numerically verified in some lower modes of the QNMs, but it may happen the saddle reduction as we go to higher modes and we may obtain other conditions. It is also interesting to discuss the physical origin of the non-perturbative contribution, which arises from the quantum tunnel effect in quantum mechanics, to the QNMs.

Not only the generalization to other geometries, there are still some questions in the study of the extremal D3/M5-branes. First, it is important to re-derive the exact conditions in different ways. In the ODE/IM method [82, 104], the QNMs conditions is identified with the Bethe roots condition for the Baxter's Q-function, which can be expressed by the WKB periods. The QNMs conditions can also be derived by using two-dimensional CFT technique [105–107]. The differential equation for the QNMs spectral problem is identified with the semiclassical limit of the differential equation for the conformal block with a degenerate field insertion in the CFT. The connection problem in the CFT then provides the QNMs conditions, which can also be expressed by the WKB periods. The re-derivations of our exact conditions reinforce the correctness of themselves. It is also interesting to discuss the meaning of the exact QNMs conditions in the context of the branes world volume theory [35].

Other direction of the future work is to compute the absorption probability of the scalar fields in the extremal D3/M5-branes metric [74, 103]. At large l limit, the absorption probability can be determined by the Gamow factor, which is the exponent of the integrals appearing in the Bohr-Sommerfeld quantization conditions for the QNMs (4.1.7) and (4.2.7). We expect that the Gamow factor is generalized to the exponent of the Borel resummed WKB period for the potential barrier interval in the Exact WKB analysis.

TBA equations and quantum Seiberg-Witten curves

In Chapter 6, we have studied the Exact WKB analysis for the quantum Seiberg-Witten curves of 4-dimensional $\mathcal{N} = 2$ SU(2) $N_f = 0, 2$ supersymmetric theories. We have determined the discontinuity of the Borel resummed WKB periods in the whole of the complex η-plane. The TBA equations governing the Borel resummed WKB periods have been derived so that the discontinuity and the asymptotic behavior of the periods are satisfied. We have computed the effective central charges of the TBA equations and found that they are proportional to the one-loop beta functions of the 4d $\mathcal{N} = 2$ theories. By using the TBA equations for $N_f = 0$ case, we have also calculated the exact QNMs condition for the extremal D3-branes, which is consistent with the Leaver's numerical method.

There are many directions for the future work of the derivation of the TBA equations. Firstly we are interested in the generalization to 4-dimensional $\mathcal{N} = 2$ SU(2) $N_f \leq 4$ theories [46, 108] and $\mathcal{N}^* = 2$ theory [73, 109, 110], whose quantum Seiberg-Witten curves form the Schrödinger type second-order differential equations. Particularly, we are interested in the TBA equations for the $N_f = 1$ theory, which compute the QNMs for the extremal M5-branes by combining with our exact QNMs conditions. The discontinuity of the Borel resummed WKB periods for the $N_f = 1$ theory is also studied in [111].

More ambitious generalization is the $\mathcal{N} = 2$ supersymmetric gauge theories with higher rank gauge group, whose quantum Seiberg-Witten curves form higher-order differential equations (for pure SU(N) case [58] and with matters [59]). A good starting point is the A_n-type ODE studied in [112], which relates to the quantum Seiberg-Witten curve for the (A_n, A_m)-type Argyres-Douglas theories [113]. The Exact WKB analysis for SU(3) theory is also studied in [114, 115]. It is also important to derive the TBA equations for Refined topological string theory [116] and 3-dimensional $\mathcal{N} = 6$ supersymmetric gauge theory [117], whose spectral curves are infinite-order differential equations (or difference equations). The Exact WKB analysis for the difference equations is considered in [118].

The open problem we are most interested in is the possibility to apply the same discussion to more general physical observables. In this thesis, we focus on the derivation of the TBA equations for the Borel resummed WKB periods. But the discontinuity and the asymptotic behavior we used to derive the TBA equations are universal character for physical observables. It is then possible to determine integral equations governing the exact physical observables even for more complicated theories, including quantum field theory and string theory.

Bibliography

[1] C. A. Hurst, "The Enumeration of Graphs in the Feynman-Dyson Technique," Proc. Roy. Soc. Lond. A **214** (1952), 44.

[2] C. M. Bender and T. T. Wu, "Statistical Analysis of Feynman Diagrams," Phys. Rev. Lett. **37** (1976), 117.

[3] F. Dyson, "Divergence of perturbation theory in quantum electrodynamics," Phys. Rev. **85** (1952), 631-632.

[4] C. M. Bender and T. T. Wu, "Anharmonic Oscillator," Phys. Rev. **184** (1969), 1231.

[5] C. M. Bender and T. T. Wu, "Anharmonic Oscillator 2: A Study of Perturbation Theory in Large Order," Phys. Rev. **D7** (1973), 1620.

[6] J. Zinn-Justin, "Perturbation Series at Large Orders in Quantum Mechanics and Field Theories: Application to the Problem of Resummation," Phys. Rept. **70** (1981), 109.

[7] M. Mariño, R. Schiappa and M. Weiss, "Nonperturbative Effects and the Large-Order Behavior of Matrix Models and Topological Strings," Commun. Num. Theor. Phys. **2** (2008), 349. [arXiv:0711.1954 [hep-th]].

[8] S. Pasquetti and R. Schiappa, "Borel and Stokes Nonperturbative Phenomena in Topological String Theory and $c = 1$ Matrix Models," Annales Henri Poincaré **11** (2010), 351. [arXiv:0907.4082 [hep-th]].

[9] J.-P. Eckmann1 and H. Epstein, "Borel Summability of the Mass and S-Matrix in ϕ^4 Models," Commun. math. Phys. **68** (1979), 245-258

[10] Alan D. Sokal, "An improvement of Watson's theorem on Borel summability," J. Math. Phys. **21** (1980), 261

[11] J. Zinn-Justin, "Perturbation Series at Large Orders in Quantum Mechanics and Field Theories: Application to the Problem of Resummation," Phys. Rept. **70** (1981), 109.

[12] T. Fujimori, S. Kamata, T. Misumi, M. Nitta and N. Sakai, "Nonperturbative contributions from complexified solutions in $\mathbb{C}P^{N-1}$models," Phys. Rev. D **94** (2016) no.10, 105002 [arXiv:1607.04205 [hep-th]].

[13] T. Fujimori, S. Kamata, T. Misumi, M. Nitta and N. Sakai, "Exact resurgent trans-series and multibion contributions to all orders," Phys. Rev. D **95** (2017) no.10, 105001 [arXiv:1702.00589 [hep-th]].

[14] T. Fujimori, S. Kamata, T. Misumi, M. Nitta and N. Sakai, "Resurgence Structure to All Orders of Multi-bions in Deformed SUSY Quantum Mechanics," PTEP **2017** (2017) no.8, 083B02 [arXiv:1705.10483 [hep-th]].

[15] T. Fujimori, M. Honda, S. Kamata, T. Misumi and N. Sakai, "Resurgence and Lefschetz thimble in three-dimensional $\mathcal{N} = 2$ supersymmetric Chern–Simons matter theories," PTEP **2018** (2018) no.12, 123B03 [arXiv:1805.12137 [hep-th]].

[16] M. Mariño and T. Reis, "Renormalons in integrable field theories," JHEP **04** (2020), 160 [arXiv:1909.12134 [hep-th]].

[17] M. Mariño and T. Reis, "A new renormalon in two dimensions," JHEP **07** (2020), 216 [arXiv:1912.06228 [hep-th]].

[18] L. Di Pietro, M. Mariño, G. Sberveglieri and M. Serone, "Resurgence and 1/N Expansion in Integrable Field Theories," JHEP **10** (2021), 166 [arXiv:2108.02647 [hep-th]].

[19] M. Marino, R. Miravitllas and T. Reis, "New renormalons from analytic trans-series," JHEP **08** (2022), 279 [arXiv:2111.11951 [hep-th]].

[20] M. Mariño, "Lectures on Non-Perturbative Effects in Large N Gauge Theories, Matrix Models and Strings," Fortsch. Phys. **62** (2014), 455-540. [arXiv:1206.6272 [hep-th]].

[21] A. Voros, "The return of the quartic oscillator. The complex WKB method," Ann. Inst. Henri Poincaré **39** (1983), 211.

[22] A. Voros, "Résurgence Quantique," Ann. Inst. Fourier **43** (1993), 1509.

[23] E. Delabaere and F. Pham, "Resurgent methods in semi-classical asymptotics," Annales de l' IHP **71** (1999), 1-94.

[24] H. Dillinger, E. Delabaere and F. Pham, "Résurgence de Voros et périodes des courbes hyperelliptiques," Annales de l'Institut Fourier **43** (1993), 163-199.

[25] K. Iwaki and T. Nakanishi, "Exact WKB analysis and cluster algebras," J. Phys. A: Math. Theor. **47** (2014), 474009 [arXiv:1401.7094 [math.CA]].

[26] K. Iwaki and T. Nakanishi, "Exact WKB analysis and cluster algebras II: Simple poles, orbifold points, and generalized cluster algebras," Int. Math. Res. Not. **2016** (2016), 4375-4417 [arXiv:1409.4641 [math.CA]].

[27] E. Delabaere, H. Dillinger and F. Pham, "Exact semiclassical expansions for one-dimensional quantum oscillators," J.Math.Phys. **38**, 6126 (1997).

[28] K. Ito, M. Mariño and H. Shu, "TBA equations and resurgent Quantum Mechanics," JHEP **01**, 228 (2019) [arXiv:1811.04812 [hep-th]].

[29] N. Sueishi, S. Kamata, T. Misumi and M. Ünsal, "On exact-WKB analysis, resurgent structure, and quantization conditions," JHEP **12** (2020), 114 [arXiv:2008.00379 [hep-th]].

[30] Y. Emery, "TBA equations and quantization conditions," JHEP **07** (2021), 171 [arXiv:2008.13680 [hep-th]].

[31] N. Sueishi, S. Kamata, T. Misumi and M. Ünsal, "Exact-WKB, complete resurgent structure, and mixed anomaly in quantum mechanics on S^1," JHEP **07** (2021), 096 [arXiv:2103.06586 [quant-ph]].

[32] S. Kamata, T. Misumi, N. Sueishi and M. Ünsal, "Exact-WKB analysis for SUSY and quantum deformed potentials: Quantum mechanics with Grassmann fields and Wess-Zumino terms," [arXiv:2111.05922 [hep-th]].

[33] B. P. Abbott *et al.* [LIGO Scientific and Virgo], "Observation of Gravitational Waves from a Binary Black Hole Merger," Phys. Rev. Lett. **116**, 061102 (2016) [arXiv:1602.03837 [gr-qc]].

[34] G. T. Horowitz and A. Strominger, "Black strings and P-branes", Nucl. Phys. B360(1991) 197-209.

[35] Y. Kurita and M. a. Sakagami, "Quasinormal modes of D3-brane black holes," Phys. Rev. D **67**, 024003 (2003) [arXiv:hep-th/0208063 [hep-th]].

[36] J. M. Maldacena, "The Large N limit of superconformal field theories and supergravity," Adv. Theor. Math. Phys. **2**, 231-252 (1998) [arXiv:hep-th/9711200 [hep-th]].

[37] E. Witten, "Anti-de Sitter space and holography," Adv. Theor. Math. Phys. **2**, 253-291 (1998) [arXiv:hep-th/9802150 [hep-th]].

[38] E. Witten, "Anti-de Sitter space, thermal phase transition, and confinement in gauge theories," Adv. Theor. Math. Phys. **2** (1998), 505-532 [arXiv:hep-th/9803131 [hep-th]].

[39] G. T. Horowitz and V. E. Hubeny, "Quasinormal modes of AdS black holes and the approach to thermal equilibrium," Phys. Rev. D **62**, 024027 (2000) [arXiv:hep-th/9909056 [hep-th]].

[40] K. Imaizumi, "Quasi-normal modes for the D3-branes and Exact WKB analysis," Phys. Lett. B **834** (2022), 137450 [arXiv:2207.09961 [hep-th]].

[41] K. Imaizumi, "Exact conditions for Quasi-normal modes of extremal M5-branes and Exact WKB analysis," [arXiv:2212.04738 [hep-th]].

[42] E. W. Leaver, "An Analytic representation for the quasi normal modes of Kerr black holes," Proc. Roy. Soc. Lond. A **402**, 285-298 (1985).

[43] B. F. Schutz and C. M. Will, "Black hole normal modes - A semianalytic approach", Astrophys. J Lett. **291** L33-36 (1985).

[44] A. Mironov and A. Morozov, "Nekrasov Functions and Exact Bohr-Sommerfeld Integrals", JHEP **1004** (2010), 040 [arXiv:0910.5670 [hep-th]].

[45] W. He and Y.-G. Miao, "Mathieu equation and Elliptic curve" Commun. Theor. Phys. **58** (2012) 827-834, [arXiv:1006.5185 [math-ph]].

[46] K. Ito, S. Kanno and T. Okubo, "Quantum periods and prepotential in $\mathcal{N} = 2$ SU(2) SQCD," JHEP **08**, 065 (2017) [arXiv:1705.09120 [hep-th]].

[47] K. Ito and H. Shu, "TBA equations for the Schrödinger equation with a regular singularity," J. Phys. A **53**, 335201 (2020) 33 [arXiv:1910.09406 [hep-th]]

[48] N. Seiberg, "Supersymmetry and non-perturbative beta functions", Phys. Lett. B **206** (1988) 630-639

[49] N. Seiberg and E. Witten, "Electric - magnetic duality, monopole condensation, and confinement in N=2 supersymmetric Yang-Mills theory," Nucl. Phys. B **426**, 19-52 (1994) [arXiv:hep-th/9407087 [hep-th]].

[50] N. Seiberg and E. Witten, "Monopoles, duality and chiral symmetry breaking in N=2 supersymmetric QCD," Nucl. Phys. B **431**, 484-550 (1994) [arXiv:hep-th/9408099 [hep-th]].

[51] F. Ferrari and A. Bilal, "The Strong coupling spectrum of the Seiberg-Witten theory," Nucl. Phys. B **469**, 387-402 (1996) [arXiv:hep-th/9602082 [hep-th]].

[52] A. Bilal and F. Ferrari, "Curves of marginal stability, and weak and strong coupling BPS spectra in N=2 supersymmetric QCD," Nucl. Phys. B **480**, 589-622 (1996) [arXiv:hep-th/9605101 [hep-th]].

[53] F. Ferrari, "Duality and BPS spectra in N=2 supersymmetric QCD," Nucl. Phys. B Proc. Suppl. **55**, no.2, 245-252 (1997) [arXiv:hep-th/9611012 [hep-th]].

[54] A. Bilal and F. Ferrari, "The BPS spectra and superconformal points in massive N=2 supersymmetric QCD," Nucl. Phys. B **516**, 175-228 (1998) [arXiv:hep-th/9706145 [hep-th]].

[55] N. A. Nekrasov, "Seiberg-Witten prepotential from instanton counting," Adv. Theor. Math. Phys. **7**, no.5, 831-864 (2003) [arXiv:hep-th/0206161 [hep-th]].

[56] N. Nekrasov and A. Okounkov, "Seiberg-Witten theory and random partitions," Prog. Math. **244**, 525-596 (2006) [arXiv:hep-th/0306238 [hep-th]].

[57] N. A. Nekrasov and S. L. Shatashvili, "Quantization of Integrable Systems and Four Dimensional Gauge Theories," [arXiv:0908.4052 [hep-th]].

[58] A. Mironov and A. Morozov, "Nekrasov Functions from Exact BS Periods: The Case of SU(N)," J. Phys. A **43**, 195401 (2010) [arXiv:0911.2396 [hep-th]].

[59] Y. Zenkevich, "Nekrasov prepotential with fundamental matter from the quantum spin chain," Phys. Lett. B **701**, 630-639 (2011) [arXiv:1103.4843 [math-ph]].

[60] K. Ito and T. Okubo, "Quantum periods for $\mathcal{N} = 2$ $SU(2)$ SQCD around the superconformal point," Nucl. Phys. B **934**, 356-379 (2018) [arXiv:1804.04815 [hep-th]].

[61] K. Ito, S. Koizumi and T. Okubo, "Quantum Seiberg-Witten curve and Universality in Argyres-Douglas theories," Phys. Lett. B **792**, 29-34 (2019) [arXiv:1903.00168 [hep-th]].

[62] K. Ito, S. Koizumi and T. Okubo, "Quantum Seiberg-Witten periods for $\mathcal{N} = 2$ $SU(N_c)$ SQCD around the superconformal point," Nucl. Phys. B **954**, 115004 (2020) [arXiv:2001.08891 [hep-th]].

[63] H. Awata and Y. Yamada, "Five-dimensional AGT Conjecture and the Deformed Virasoro Algebra," JHEP **01**, 125 (2010) [arXiv:0910.4431 [hep-th]].

[64] H. Awata, H. Fuji, H. Kanno, M. Manabe and Y. Yamada, "Localization with a Surface Operator, Irregular Conformal Blocks and Open Topological String," Adv. Theor. Math. Phys. **16**, no.3, 725-804 (2012) [arXiv:1008.0574 [hep-th]].

[65] K. Imaizumi, "Exact WKB analysis and TBA equations for the Mathieu equation," Phys. Lett. B **806** (2020), 135500 [arXiv:2002.06829 [hep-th]].

[66] K. Imaizumi, "Quantum periods and TBA equations for $\mathcal{N} = 2$ $SU(2)$ $N_f = 2$ SQCD with flavor symmetry," Phys. Lett. B **816** (2021), 136270 [arXiv:2103.02248 [hep-th]].

[67] G. Aminov, A. Grassi and Y. Hatsuda, "Black Hole Quasinormal Modes and Seiberg–Witten Theory," Annales Henri Poincare **23** (2022) no.6, 1951-1977 [arXiv:2006.06111 [hep-th]].

[68] M. Bianchi, D. Consoli, A. Grillo and J. F. Morales, "QNMs of branes, BHs and fuzzballs from quantum SW geometries," Phys. Lett. B **824**, 136837 (2022) [arXiv:2105.04245 [hep-th]].

[69] M. Bianchi, D. Consoli, A. Grillo and J. F. Morales, "More on the SW-QNM correspondence," JHEP **01**, 024 (2022) [arXiv:2109.09804 [hep-th]].

[70] D. Gaiotto, G. W. Moore and A. Neitzke, "Wall-crossing, Hitchin systems, and the WKB approximation," Adv. Math. **234** (2013), 239-403 [arXiv:0907.3987 [hep-th]].

[71] J. Zinn-Justin and U. D. Jentschura, "Multi-instantons and exact results I: Conjectures, WKB expansions, and instanton interactions," Annals Phys. **313** (2004), 197-267 [arXiv:quant-ph/0501136 [quant-ph]].

[72] J. Zinn-Justin and U. D. Jentschura, "Multi-instantons and exact results II: Specific cases, higher-order effects, and numerical calculations," Annals Phys. **313** (2004), 269-325 [arXiv:quant-ph/0501137 [quant-ph]].

[73] G. Başar and G. V. Dunne, "Resurgence and the Nekrasov-Shatashvili limit: connecting weak and strong coupling in the Mathieu and Lamé systems," JHEP **02** (2015), 160 [arXiv:1501.05671 [hep-th]].

[74] I. R. Klebanov, "World volume approach to absorption by nondilatonic branes," Nucl. Phys. B **496** (1997), 231-242 [arXiv:hep-th/9702076 [hep-th]].

[75] E. W. Leaver, "Quasinormal modes of reissner-nordstro ¨ m black holes," Phys. Rev. D **41**, 2986-2997 (1990).

[76] S. Prem Kumar, A. O'Bannon, A. Pribytok and R. Rodgers, "Holographic Coulomb branch solitons, quasinormal modes, and black holes," JHEP **05** (2021), 109 [arXiv:2011.13859 [hep-th]].

[77] L. Motl, "An Analytical computation of asymptotic Schwarzschild quasinormal frequencies," Adv. Theor. Math. Phys. **6**, 1135-1162 (2003) [arXiv:gr-qc/0212096 [gr-qc]].

[78] N. Andersson and C. J. Howls, "The Asymptotic quasinormal mode spectrum of nonrotating black holes," Class. Quant. Grav. **21**, 1623-1642 (2004) [arXiv:gr-qc/0307020 [gr-qc]].

[79] L. Motl and A. Neitzke, "Asymptotic black hole quasinormal frequencies," Adv. Theor. Math. Phys. **7**, 307-330 (2003) [gr-qc/0301173].

[80] S. S. Gubser, I. R. Klebanov and A. W. Peet, "Entropy and temperature of black 3-branes," Phys. Rev. D **54**, 3915-3919 (1996) [arXiv:hep-th/9602135 [hep-th]].

[81] R. Güven, "Black p-brane solutions of $D = 11$ supergravity theory," Phys. Lett. B **276**, 49-55 (1992).

[82] D. Fioravanti, D. Gregori and H. Shu, "Integrability, susy $SU(2)$ matter gauge theories and black holes," [arXiv:2208.14031 [hep-th]].

[83] N. Oshita, "Ease of excitation of black hole ringing: Quantifying the importance of overtones by the excitation factors," Phys. Rev. D **104** (2021) no.12, 12 [arXiv:2109.09757 [gr-qc]].

[84] S. Codesido and M. Marino, "Holomorphic Anomaly and Quantum Mechanics," J. Phys. A **51** (2018) no.5, 055402 [arXiv:1612.07687 [hep-th]].

[85] L. F. Alday, J. Maldacena, A. Sever and P. Vieira, "Y-system for Scattering Amplitudes," J. Phys. A **43**, 485401 (2010) [arXiv:1002.2459 [hep-th]].

[86] N. Dorey, V. V. Khoze and M. P. Mattis, "On N=2 supersymmetric QCD with four flavors," Nucl. Phys. B **492** (1997), 607-622 [arXiv:hep-th/9611016 [hep-th]].

[87] L. F. Alday, D. Gaiotto and Y. Tachikawa, "Liouville Correlation Functions from Four-dimensional Gauge Theories," Lett. Math. Phys. **91** (2010), 167-197 [arXiv:0906.3219 [hep-th]].

[88] E. Witten and D. Olive, "Supersymmetry Algebras That Include Topological Charges," Phys. Lett. B **78** (1978), 97-101

[89] D. Gaiotto, G. W. Moore and A. Neitzke, "Four-dimensional wall-crossing via three-dimensional field theory," Commun. Math. Phys. **299** (2010), 163-224 [arXiv:0807.4723 [hep-th]].

[90] D. Gaiotto, "Opers and TBA," [arXiv:1403.6137 [hep-th]].

[91] A. Grassi, J. Gu and M. Mariño, "Non-perturbative approaches to the quantum Seiberg-Witten curve," JHEP **07** (2020), 106 [arXiv:1908.07065 [hep-th]].

[92] D. Fioravanti and D. Gregori, "Integrability and cycles of deformed $\mathcal{N} = 2$ gauge theory," Phys. Lett. B **804** (2020), 135376 [arXiv:1908.08030 [hep-th]].

[93] A. B. Zamolodchikov, "On the thermodynamic Bethe ansatz equation in sinh-Gordon model," J. Phys. A **39** (2006), 12863-12887 [arXiv:hep-th/0005181 [hep-th]].

[94] A. B. Zamolodchikov, "Quantum Field Theories in Two Dimensions," World Scientific (2012), vol. 2.

[95] A. B. Zamolodchikov, "Thermodynamic Bethe Ansatz in Relativistic Models. Scaling Three State Potts and Lee-Yang Models," Nucl. Phys. B **342**, 695-720 (1990).

[96] T. R. Klassen and E. Melzer, "Purely Elastic Scattering Theories and their Ultraviolet Limits," Nucl. Phys. B **338** 485-528 (1990).

[97] S. Cecotti and M. Del Zotto, "Y systems, Q systems, and 4D $\mathcal{N} = 2$ supersymmetric QFT," J. Phys. A **47** (2014) no.47, 474001 [arXiv:1403.7613 [hep-th]].

[98] A. Ceresole, R. D'Auria and S. Ferrara, "On the geometry of moduli space of vacua in N=2 supersymmetric Yang-Mills theory," Phys. Lett. B **339** (1994), 71-76 [arXiv:hep-th/9408036 [hep-th]].

[99] M. Matone, "Instantons and recursion relations in N=2 SUSY gauge theory," Phys. Lett. B **357** (1995), 342-348 [arXiv:hep-th/9506102 [hep-th]].

[100] T. Eguchi and S. K. Yang, "Prepotentials of N=2 supersymmetric gauge theories and soliton equations," Mod. Phys. Lett. A **11** (1996), 131-138 [arXiv:hep-th/9510183 [hep-th]].

[101] J. Sonnenschein, S. Theisen and S. Yankielowicz, "On the relation between the holomorphic prepotential and the quantum moduli in SUSY gauge theories," Phys. Lett. B **367** (1996), 145-150 [arXiv:hep-th/9510129 [hep-th]].

[102] P. C. Argyres, M. R. Plesser, N. Seiberg and E. Witten, "New N=2 superconformal field theories in four-dimensions," Nucl. Phys. B **461**, 71-84 (1996) [arXiv:hep-th/9511154 [hep-th]].

[103] S. S. Gubser and A. Hashimoto, "Exact absorption probabilities for the D3-brane," Commun. Math. Phys. **203**, 325-340 (1999) [arXiv:hep-th/9805140 [hep-th]].

[104] D. Fioravanti and D. Gregori, "A new method for exact results on Quasinormal Modes of Black Holes," [arXiv:2112.11434 [hep-th]].

[105] G. Bonelli, C. Iossa, D. P. Lichtig and A. Tanzini, "Exact solution of Kerr black hole perturbations via CFT2 and instanton counting: Greybody factor, quasinormal modes, and Love numbers," Phys. Rev. D **105** (2022) no.4, 044047 [arXiv:2105.04483 [hep-th]].

[106] G. Bonelli, C. Iossa, D. P. Lichtig and A. Tanzini, "Irregular Liouville correlators and connection formulae for Heun functions," [arXiv:2201.04491 [hep-th]].

[107] D. Consoli, F. Fucito, J. F. Morales and R. Poghossian, "CFT description of BH's and ECO's: QNMs, superradiance, echoes and tidal responses," [arXiv:2206.09437 [hep-th]].

[108] S. K. Ashok, D. P. Jatkar, R. R. John, M. Raman and J. Troost, "Exact WKB analysis of $\mathcal{N} = 2$ gauge theories," JHEP **07**, 115 (2016) [arXiv:1604.05520 [hep-th]].

[109] W. He, "Combinatorial approach to Mathieu and Lamé equations," J. Math. Phys. **56**, no.7, 072302 (2015) [arXiv:1108.0300 [math-ph]].

[110] A. K. Kashani-Poor and J. Troost, "Quantum geometry from the toroidal block," JHEP **08**, 117 (2014) [arXiv:1404.7378 [hep-th]].

[111] A. Grassi, Q. Hao and A. Neitzke, "Exact WKB methods in SU(2) $N_f = 1$," JHEP **01** (2022), 046 [arXiv:2105.03777 [hep-th]].

[112] P. Dorey, C. Dunning and R. Tateo, "Differential equations for general SU(n) Bethe ansatz systems," J. Phys. A **33**, 8427-8442 (2000) [arXiv:hep-th/0008039 [hep-th]].

[113] K. Ito and H. Shu, "ODE/IM correspondence and the Argyres-Douglas theory," JHEP **08**, 071 (2017) [arXiv:1707.03596 [hep-th]].

[114] F. Yan, "Exact WKB and the quantum Seiberg-Witten curve for 4d N = 2 pure SU(3) Yang-Mills. Abelianization," JHEP **03** (2022), 164 [arXiv:2012.15658 [hep-th]].

[115] K. Ito, T. Kondo and H. Shu, "Wall-crossing of TBA equations and WKB periods for the third order ODE," Nucl. Phys. B **979** (2022), 115788 [arXiv:2111.11047 [hep-th]].

[116] M. Aganagic, M. C. N. Cheng, R. Dijkgraaf, D. Krefl and C. Vafa, "Quantum Geometry of Refined Topological Strings," JHEP **11** (2012), 019 [arXiv:1105.0630 [hep-th]].

[117] Y. Hatsuda, M. Marino, S. Moriyama and K. Okuyama, "Non-perturbative effects and the refined topological string," JHEP **09** (2014), 168 [arXiv:1306.1734 [hep-th]].

[118] A. K. Kashani-Poor, "Quantization condition from exact WKB for difference equations," JHEP **06** (2016), 180 [arXiv:1604.01690 [hep-th]].